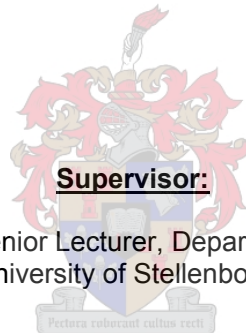


THE CHARACTERISATION OF SOUTH AFRICAN SEA STORMS

by

K R MacHutchon

Thesis presented in fulfilment of the requirements for
the Degree of Master of Science in Civil Engineering
At the University of Stellenbosch



Supervisor:

Mr DE Bosman, Senior Lecturer, Department of Engineering,
University of Stellenbosch

STELLENBOSCH

December 2006

DECLARATION

I, the undersigned, hereby declare that the work contained in this thesis is my own original work and that I have not previously in its entirety or in part submitted it to any other University for a degree.

Signature:

Date:



ABSTRACT

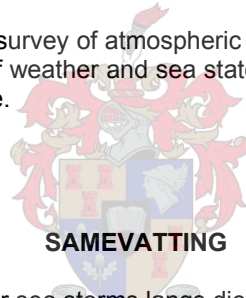
This research provides an overview of sea storms around the South African Coast in terms of weather types, characteristic wave statistics, storm processes and wave energy.

Sea Storm Profiles are unique to the particular storm events causing them, but they can be associated with Equivalent Wave Energy (EWE) Storm Profiles, which are representative of them and have a linear, symmetric, "Capital Lambda" (Λ), shape. The actual storm profile and the EWE Profile are equivalent in wave energy, and the benefit of the EWE is that it is regular and can be readily compared with another EWE Storm Profile for analysis, and for the comparison of impacts.

The ability to compare the impacts of Sea Storms from different areas, on the basis of characteristic Equivalent Wave Energy (EWE) Storm Profiles within the South African Coastal Regions, is considered to be advantageous. This will allow Engineers to apply the knowledge gained in one area to another with a similar EWE Storm Profile, with more confidence.

There will always be the need for site-specific investigations, data recording, data analysis and interpretations in Coastal Engineering Work, but one needs to start with an understanding of the general nature of the coastal region in which one is working. This research adds to the background "Body of Knowledge" relating to the character of the sea storms in the Regions around South Africa.

The study is based on a literature survey of atmospheric weather, sea wave theory and wave climates, as well as the analysis of weather and sea state data at selected recording stations around the South African Coastline.



SAMEVATTING

Hierdie navorsing bied 'n oorsig oor see storms langs die Suid Afrikaanse Kus in terme van weertipes, karakteristieke golfdata, stormprosesse en golfenergie.

See Storm Profile is uniek aan die besondere storm-gebeurtenisse waardeur hulle veroorsaak word, maar hulle kan geassosieer word met verteenwoordigende Ekwiwalente Golf Energie (EGE) Storm Profile wat 'n liniêre, simmetriese, hoofletter Lambda (Λ) vorm het. Die werklike Storm Profiel en die EGE Profiel is ekwiwalent in terme van golf energie. Die voordeel van die EGE is dat dit reëlmatig is en geredelik met 'n ander EGE Storm Profiel vergelyk kan word vir analise en impak evaluasie doeleindes.

Die moontlikheid om die impak van See Storms van verskillende gebiede op grond van karakteristieke Ekiwalente Golf Energie (EGE) Storm Profile binne die Suid Afrikaanse Kusgebiede te kan vergelyk, word as nuttig beskou. Die moontlikheid stel ingenieurs in staat om kennis wat in een gebied opgebou is, met meer vertroue op 'n ander gebied met 'n soortgelyke EGE Storm Profiel toe te pas.

Terrein-spesifieke ondersoeke, data opnames, data analise en interpretasie sal altyd nodig wees vir Kus Ingenieurswerke, maar 'n redelike begrip van die algemene aard van 'n spesifieke kusgebied is nodig by die aanvang van 'n projek. Hierdie ondersoek dra by tot die agtergrond kennis oor die aard van see storms in die kusgebiede rondom Suid Afrika.

Die navorsing is gegrond op 'n literatuur-studie van atmosferiese weer, seegolf-teorie, en golf-klimaat, sowel as die ontleding van weer- en see-toestand data, verkry van 'n aantal meet-stasies langs die Suid Afrikaanse kuslyn.

ACKNOWLEDGEMENTS

Learning and Continuing Professional Development Programmes always make demands on the person in the process, as well as those giving input and support to that person. As far as I am concerned, I have benefited greatly by the process of researching and preparing this Thesis. I have certainly learnt a great deal and made very good friends with those who have assisted and encouraged me in the process.

In this regard, my supervisor Eddie Bosman at the University of Stellenbosch, takes the lead. He has always been available to me to brainstorm new ideas and to review progress at regular intervals. Eddie has been an inspiration to me and has guided me through the process, always encouraging me to be meticulous in detail and specific in research.

Marius Rossouw, originally of the of the CSIR and more lately of Prestedge, Retief Dresdner and Wijnberg, Consulting Engineers, has also been a source of great inspiration to me. I am grateful for his valuable advice during my research.

Ursula Von St Ange, of the CSIR, has always been very prepared to collect and forward data to me for analysis, and I am very grateful to her, for her support.

I would also like to acknowledge and thank the CSIR, as an organisation, for its support with regard to the provision of data and providing access to its Library, during my research.

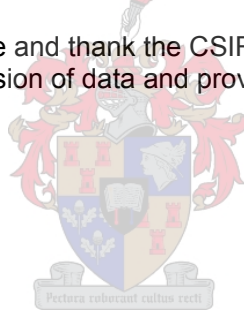


TABLE OF CONTENTS

Declaration	ii
Abstract / Samevatting	iii
Acknowledgements	iv
Table of Contents	v
List of Tables	viii
List of Figures	ix
List of Appendices	xiv
Nomenclature	xv
Definition of Terms	xvii
1. INTRODUCTION	1
1.1 General	1
1.2 Objectives of the Research	1
1.3 Methodology of the Research	1
2. LITERATURE SURVEY	3
2.1 Atmospheric Weather	3
2.1.1 Global Atmospheric Weather systems	3
2.1.2 Air Mass Source Regions	4
2.1.3 Regional Atmospheric Circulation Patterns and Weather Types affecting South Africa	5
2.1.4 Weather Deviations and Local Synoptic Pattern Types	6
2.1.5 Synoptic Pattern Types	8
2.2 Sea Waves	17
2.2.1 General	17
2.2.2 Wind Wave Formation Mechanisms	20
2.2.3 Momentum transfer at the air-sea interface	24
2.2.4 Laboratory Studies of Capillary Waves and Ripples	26
2.2.5 Sea Waves Climates	28
2.2.6 Wave Forecasting Models	31

2.3	Wave Climates	33
2.3.1	Major Wind Belts	33
2.3.2	Major Wave Climates	34
2.3.3	South African Wind Wave Climates	35
2.4	South African Ocean Currents	36
2.4.1	General	36
2.4.2	The Agulhas Current and Counter Current	37
2.4.3	The South Atlantic Current	40
2.4.4	The Benguela Current	40
2.5	Summary of Literature Survey	41
3.	AVAILABLE WEATHER AND SEA STATE DATA AT SELECTED RECORDING STATIONS ON THE SOUTH AFRICAN COASTLINE	42
3.1	Meteorological Weather Data	42
3.1.1	Synoptic Charts	42
3.1.2	Weather Deviations and Synoptic Patterns	42
3.2	Wave and Wind Data Sets	43
3.2.1	Port Nolloth Area	44
3.2.2	Agulhas Bank Area	45
3.2.3	Durban Area	46
4.	ANALYSIS OF DATA	47
4.1	Weather Types and Local Synoptic Patterns around the South African Coast:	47
4.1.1	Annual Distribution of Weather Types and Local Synoptic Patterns causing Atmospheric Storms	47
4.1.2	Regional Wind and Wave Directions	49
4.2	Statistical Analysis of Wave Heights	50
4.2.1	General	50
4.2.2	Port Nolloth Area	50
4.2.3	Cape Point Area	51
4.2.4	Agulhas Bank Area	52
4.2.5	Durban Area	52
4.2.6	Combined Frequency of Occurrence and Probability of Exceedance Curves for the Different Areas	53
4.3	Analysis of Sea Storms	54
4.3.1	Definition of a Storm and Details of Parameters	54
4.3.2	The Offshore Storm Process	59
4.3.3	Storm Passage Variations in relation to a fixed Position	63
4.3.4	Annual Frequencies of Sea Storms around South Africa	66
4.3.5	Sea Storm Profile	67

4.3.5	South Africa Area Sea State and Sea Storm Profiles	68
4.3.7	Wave Energy and Energy Flux	71
4.3.8	Equivalent Wave Energy (EWE) Storm Profiles	74
5	FINDINGS	82
5.1	Correlation of Sea Storms with Weather Type and Synoptic Patterns	82
5.2	Wave Statistics	84
5.3	Wave Climates	84
5.4	Sea Storm Processes	84
5.5	Storm Frequencies	85
5.6	Sea Storm Thresholds, Maximum Intensities and Storm Wave Peak Periods	86
5.7	Storm Wave Energy Levels	86
5.8	Characteristics of Sea Storms	87
5.9	Proposed Sea Storm Regions	90
6.	SUMMARY AND CONCLUSIONS	92
	REFERENCES	96



LIST OF TABLES

Table 2.1:	Frequency of occurrence of the Weather Deviations and Synoptic Pattern Types
Table 2.2:	Beaufort scale with Significant Wave Heights
Table 2.3:	Major Wind Belts of the World
Table 3.1:	Annual Frequency Distribution of Synoptic Patterns
Table 3.2:	Details of Analysed Wave Data
Table 3.3:	Periods of Data Analysed for the Port Nolloth Area
Table 3.4:	Periods of Data Analysed for the Agulhas Bank Area
Table 3.5:	Periods of Data Analysed for the Durban Area
Table 4.1:	Grouped Weather Deviations and Synoptic Patterns effecting sea storms around the South African Coastline
Table 4.2	Distribution of General Peak Wave Periods (T_p)
Table 4.3:	Average Peak Storm Wave Periods ($\overline{T_p}$) for the Wave Climate Regions around the South African Coast
Table 5.1:	Storm Thresholds, Average Maximum Storm Intensities, and the Average Storm Wave Peak periods
Table 5.2:	Average Storm Energy Levels
Table 5.3:	Steepness ratios for Regional EWE Storms
Table 5.4:	Storm Duration Ratios
Table 5.5:	Characteristics of South African Sea Storms

LIST OF FIGURES

- Figure 2.1:** Global Weather System Components
- Figure 2.2:** Global Air Mass Source Regions
- Figure 2.3:** Tri-Cellular Model of Atmospheric Circulation
- Figure 2.4:** Composite diagram showing the important features of the surface atmospheric circulation over South Africa
- Figure 2.5:** A schematic illustration of a typical surface sequence of weather disturbances over Southern Africa
- Figure 2.6:** Schematic representation of the near surface and 500hPa circulation associated with the Continental High Type Types
- Figure 2.7:** Sea Level Synoptic Chart showing typical Continental High Conditions
- Figure 2.8:** Schematic representation of the near surface
- Figure 2.9:** Sea Level Synoptic Chart showing West Coast Trough Conditions
- Figure 2.10:** Schematic representation of the near surface and 500hPa circulation associated with the Westerly Atmospheric Wave and Cold Front Type of weather
- Figure 2.11:** Sea Level Synoptic Chart showing Westerly Atmospheric Wave and Cold Front Conditions.
- Figure 2.12:** Schematic representation of the near surface and 500hPa circulation associated with the Cut-off Low Type of weather
- Figure 2.13a:** Sea Level Synoptic Chart showing Cut-off Low Conditions (Day 1)
- Figure 2.13b:** Sea Level Synoptic Chart showing Cut-off Low Conditions (Day 2)
- Figure 2.14:** Schematic representation of the near surface and 500hPa circulation associated with the Easterly Wave Type of weather
- Figure 2.15:** Sea Level Synoptic Chart showing Easterly Atmospheric Wave Conditions
- Figure 2.16:** Graph showing the Significant Wave Height (H_s) and the Beaufort Scale as a function of Wind Speed

- Figure 2.17.** Graph showing the Significant Wave Height (H_s) and the Beaufort Scale as a function of Wind Speed
- Figure 2.18:** Gravity wave Continuum Diagram
- Figure 2.19.** Diagram showing areas of high velocity and Low-pressure over wave formation.
- Figure 2.20.** Diagram showing areas of Laminar and Turbulent Flow over a waveform
- Figure 2.21.** Diagram showing areas of Laminar and Turbulent flow over a waveform, and possible changes in waveform shape, due to relative movement between water molecules and the wind.
- Figure 2.22.** View of parasitic capillary waves on the leeward side of wavelets
- Figure 2.23:** Observed Drag Coefficients in the open sea for varying wind Speeds above 6.0 m/sec.
- Figure 2.24:** Observed Drag Coefficients in the open sea for low wind speeds
- Figure 2.25:** Location of the high shear layer at the outer edge of the separation bubble on a steep laboratory wave
- Figure 2.26:** Conceptual model of Burst and Sweep flows around the Separation Bubble
- Figure 2.27:** Diagram of Air flow jet reattachment downstream of a separation
- Figure 3.28:** Typical 20 minute Wave Data Record off Cape point (Slangkop) in the Southern Coast Storm Wave Region
- Figure 3.29:** Section of Typical Time Series Wave Profile
- Figure 3.30a:** Typical Autocovariance Functions of the Time Series Data
- Figure 3.30b:** Normalised Autocovariance Functions of the Time Series Data
- Figure 3.31:** Wave Spectrum showing Energy as a function of Frequency
- Figure 2.32:** Major Wind Belts of the World
- Figure 2.33:** Major Wave Climates of World Coasts
- Figure 2.34:** Modified Major Wave Climates of South African Coast
- Figure 2.35:** Diagrammatic layout of Dominant Ocean currents around South Africa
- Figure 2.36:** Layout showing the Agulhas current in the East Coast Swell Region
- Figure 2.37:** Large Scale circulation of the Agulhas Current system

- Figure 2.38:** Satellite image of Agulhas Retroflexion
- Figure 3.1** Location of Wave Recording Station with Water Depths
- Figure 3.2:** Annual Periods of Data Analysed from the Port Nolloth Area
- Figure 3.3:** Annual Periods of Data Analysed from the Agulhas Bank Area
- Figure 3.4:** Annual Periods of Data Analysed from the Durban Area
- Figure 4.1:** Graphs of Combined Regional Weather Deviations and Synoptic Pattern Types
- Figure 4.2:** Wind Direction Polar Diagram for the FA Platform for the Year 1998
- Figure 4.3:** Wave Direction Distributions
- Figure 4.4(a):** Frequency of Occurrence and Probability of Exceedance of H_{m0} - Port Nolloth
- Figure 4.4(b):** Percentage Exceedance Data and Fitted distribution Curves for H_{m0} - Port Nolloth
- Figure 4.5(a):** Frequency of Occurrence and Probability of Exceedance of H_{m0} - Cape Point
- Figure 4.5(b):** Percentage Exceedance Data and Fitted distribution Curves for H_{m0} - Cape Point
- Figure 4.6(a):** Frequency of Occurrence and Probability of Exceedance of H_{m0} - Agulhas Bank
- Figure 4.6(b):** Percentage Exceedance Data and Fitted distribution Curves for H_{m0} - Agulhas Bank
- Figure 4.7(a):** Frequency of Occurrence, Probability of Exceedance and Percentage of Exceedance of H_{m0} -Durban
- Figure 4.7(b):** Percentage Exceedance Data and Fitted distribution Curves for H_{m0} - Durban
- Figure 4.8:** Combined Frequency of Occurrence Curves for H_{m0} for the different Areas
- Figure 4.9:** Combined Probability of Exceedance of H_{m0} for the different Areas
- Figure 4.10:** Satellite Image of the West and Part-Southern Coast of South Africa, showing typical Cold Front cloud features
- Figure 4.11:** Synoptic Chart of the of the same area shown in the satellite image in Figure 4.10

- Figure 4.12:** Two typical South African Sea Storm Profiles
- Figure 4.13:** Percentage Frequency of Occurrence of General Deep Water Peak Wave Periods (T_p)
- Figure 4.14:** Graph showing profile of a Typical Storm off the Southern Coast of South Africa
- Figure 4.15:** The Profile for the second storm on the Agulhas Bank Area in June 1998
- Figure 4.16(a):** Cold Front movement from 2006/05/01 to 2006/05/02.
- Figure 4.16(b):** Cold Front movement from 2006/05/03 to 2006/05/04.
- Figure 4.16(c):** Cold Front movement from 2006/05/05 to 2006/05/06.
- Figure 4.17:** Schematic generalised representation of a storm passage on the south coast of the Southern Hemisphere land mass, showing the variation in wind direction, wind speed, wave height and surge characteristics
- Figure 4.18:** Storm Cycle Diagram
- Figure 4.19:** Illustrative plot of wind Directions at 'A'
- Figure 4.20:** Graphs of the Annual Frequencies of the Sea Storms, in the different representative areas around South Africa
- Figure 4.21:** Storm Parameter Diagram
- Figure 4.22:** Monthly Sea State Profiles, on the Agulhas Bank for the year 1998
- Figure 4.23:** Typical Monthly Sea State Profiles for the Port Nolloth Area with storms shown shaded.
- Figure 4.24:** Typical Monthly Sea State Profiles for the Cape Point Area with storms shown shaded.
- Figure 4.25:** Typical Monthly Sea State Profile for the Agulhas Bank Area
- Figure 4.26:** Typical Monthly Sea State Profile for the Durban Area
- Figure 4.27:** Typical Sea State Profile incorporating a single Storm
- Figure 4.28:** Diagrammatic Process of EWE Storm Profile Development
- Figure 4.29:** Typical Plots of Actual and Equivalent Wave Energy Storm Profiles for the Port Nolloth Area
- Figure 4.30:** Typical Plots of Actual and Equivalent Wave Energy Storm Profiles for the Cape Point Area
- Figure 4.31:** Typical Plots of Actual and Equivalent Wave Energy Storm Profiles for the Agulhas Bank Area

- Figure 4.32:** Typical Plots of Actual and Equivalent Wave Energy Storm Profiles for the Durban Area
- Figure 4.33:** Area Average Equivalent Wave Energy (EWE) Storm Profiles for the Sea Storm Areas around South Africa
- Figure 5.1:** Graphs showing the Monthly Frequencies of Occurrence of Weather Types and Sea Storms in the different Regions
- Figure 5.2:** Diagram illustrating the Offshore Storm Process
- Figure 5.3:** Average Monthly Occurrences, of the Storms in the Different Regions
- Figure 5.4:** Average EWE Storm Profile for the South African Coastlines
- Figure 5.5:** South African Sea Storm Regions
- Figure 5.6:** Marine METAREA VII



LIST OF APPENDICES

- APPENDIX A -** Notes on Very Large (Freak) Waves that occur in the East London Sea Storm Area.
- APPENDIX B -** Graphs showing Profiles of Sea Storms in the Agulhas Bank Area for the Year 1998
- APPENDIX C -** Typical Storm Energy Flux Calculations
- APPENDIX D -** Typical Equivalent Wave Energy Storm Profile Calculations



NOMENCLATURE

<i>Symbols:</i>	H_s	Significant Wave Height (m)
	c	Velocity of wave form (m/sec)
	s	Ratio of the density of fluids
	ρ_a	Density of air (kg/m^3)
	ρ_w	Density of water (kg/m^3)
	S_c	Sheltering coefficient
	u^*	Friction velocity (m/sec)
	u_{10}	Wind speed at 10m height (m/sec)
	τ	Shear Stress
	C_D	Drag Coefficient
	Z_0	Roughness length
	C_p	Phase velocity of characteristic waves
	K_p	Wave number = $\frac{2\pi}{L}$
	$\eta(t)$	Sea surface elevations above and below a fixed datum as a time series
	t	variable of time (sec)
	$Z(t)$	Auto-covariance function of time series data
	T_p	Spectral peak wave period
	H_{m0}	Estimate of Significant Wave height = $4\sqrt{m_0}$
	m_0	Zeroth moment of Spectral Density
	m_1	
	T_z	Average zero upcrossing period (sec)
	L	Wavelength (m)
	E_p	Potential Energy (Joules/m length of wave crest)
	E_k	Kinetic Energy (Joules/m length of wave crest)

The Characterisation of South African Sea Storms

E_T	Total Energy (Joules/m length of wave crest)
\bar{E}	Specific Energy or Energy Density (Joules/m ²)
$\langle \eta^2 \rangle^{.5}$	Standard deviation of surface displacements
J or \bar{P}	Wave energy Flux or Wave Power (Joules /sec/m length of wave crest)
C_g	Wave group velocity (or celerity) (m/sec)
\bar{P}_o	Wave Power in deep sea
\bar{E}_o	Specific energy in deep water
C_o	Wave Velocity (or celerity) in deep water (m/sec)



DEFINITIONS OF TERMS

Weather is defined as being the day-to-day variations of meteorological conditions in the atmosphere, especially the wind, clouds, rain and temperature.

Synoptic Patterns are defined as being the wide area layouts, or configurations, of the high and low pressure areas, as well as the intermediate transitions areas between these features, in the atmosphere. Synoptic patterns are depicted by isobars.

Atmospheric Waves are defined as being wave shaped groups of isobars, which move across a region in the same direction of travel as the synoptic pattern.

Sea Waves are defined as being surface gravity waves, with periods of between approximately 3 and 25 seconds, which are formed on the surface of the sea by winds.

Storm Peak Threshold (SPT) is defined as “the sea state with a maximum significant wave height equal to 1.5 x the annual average significant wave height for the site of the Storm” [Boccotti, 2000].

Storm Threshold (ST) is defined as being equal to the Annual Average Significant Wave Height for the Area.

Storm Peak Duration (SPD) is defined as “the time that the sea state exceeds the Storm Peak Threshold, provided that it is greater than a 12 hour continuous, and does not fall below this threshold, before rising again, for a continuous period of less than 12 hours.

Storm Duration (SD) is defined as “the time that the sea state exceeds the Storm Threshold, with at least one Storm Peak in the period”.

Maximum Storm Intensity ($H_{m0 \text{ (max)}}$) is significant wave of the highest sea state during the storm.

Peak Period (T_p) is the Spectral Peak Period = $1/f_p$.

A Storm Profile is the plot of the sea state intensities in excess of the storm threshold level.

The Equivalent Wave Energy (EWE) Storm Profile is a symmetrical triangular profile plot of sea states, which has the same storm threshold, maximum intensity, maximum significant wave height and storm energy level, as the actual storm.

1. INTRODUCTION

1.1 General

Sea Storms are high-energy events of finite duration, which effect Ships at sea, Offshore Structures, Coastal Engineering Structures, Coastal Engineering Construction Works and Natural Coastlines.

Waves, arising from sea storms, are probably the most significant hydraulic parameter in the Coastal Engineering Design and Risk Management Process. An understanding and forecasting of storm events, as well as the ability to mitigate their negative impacts, are important aspects of work in the Coastal and Near Offshore Zones.

Significant factors which govern the impact of Sea Storm, include:

- Their Intensities
- Their duration,
- Their Wave Energy Levels, which are a function of wave heights (H_{m0}) and Periods (T_p), and
- Their frequency of occurrence.

Storm Durations affect the construction stages of a project more than the permanent works due to the fact that they can cause:

- Damage to the exposed and vulnerable construction faces, and
- Increases downtime periods,

The frequency of occurrence of storms also affects construction stages more than permanent works, due to the fact that a second and third storm, occurring soon after an earlier one, can compound damage from the earlier storm/s, which may not have been fully repaired at the time.

1.2 Objectives of the Research

The objectives of this research are to characterise Sea Storm Regions and Sea Storm Events around the South African Coast so as to be in a better position to manage the Construction Risks, in the field Coastal and near Offshore Engineering, in the Country.

1.3 Methodology of the Research

The objectives this research were achieved in the following way:

Firstly, a literature survey was conducted of the following topics, which all relate to the issues to be dealt with:

- **Atmospheric Weather** around the South African Coast
- **Ocean Wave Theory**, including wind generation of waves, wave forecasting models, drag, stress, friction velocity and roughness length, as well as issues related to short and long waves
- **Wave Climates**, including major wave climates as well as South African wave climates, and
- **Offshore Ocean Currents** around the South African Coastline

Secondly, weather and sea state data were collected from selected recording stations around the South African Coastline to identify Storm Regions. The identification of the Storm Regions was based on the synoptic patterns causing the sea storms in the regions, the regional wind and wave directions, sea state parameters, storm parameters and the frequency of storms in the regions.

Thirdly, the above data were analysed to identify aspects of the environment, and sea storms that could be used to characterise the latter, on an individual and regional, basis around the South African Coastline. In this regard the following issues were covered:

- The weather
- Wave Statistics
- Sea storm details

Fourthly, findings relating to the characterisation of sea storms, and sea storm regions, around the South African coastline were drawn from the above analysis.

Finally, conclusions were drawn from the findings, to provide Coastal Engineers with a sound basis for the identification of storm types and for the evaluation of storm impacts.

It is considered that this research could contribute towards the better management of construction risk in the field of coastal engineering.



2. LITERATURE SURVEY

A survey of current literature on Atmospheric Weather, Sea Waves, Wave Climates and Offshore Ocean Currents was carried to provide a general background to the topic of Sea storms, which is the focus of this study. Relevant details arising from the literature survey have been included below.

2.1. Atmospheric Weather

The weather is controlled by air masses, comprising vast bodies of air, which may stay in one location for a significant number of weeks or even months. These locations are known as source regions and while they are there the air masses acquire the same general characteristics whether warm or cold, dry or humid, throughout their entire depth.

Eventually the different air masses are drawn into, or displaced by, air masses from other source regions and this interaction causes most of the depressions, and fronts, that are usually associated with weather systems [Watts, 2004].

2.1.1 Global Atmospheric Weather Systems

The world's weather system can be reduced, in its most basic form, to the following components, shown diagrammatically in Figure 2.1

- (i) Polar High Pressure regions
- (ii) Temperate Low Pressure Belts, and the Polar Fronts
- (iii) Sub-Tropical High Pressure Belts, and the permanent anticyclones
- (iv) Equatorial Low Pressure belts and the Inter-tropical Convergence Zone, which divides the Southern Hemisphere air from the Northern Hemisphere air.

Pectora roborant cultus recti

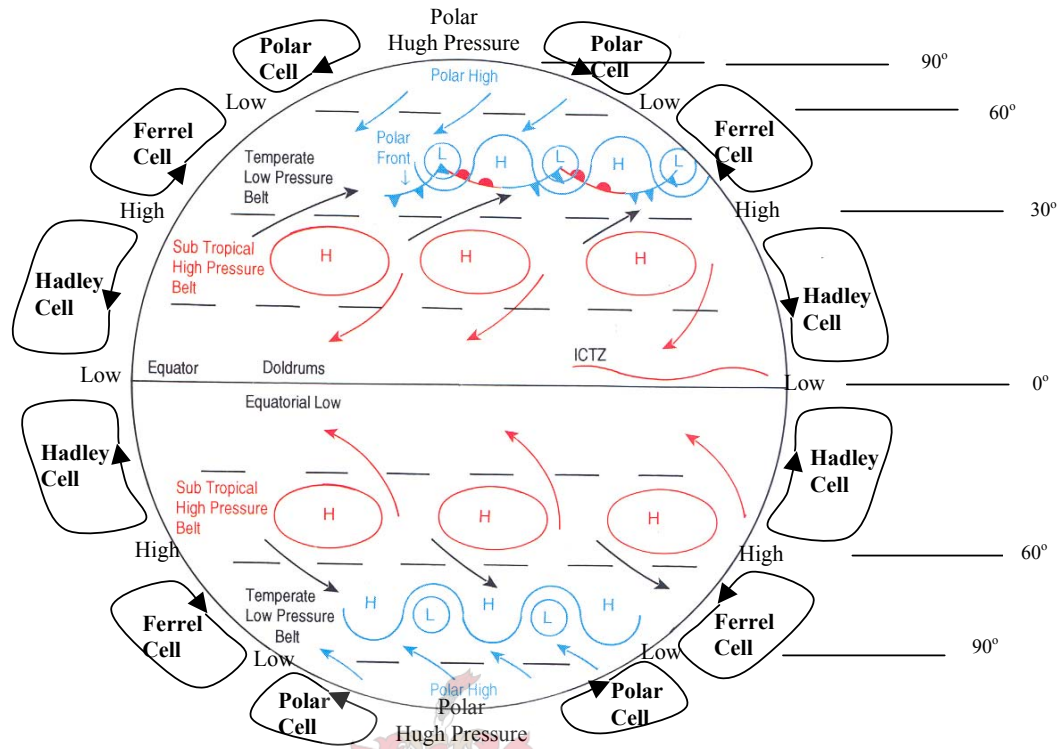


Figure 2.1: Global Weather System Components [Watts, 2004, modified]

2.1.2 Air Mass Source Regions

Air masses have the following principal global source regions [A watts, 2001]:

- | | | |
|-------|-----------------------|----|
| (i) | Marine Tropical: | mT |
| (ii) | Marine Polar: | mP |
| (iii) | Equatorial: | E |
| (iv) | Continental Polar: | cP |
| (v) | Continental Tropical: | cT |
| (vi) | Arctic: | A |
| (vii) | Ant-arctic: | AA |

The above air masses sources are shown in Figure 2.2 and it can be seen that Southern Africa is influenced by the following sources:

- (i) The Continental Tropical source over Southern Africa
- (ii) The Marine Tropical source (dry) over the Southern Atlantic Ocean
- (iii) The Marine Tropical source (moist) over the Southern Indian Ocean
- (iv) The Belt of Moving Cyclones of the Polar Front Zone, to the South of Southern Africa

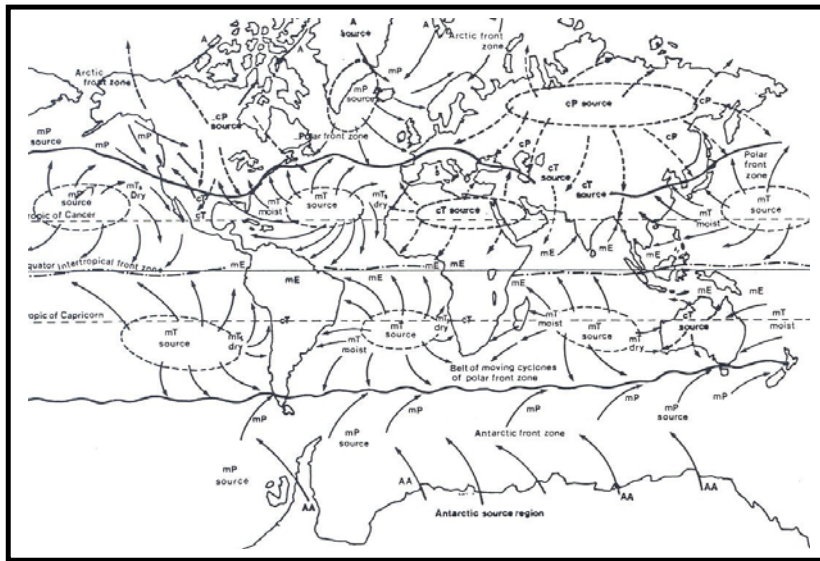


Figure 2.2: Global Air Mass Source Regions [Watts, 2004]

2.1.3 Regional Atmospheric Circulation Patterns and Weather Types affecting South Africa

The climate and weather of Southern Africa are influenced by the mean circulation of the atmosphere over the sub-continent, and by local deviations from that mean. Due to Southern Africa's location in the sub-tropics, it is affected by circulation systems prevailing in both the tropics to the north and temperate latitudes to the south. At the same time it is dominated by the high-pressure systems that, when averaged, constitute the semi-permanent, subtropical high-pressure cells of the general circulation of the southern hemisphere [Watts, 2004].

(a) Over-land Circulation Patterns

Except near the surface, the mean circulation of the atmosphere over the Southern Africa land mass is anti-clockwise, or anti-cyclonic, throughout the year. In winter the mean anticyclone intensifies and moves northward. Upper-level circumpolar westerlies expand and displace the upper tropical easterlies towards the equator. The near-surface circulation over the land, at 850 hPa in January, consists of a weak low-pressure area centred over the central interior and linked, by a trough, across the Northern Cape and Botswana to a tropical low north of Botswana. The centre of the latter feature wanders in an east-west direction along the southern branch of the Inter Tropical Convergence Zone in the region of the Congo Air Boundary and occasionally southward towards Namibia, Botswana, or Zimbabwe. Over the Northern Cape a weak ridge is to be observed. In contrast to the January situation, the low-level July mean pressure field at 850 hPa is strongly anticyclonic over the inland areas. The change to a single high-pressure cell takes place by March, resulting in a northerly flow of moist air from the tropics over the western parts over southern Africa at a time when the air masses over Zimbabwe, Zambia and northern Botswana and Namibia are still moist [Tyson et al, 2000].

(b) Marine Circulation Patterns

The wind and therefore the sea wave patterns in the South Atlantic and South Indian Oceans are influenced by a number of dominant meteorological features, in a similar way to that for the land circulation patterns, referred to above.

Heated air, which rises in the tropics near the equator, moves southward and descends in the vicinity of latitude 30°S, to form the so called Hadley cell. This descending air causes two semi-permanent high pressure systems, the South Atlantic High and the South Indian High, with the air moving in an anti-cyclonic way around the centre of the high pressure system.

South of the Hadley cell, the Ferrel Westerlies spiral east-wards around the globe. Disturbed air in the Ferrel westerlies creates the low pressure system of the South Atlantic. Once formed, these low-pressure systems are moved from west to east within the Ferrel westerly wind system shown diagrammatically in Figure 2.3. It is the passage of these atmospheric depressions, with their associated cold fronts and wind fields that are the main generating source of large sea waves affecting the South African coastline [Rossouw (J), 1989].

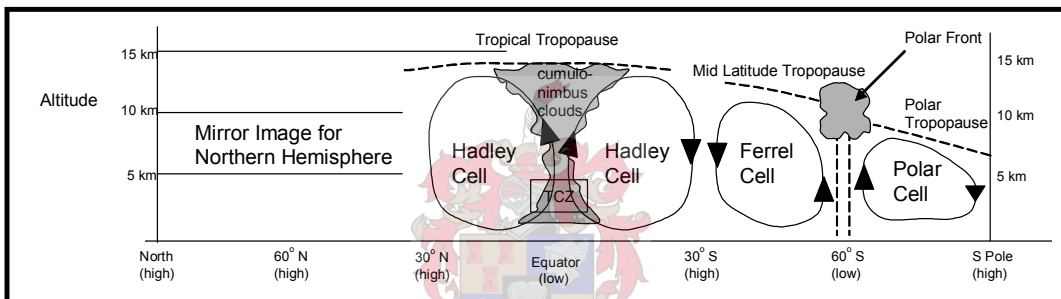


Figure 2.3: Tri-Cellular Model of Atmospheric Circulation

2.1.4 Weather Deviations and Local Synoptic Pattern Types

The main elements affecting the day-to-day weather of Southern Africa are caused by tropical, subtropical and temperate weather features.

The *tropical influence* on Southern African weather is affected through tropical easterly air flow, with the occurrence of easterly atmospheric waves and low pressure areas. (Refer to Figure 2.4 for examples of atmospheric waves).

The *subtropical influence* is affected through the semi-permanent Continental High as well as the South Atlantic Anticyclone and the South Indian Anticyclone, as shown in the composite diagram in Figure 2.4. The systems comprise the elements of the discontinuous high pressure belt that circles the southern hemisphere at about 30°S.

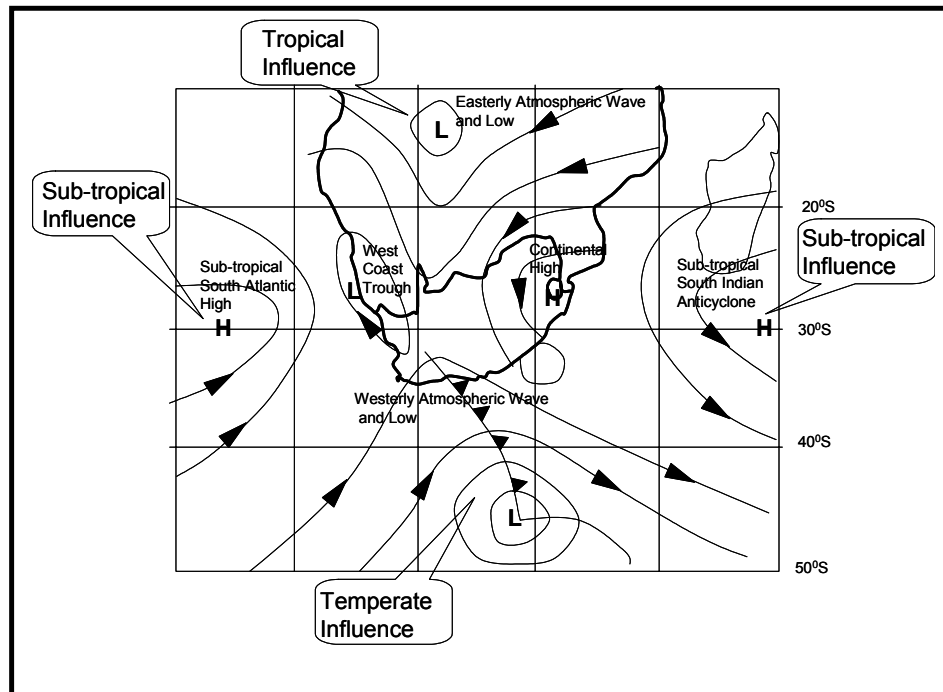


Figure 2.4: Composite diagram showing the important features of the surface atmospheric circulation over South Africa [Tyson et al, 2000].

The Southern Atlantic and Indian Ocean Anticyclones vary significantly in position throughout the year. Both cells move about 6° northward in winter. The Atlantic high shows a yearly cycle in its latitudinal position while the Indian high undergoes a half-yearly zonal oscillation. The monthly longitudinal shifts in the position of the Atlantic high are up to double those of its latitudinal variation and do not materially affect the weather of the subcontinent. On the scale of days, however, the high may ridge eastward and to the south of the continent. Extended ridging leads to breaking off (sometimes referred to as budding) of a separate high, which drifts eastward into the Indian Ocean before being subsumed into the South Indian high. In so doing the freshly formed ridging anticyclone in the westerlies may strongly affect the weather of South Africa. The seasonal east-west shifts of the high in the Indian Ocean (up to 24°) have important effects on the summer and winter weather of the eastern parts of southern Africa.

Temperate influence is exerted through traveling deviations in the westerlies that take the form of westerly atmospheric waves with cold fronts and lows.

Of a more local nature are west-coast troughs and the smaller-scale and shallow coastal lows.

Underlying a considerable day-to-day variability in weather, it is possible to discern a tendency for the occurrence of typical sequences in the passage of disturbances to the south of the subcontinent. These sequences seldom occur for long enough to impose a predictable regularity on the weather, but occasionally they may establish themselves clearly for short periods. Such a 6-day sequence is illustrated schematically in Figure 2.5.

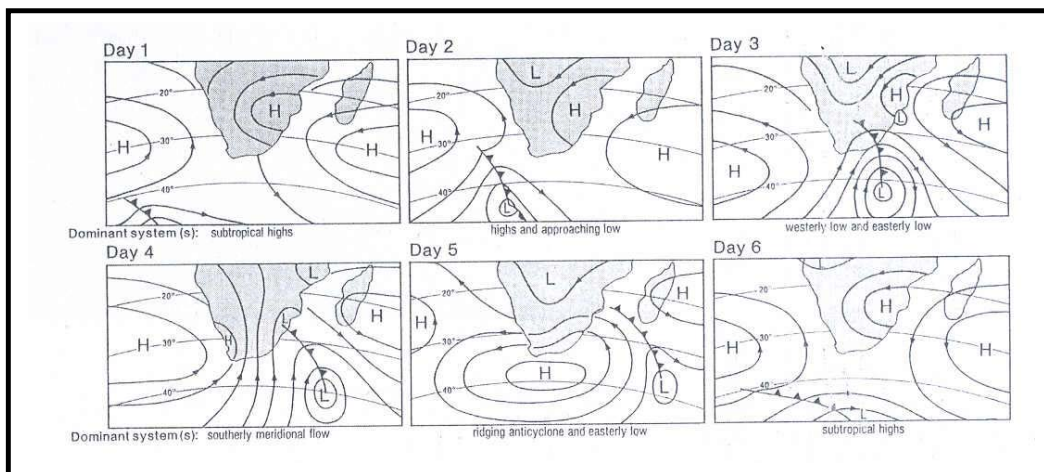


Figure 2.5: A schematic illustration of a typical surface sequence of weather disturbances over Southern Africa [Tyson et al, 2000]

On *day 1* the circulation is dominated by subtropical highs. Thereafter a low in the westerlies drifts eastward to trail its cold front across the southern part of South Africa by *day 3*. At the same time an easterly atmospheric wave develops to the north. By *day 4* the low is moving off the east coast and strong southerly meridional flow sweeps across the subcontinent. At the same time the Atlantic high begins to ridge eastward towards Cape Town. By *day 5* a large ridging anticyclone has broken free of its parent Atlantic High and is drifting around the tip of Africa and into the Indian Ocean. By *day 6* the ridging high has been amalgamated into the Indian high and the circulation pattern has reverted to one similar to that prevailing originally on *day 1*. [Tyson et al, 2000]

2.1.5 Synoptic Pattern Types

The principal synoptic patterns, which incorporate generalized near-surface circulation types and their attendant upper level counterparts, and which effect the sea storms around the South African Coast, have been identified as follows:

- (i) Continental Highs
- (ii) West Coast Troughs
- (iii) Westerly Atmospheric Waves and Cold Fronts
- (iv) Cut-off Lows, and
- (v) Easterly Atmospheric Waves

(a) Continental High

Fine weather and mildly disturbed conditions are invariably associated with the generation of anti-cyclonic vorticity in large subtropical anti-cyclones centered over the sub-continent and surrounding sea areas. They are associated with divergence in the near surface wind field, strong subsidence throughout a deep layer, the occurrence of inversions, fine clear conditions and little or no rainfall.

The surface divergence is accompanied by convergence in the uppermost levels of the troposphere and this, together with descent in the pole-ward limb of the tropical Hadley cell, produces subsidence throughout the 500hPa surfaces and into the lower layers.

The frequency of occurrence of anticyclones reaches a maximum over the interior plateau in June and July with a minimum during December. The dominant effect of winter subsidence over the inland areas is such that the mean vertical motions, averaged over the year, are downward. Clearly there must be times when upward motion dominates, otherwise no weather would occur, but this circulation is generally localised within the system producing it and subsidence continues to prevail elsewhere.

Anticyclones generally either travel around, or they block, other air masses. Travelling highs tend to circulate around the temperate latitudes with local lows. In other cases, such as the situation over Southern Africa, they tend to be more static and only allow lows to move in, for any length of time, when they move northwards, during the winter months. This process allows the southerly Storm Wave Climate region to move closer to the South African Coastline where it has a significant effect on the sea storms in the southern area.

A schematic representation of the near surface and 500hPa (5 000 m altitude) circulations associated with the Continental High Type of Weather has is presented in Figure 2.6.

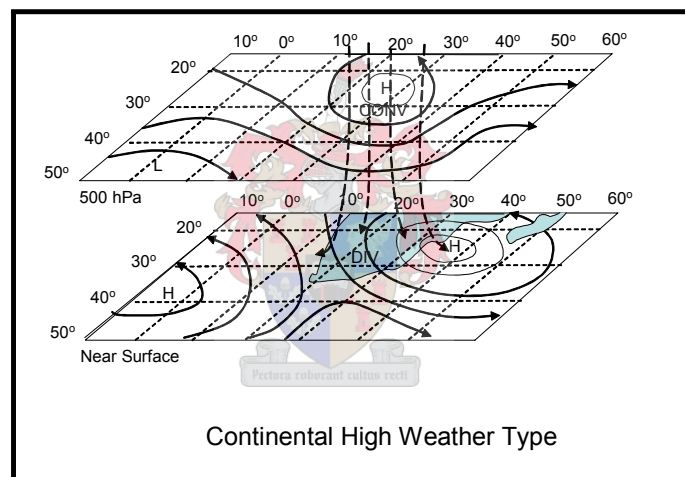


Figure 2.6: Schematic representation of the near surface and 500hPa circulation associated with the Continental High Type Types [Tyson et al, 2000, redrawn]

Details of the Sea Level Synoptic Chart showing typical Continental High Conditions is given in Figure 2.7 where the feature has been marked

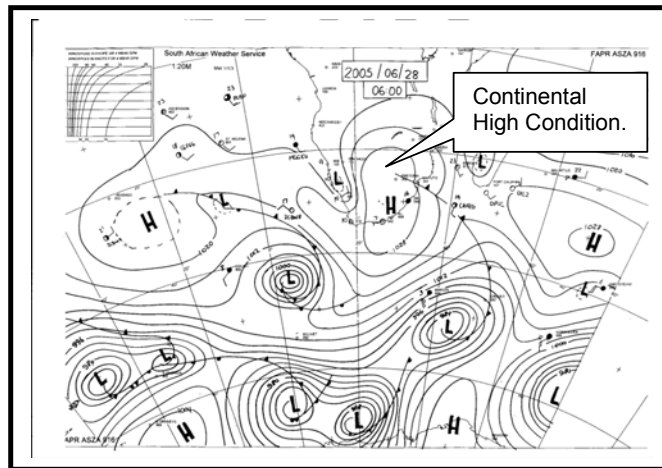


Figure 2.7: Sea Level Synoptic Chart showing typical Continental High Conditions [South African Weather Services]

Synoptic Charts are graphical representations of the surface weather across a region at a single point in time. The charts are compiled from information collected from a number of weather stations in the area, and they are presented in accordance with international standards [Reynolds, 2004].

The charts include a broad spectrum of information on the weather, including details on the following principal elements:

- (i) The Mean Sea Level Pressure at the recording station that provided the information, plotted to the top and right of the location of the station. The location of the station is marked on the chart as a circle.
- (ii) Contours of Equal Pressure, known as isobars, across the region, with local areas of high and low pressure being marked with an “H” and “L” respectively.
- (iii) Temperature fronts, comprising cold and warm fronts, which are shown as triangular spikes and rounded semi-circles respectively, along the lines of the fronts.
- (iv) Wind Directions and Speeds, represented by “shafts” pointing towards the centre of the different stations along the direction from which the wind is blowing, and “barbs” at the ends of the shafts, respectively. The wind speeds are reported to the nearest knot (approximately 0.5 m/sec), and they are rounded to the nearest 5 knots before being plotted. The “barbs “ are plotted on the right hand side of the shafts, looking towards the station, in the Southern Hemisphere, and on the left hand side in the Northern Hemisphere.
- (v) Cloud Cover, represented by the percentage of the station circle that is shaded.

(b) West-coast Troughs

A surface trough of low pressure over the west coast and an upper-tropospheric westerly atmospheric wave to the west of the continent result in a situation conducive to widespread rains over the western parts of South Africa. Surface convergence and upper-level divergence ahead of the trough combine to produce the conditions necessary for general upward vertical motion. Cyclonic disturbances originating as west-coast troughs tend to follow a south-easterly trajectory as they move into the Indian Ocean. They also appear to develop only at times of active tropical convection, suggesting a dynamic link with the easterlies in their formation.

A Schematic representation of the near surface and 500hPa circulation associated with the West Coast Trough Type of weather is given in Figure 2.8.

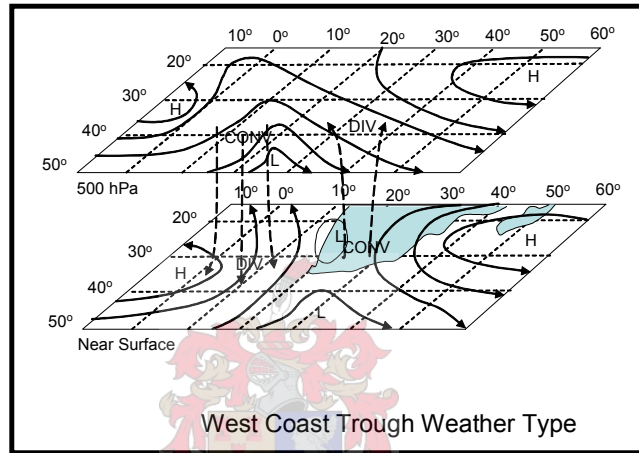


Figure 2.8: Schematic representation of the near surface and 500hPa circulation associated with the West Coast Trough Type of weather. [Tyson et al, 2000, redrawn]

Details of a Sea Level Synoptic Chart showing the West Coast Trough Condition, together with the Continental High Condition, are given in Figure 2.9, where the features have been marked

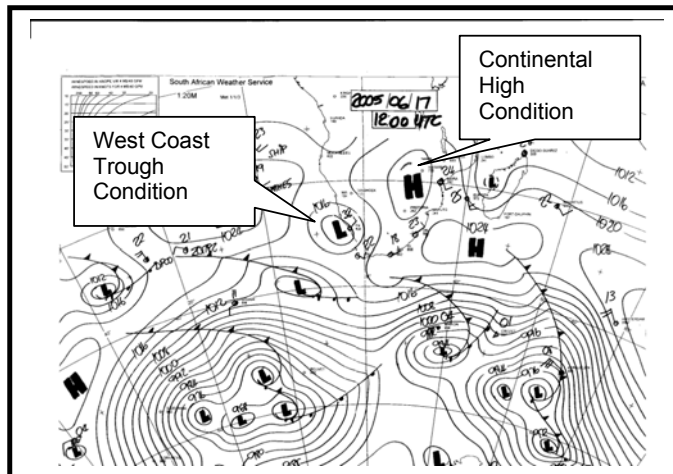


Figure 2.9: Sea Level Synoptic Chart showing West Coast Trough Conditions [South African Weather Services]

(c) Westerly Atmospheric Waves and Cold Fronts

Westerly Atmospheric Waves and cold fronts are important determinants of the weather and climate of Southern Africa, and in particular of South Africa. Westerly Atmospheric Waves can occur either independently or together with Cold Fronts, Depressions and Cut-off Lows.

Westerly Atmospheric Waves are unstable, Rossby Waves, that are normally tilted westward with height. Closed isobars may be present at the surface, but there is no closed circulation in the upper air. Westerly Atmospheric Waves have a peak frequency of occurrence of 2 to 8 days. The conservation of absolute vorticity and the change in radius of curvature in the wave produces surface convergence, with south easterly air flow, to the rear of the trough; whereas at the 500 hPa level and above, divergence occurs to the east and ahead of the trough.

Cold Fronts are associated with invasions of cold air from the south and south-west that produce characteristic cold snaps of a few day's duration, and it is useful to discuss them separately. They occur most frequently in winter when the amplitude of westerly disturbances is greatest. They also produce conditions favourable for the promotion of convection to the rear of the front, where low-level convergence in airflow with a marked southerly component is at a maximum. Ahead of the front, in airflow with pronounced northerly component, divergence and subsidence are responsible for stable and generally cloud-free conditions. Cold fronts are associated with distinctive bands of clouds, which may extend far inland. The wind shift across the front is usually associated with a pronounced reversal of direction and changes in wind speed and gustiness, although the passage of the preceding coastal low may produce even more pronounced shifts at the surface.

A Schematic representation of the near surface and 500hPa circulation associated with the Westerly Atmospheric Wave and Cold Front Type of weather is presented in Figure 2.10.

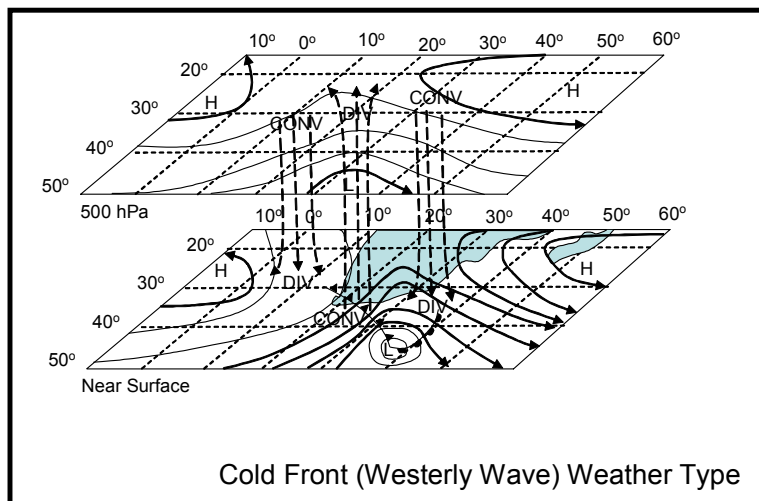


Figure 2.10: Schematic representation of the near surface and 500hPa circulation associated with the Westerly Atmospheric Wave and Cold Front Type of weather. [Tyson et al, 2000, redrawn]

Details of a Sea Level Synoptic Chart showing Westerly Atmospheric Wave and Cold Front Conditions is given in Figure 2.11, where the features have been marked.

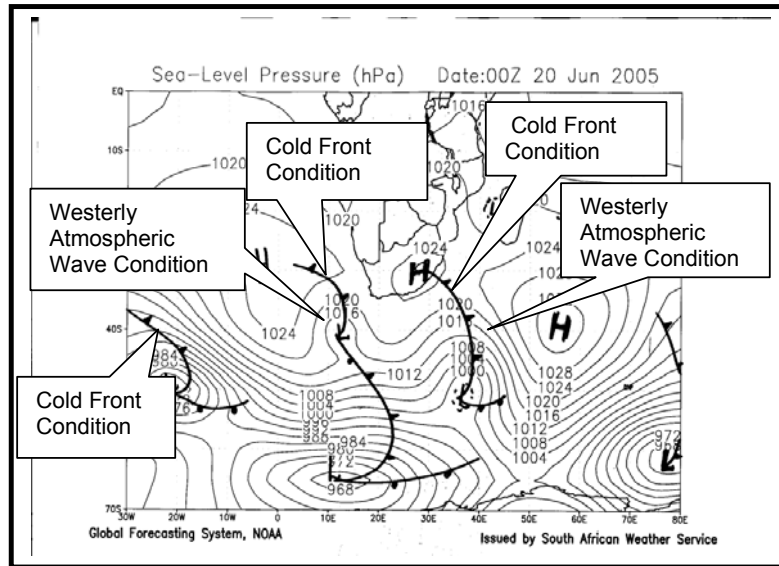


Figure 2.11: Sea Level Synoptic Chart showing Westerly Atmospheric Wave and Cold Front Conditions [South African Weather Services]

(d) Cut-off lows

The Cut-off Low is a feature that is a cold-cored depression, which starts as a trough in the upper westerlies and deepens into a closed circulation extending downward to the surface and which become displaced equatorward out of the basic westerly current. Cut-off lows are unstable, baroclinic systems that slope to the west with increasing heights and are associated with strong convergence and vertical motion, particularly while they are deepening. The source of major divergence, necessary to act together with the surface convergence to produce the deep uplift that is observed in cut-off lows, occurs at a level much higher than the 500 hPa surface. Cut-off lows account for many of the flood-producing rains observed over South Africa.

A Schematic representation of the near surface and 500hPa circulation associated with the Cut-off Low Type of weather is given in Figure 2.12.

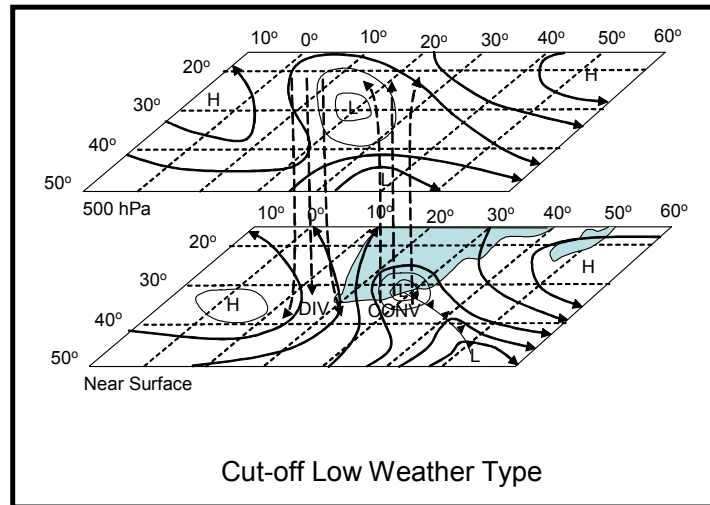


Figure 2.12: Schematic representation of the near surface and 500hPa circulation associated with the Cut-off Low Type of weather. [Tyson et al, 2000, redrawn]

Details of a Sea Level Synoptic Chart showing Cut-off Low Conditions is given in Figures 2.13a and 2.13b, where the features have been marked.

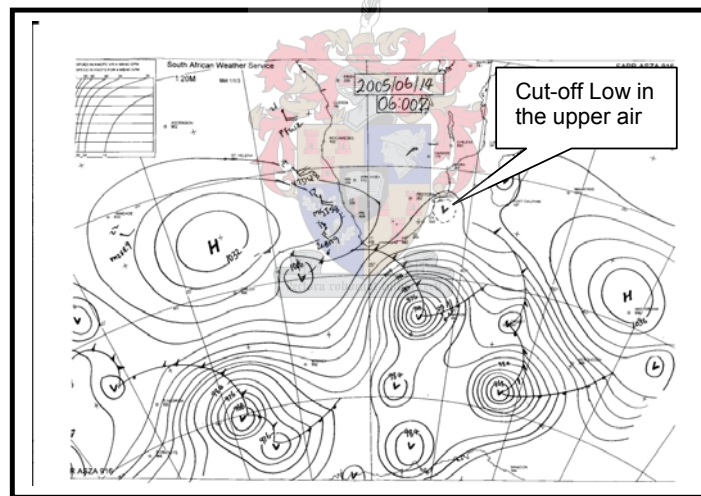


Figure 2.13a: Sea Level Synoptic Chart showing Cut-off Low Conditions (Day 1) [South African Weather Services]

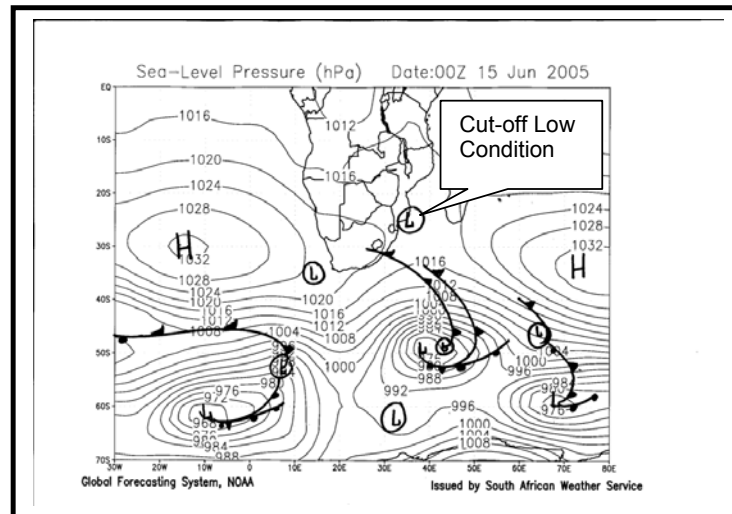


Figure 2.13b: Sea Level Synoptic Chart showing Cut-off Low Condition (Day 2) [South African Weather Services]

(e) Easterly Atmospheric Waves

Disturbances in the tropical easterly flow occurring around the northern sector of subtropical anticyclones take the form of easterly atmospheric waves and lows. They are usually associated with the Inter-Tropical Convergence Zone and the warm, humid easterly winds between the Zone and the subtropical high-pressure belt. Unlike their counterparts over the tropical North Atlantic Ocean and the Caribbean Sea, easterly atmospheric waves over southern Africa are semi-stationary in character. They form in deep easterly currents in the vicinity of an easterly jet. The atmospheric waves are relatively stable features, and they usually take the form of open atmospheric waves or cool-colored closed lows which are evident at lower levels (850 hPa and 700hPa), weakly developed at 500 hPa (5000m altitude) and generally absent in the upper troposphere, where they are replaced by a warm-cored ridge of high pressure. Since the systems are relative stable, their axes are not displaced with height, as is the case with their unstable counterparts in the westerlies.

Low-level convergence occurs to the east of the surface trough, while at 500 hPa or above the flow is divergent. The consequence is strong uplift, which may sustain rainfall in the absence of pronounced instability. With the presence of unstable air, good rains, often occurring in rainy spells of a few days' duration, may occur over wide areas to the east of the trough in association with winds of a northerly component. Ahead of and to the west of the trough, and consequent upon surface divergence and upper level convergence, subsidence ensures no rainfall, clear skies and hot conditions.

Typical 850 hPa circulation patterns associated with a midsummer tropically induced easterly atmospheric wave disturbance produced extensive scattered rainfall over north-eastern South Africa.

A Schematic representation of the near surface and 500hPa circulation associated with the Easterly Atmospheric Wave Type of weather is given in Figure 2.14.

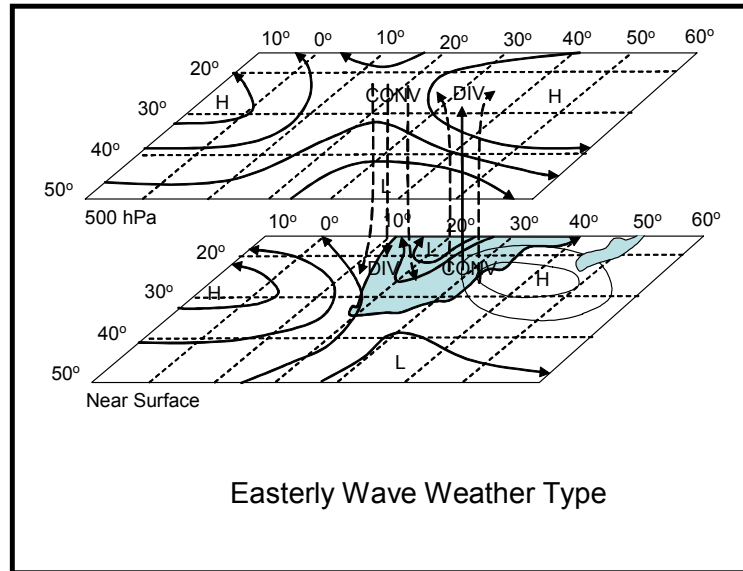


Figure 2.14: Schematic representation of the near surface and 500hPa circulation associated with the Easterly Atmospheric Wave Type of weather. [Tyson et al, 2000, redrawn]

Details of a Sea Level Synoptic Chart showing Easterly Atmospheric Wave Conditions is given in Figure 2.15, where the features have been marked.

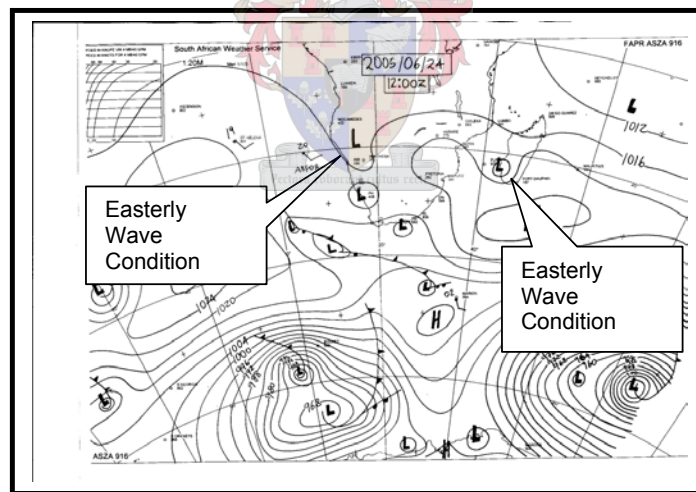


Figure 2.15: Sea Level Synoptic Chart showing Easterly Atmospheric Wave Conditions [South African Weather Services]

2.2 Sea Waves

The Atmospheric Weather Types and Synoptic Patterns, that have been identified and discussed in 2.1 above, directly effect the sea surfaces over which the occur. The pressure differentials and gradients in the atmosphere cause air masses to move around and build up kinetic energy, which is transferred to the sea surface causing sea waves to are build up.

2.2.1 General

Wind generated sea waves are a special type of water wave which is formed by the action of wind on the air-water interface. The characteristics of sea waves are determined by the coupling process between the boundary layers of the air and the water, and they are significantly affected by the following factors:

- The **motion of the wave surface**,
- The local **wind speed and direction**, and
- The **turbulence in the air and water boundary layers** [Toba, 1988 and Csanady, 2001]

Wind speeds can be related to visual descriptions of the sea states and visually assessed wave heights by the Beaufort Scale. The scale is not linked to measured wave values such as wave height, wave period or wave direction, but it is considered to be useful from the point of view of obtaining an understanding of how the state of the sea surface builds up from ripples to exceptionally high waves, as the wind speed increases.

The Beaufort scale ranges from 2 to 12, and it is based on the assumption that the sea waves are fully developed. The scale includes descriptions of the waves in the different categories of wind speed, and details of the scale have been given, together with the following data, in Table 2.2:

- (i) The respective ranges of wind speed, which are incorporated into the scale,
- (ii) The respective significant wave heights, which are incorporated into the scale, and
- (iii) The fetch and time required for a fully developed sea at the different levels of the scale

Table 2.2: Beaufort scale with Significant Wave Heights [J Simm and Cruickshank,1998]

Beaufort Scale	Name	Wind Speed					State of Sea Surface	Wave height (Hs)	Fetch required for Fully Developed (FD) Sea		Time required for Fully Developed (FD) Sea (hrs)
		knots		m/s					km	= say	
		Min	Max	Min.	Max.	Ave					
0	Calm	< 1		0.0	to 0.2	0.1	Sea like a mirror	0.0		0	0
1	Light air	1 to 3		0.3	to 1.5	0.9	Ripples with appearance of scales; no foam crest	0.2	+/- 40	= say 40	> 8 = say 8
2	Light Breeze	4 to 6		1.6	to 3.3	2.5	Small wavelets; crests have glassy appearance but do not break	0.4	+/- 50	= say 50	> 9 = say 9
3	Gentle Breeze	7 to 10		3.4	to 5.4	4.4	Large wavelets; crests begin to break; scattered white horses	0.8	+/- 120	= say 120	> 9 = say 9
4	Moderate Breeze	11 to 16		5.5	to 7.9	6.7	Small waves, becoming larger: fairly frequent white horses	1.5	+/- 220	= say 220	> 12 = say 12
5	Fresh Breeze	17 to 21		8.0	to 10.7	9.4	Moderate waves taking longer to form; many white horses and a chance of some spray	2.0	+/- 400	= say 400	> 18 = say 18
6	Strong Breeze	22 to 27		10.8	to 13.8	12.3	Large waves forming; white foam crests extensive everywhere and spray probable	3.5	+/- 600	= say 600	> 25 = say 25
7	Moderate gale	28 to 33		13.9	to 17.1	15.5	Sea heaps up and white foam from breaking waves begins to be blown in streaks; spindrift begins to be seen	5.0	+/- 800	= say 800	> 30 = say 30
8	Fresh gale	34 to 40		17.2	to 20.7	19.0	Moderately high waves of greater length; edges of crests break into spindrift; foam is blown in well marked streaks	7.5	> 1000	= say 1000	> 35 = say 35
9	Strong gale	41 to 47		20.8	to 24.4	22.6	High waves; dense streaks of foam; sea begins to roll; spray may effect visibility	9.5	> 1000	= say 1100	> 35 = say 40
10	Whole gale	48 to 55		24.5	to 28.4	26.5	Very high waves with overhanging crests; sea surface takes on white a white appearance as foam in great batches is blown in very dense streaks; rolling of sea is heavy and visibility is reduced	12.0	> 1000	= say 1200	> 35 = say 45
11	Storm	56 to 64		28.5	to 32.7	30.6	Exceptionally high waves; sea covered with long white patches of foam; small and medium sized ships might be lost to view behind waves for long times; visibility further reduced	15.0	> 1000	= say 1300	> 35 = say 50
12	Hurricane	> 64		32.7	to 35.0	33.9	Air filled with foam and spray; sea completely white and driving spray; visibility greatly reduced	> 18.0	> 1000	= say 1500	> 35 = say 60

Details of Wind Speed, Fetch and Times required for the Full Development (FD) of the sea, which have been derived from the data in Table 2.2, have been plotted against Significant Wave Heights in Figure 2.16. Exponential trend curves have been fitted to the data for a clearer illustration the relationship between the variables.

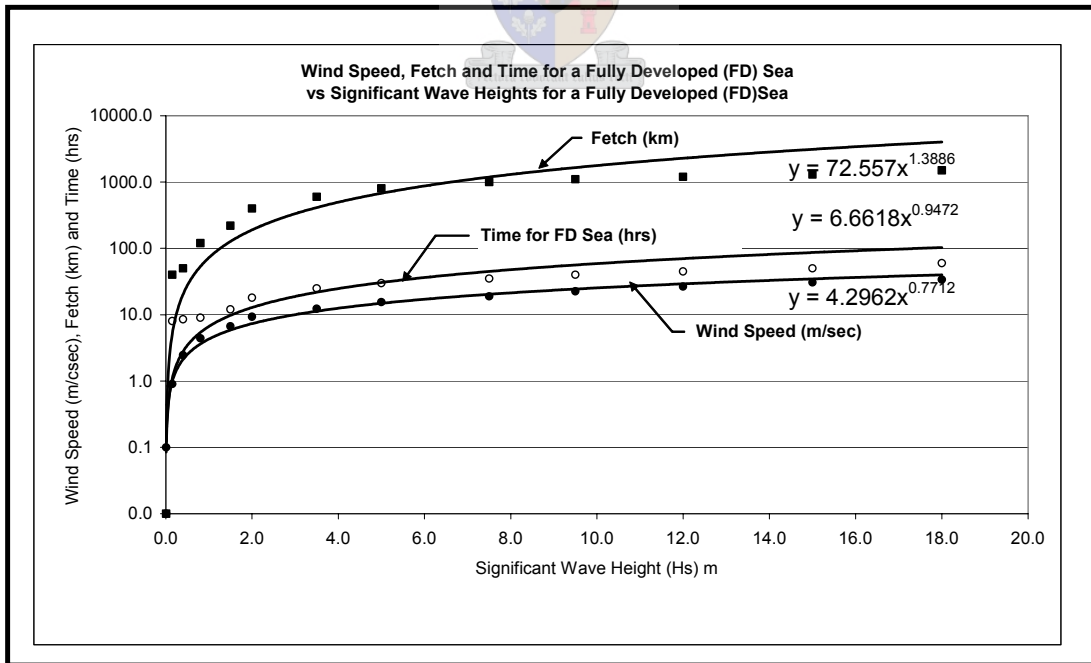


Figure 2.16. Graph showing Wind Speeds, Fetches and Times required for the Full Development (FD) of the Sea, for given Significant Wave Heights

The Coastal Engineering Manual (CEM) provides wave prediction nomograms in Chapter 2 “Meteorological and Wave Climates” of Part 11 of the Manual. These nomograms provide information on fully developed wave heights, as a function of wind speed, for both Fetch-limited and Duration-limited conditions. An initial, indicative, order of magnitude comparison of the information gained from the nomograms in the CEM and from the graphs in Figure 2.16, indicates that they correspond reasonably well. It would undoubtedly be very worthwhile to carry out a more detailed comparison of the information, but this is considered to be beyond the scope of this study.

As can be seen from the descriptions of the sea states in the Beaufort Scale, sea waves can be considered start from **ripples** and **wavelets** (described as small and large), before proceeding to **waves** (described as moderate, large and heaped) and **high waves** (described as moderately high, high, very high and exceptionally high), with the on-going transfer of energy from the wind to the sea.

The wave continuum, based on the Beaufort scale, has been shown graphically in Figure 2.17 and diagrammatically in Figure 2.18.

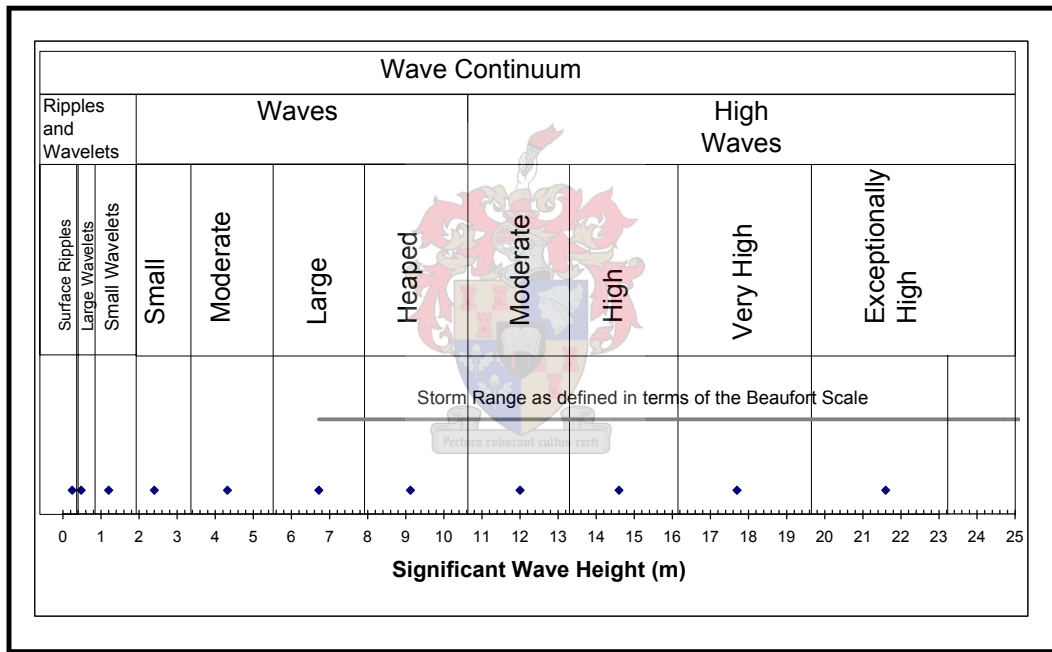


Figure 2.17. Graph showing the Significant Wave Height (Hs) and the Beaufort Scale as a function of Wind Speed

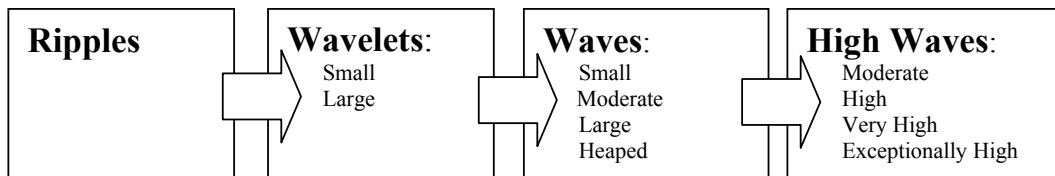


Figure 2.18: Gravity wave Continuum Diagram

2.2.2 The Wind-Wave Formation Mechanisms.

The surface water wave generation problem can be viewed as a shear flow stability problem in the presence of a flexible boundary. [Farrell et al, 2005]

Wind can be considered to be the velocity at which the air moves, that is, a strong wind corresponds to a high velocity, and vice versa. On this basis one can say the velocity at which the air moves over the water causes the waves.

The commonly observed process, of surface water wave excitation by wind, resisted comprehensive theoretical explanation for a long time due to the fact that wave growth predictions did not agree with observations.

Early theories relating to wind generated waves are reviewed in the following sections.

(a) Instability Theory

The Kelvin-Helmholtz instability theory was one of the early theories for the formation of wind-waves, but it is not generally regarded as a primary mechanism for the generation of the phenomenon. The theory assumes that Bernoulli suction, coherently 180 degrees out of phase with the surface elevation, produces exponential growth of the elevation, but the problem with the theory is that instability requires that the suction exceeds the gravitational restoring force and this would require wind speeds substantially in excess of the observed wave generating wind speeds.[Farrell et al, 2005]

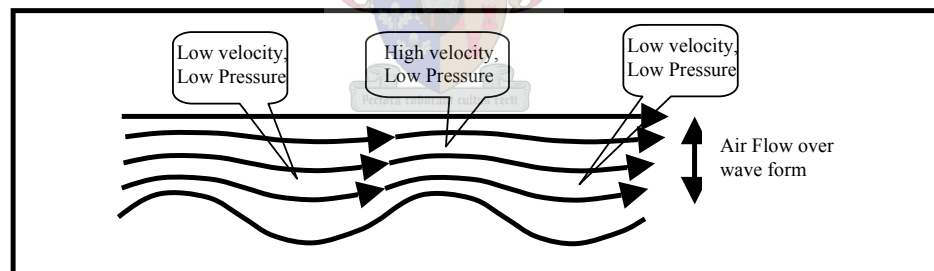


Figure 2.19. Diagram showing areas of high velocity and low-pressure over wave formation.

When two fluids of different densities overlay each other, the common boundaries are flat and horizontal at rest. If one fluid moves relative to the other, without turbulence, and the boundary is disturbed very slightly to form sea waves, the waves will grow if the relative velocity is great enough. The required velocity is that of the waves multiplied by a factor so that the longer, faster waves require a greater velocity to cause them to build. Similarly, very slow wavelets are built up by very slow movement between the fluids. [Russell,1954]

Very small waves, a few centimetres long, do not obey the laws of sea waves as they are propagated by gravity and surface tension, whereas the larger sea waves are propagated by gravity only.

Gravity causes longer waves to travel faster, whereas surface tension causes shorter waves to travel faster. The result of these actions is that longer waves and very short waves travel fast, and that intermediate waves travel at the slowest possible speeds. The particular wind, which will just build up the slowest wave is the slowest wind that will cause any waves to build up at all. The slowest wave in water has the following length and velocity [Russell, 1954]:

- A wave length of 1.69 cm (16,9 mm), and
- A velocity is 23 cm/sec (230 mm/sec or 0.23 m/sec)

The general theory, applied to any two fluids, shows that waves are built up if

the relative velocity between them exceeds $v_{crit.} = c \frac{(1+s)}{\sqrt{s}}$

Where: c = the velocity of the wave form
 s = the ratio of the densities of the fluids
 Say c = 0.23 m/sec
 ρ_a = 1.2 kg/m³
 ρ_w = 1000 kg/m³

$$\begin{aligned} \rho_a / \rho_w &= 1.2 / 1000 \\ &= 1.2 \times 10^{-3} \\ &= 0.0012 \end{aligned}$$

$$\begin{aligned} \text{Therefore } v_{crit.} &= 0.23 \times (1.0012) / \sqrt{0.0012} \\ &= 6.58 \text{ m/sec.} \end{aligned}$$

As mentioned above, this velocity is significantly greater than the observed velocity of the wind, which causes the first waves, and therefore the theoretical predictions are incorrect in the case of ocean wind-waves. [Russell, 1954]

It is apparent that the instability theory is more relevant to less dense liquids or the cases where the difference in densities between the two fluids is very much less than that between air and water.

(b) Sheltering Theory

In 1924 Jeffreys introduced a theory based on laminar and turbulent flows over the windward and leeward slopes of the waves, respectively, as shown in Figure 2.20. An eddy is assumed to exist in the air space between the water surface and the air leaving the crest. The combination of laminar and turbulent flow across the wave has the effect of applying a force to it. This force can be calculated on the basis of the area of the wave that offers resistance to the wind, and working backwards from the observed minimum velocities, Jeffreys calculated that the percentage of height that offered resistance to the wind was about 27% of the total wave height. He called this percentage the "Sheltering Coefficient" as it reflected the height of the wave that sheltered the next wave.

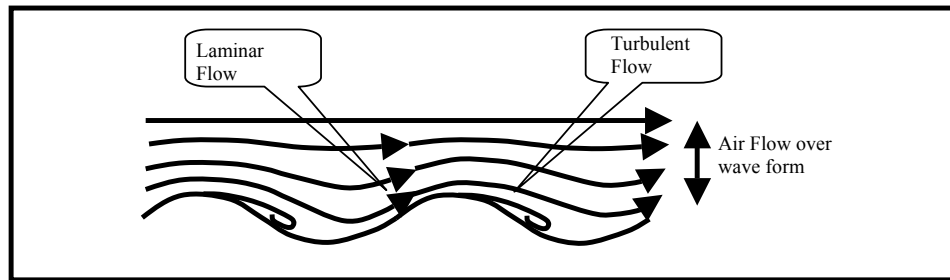


Figure 2.20. Diagram showing areas of Laminar and Turbulent Flow over a waveform

Jeffreys theory does not state that the height of a rigid wave form, which offers resistance to the wind, is 27% of the total height of the wave. It says that 27% of the height of a modulating flow pattern, which is moving backwards relative to the direction of the wind, at a speed of the waveform, will offer resistance to the wind.

The theory of sheltering is most satisfactory in its explanation of the behaviour of initial waves. A sheltering coefficient, " s_c " equal to 27% of the wave height is found to be applicable for the slowest wind velocity of 1.1m/sec. In this case the velocity and length of the first waves are found to be 37 cm/sec and 8 cm respectively. These values are reasonable when compared to observations. The theory can be used to predict that a gust of wind disturbing the water will generate slow and faster waves, which are parallel and long crested at right angles to the wind, but it does not account for the fact that other waves are generated at the same time [Russell, 1954]. A gust of wind that is stronger than the critical wind speed will generate waves of many lengths, some longer and some shorter than 8 cm, and they will all exist at the same time in a short crested wave field.

The Theory of sheltering is adequate for the initial formation of waves, but it fails when applied to their later development and in the calculation of frictional drag between the wind and the water.

(c) Rough Turbulent Theory

Jeffrey's theory only considers the relative velocity between the waves and the wind, and it does not consider the differential movement of the wind relative to the water. If one considered the relative movement between to actual water particles and the wind, the flow pattern would be completely different as the wind shear could be considered to drag the surface water molecules along, forcing them to build up at the peak of the wave, where they could either be separated from the body of the water in the high velocity and highly turbulent wind, or the could roll over and collapse down the leeward face of the wave, as shown diagrammatically in Figure 2.21.

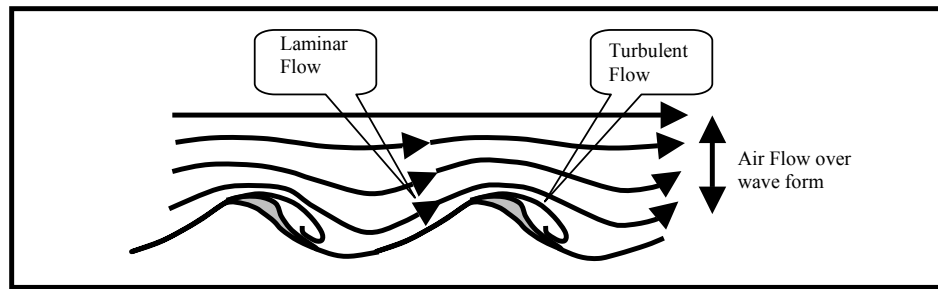


Figure 2.21. Diagram showing areas of Laminar and Turbulent flow over a waveform, and possible changes in waveform shape, due to relative movement between water molecules and the wind.

The collapsing water molecules described above could be considered to cause the parasitic capillary waves, commonly viewed on the leeward side of wavelets and shown in Figure 2.22.

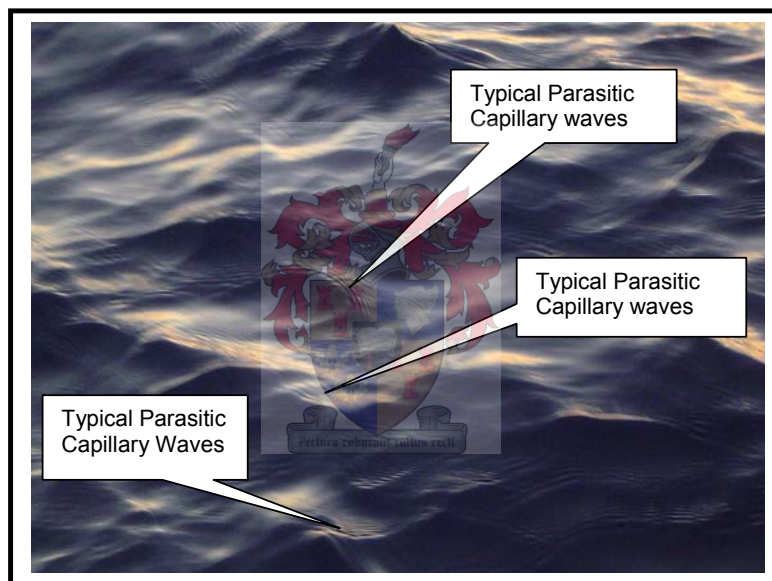


Figure 2.22. View of parasitic capillary waves on the leeward side of wavelets

Sverdrup and Munk (1947) proposed that the generation of waves is caused by a combination of the following mechanisms:

- Partial pressure on the wave form as in the sheltering theory, and
- Partial shear of the wave particles themselves by tangential stresses

In the application of this theory a much smaller sheltering coefficient of 1.35% is used. Munk (1947) also proposed that the tangential stress, or wind drag, varied with the square of the wind speed **so long as the wind speed exceeded 7.0m/sec**. The theory is therefore based, to all intents and purposes on the laws of turbulent flow over (a) rough plane.

The rate at which waves acquire energy is simply the uniform tangential stress multiplied by the rate at which the surface particles progress forwards. A corollary of

this is that, if there were no forward progression at the surface, tangential stress would not build up the wave height.

Sea waves, which are moving slower than the wind, receive energy from the wind principally by means of tangential stress, through either friction or turbulence mechanisms, while waves, which move faster than the wind, receive their energy in the same way but it is transferred back to the air by the push of the wave form on the air in front of it. [Russell, 1954]

Other wave dissipation processes include:

- (i) Turbulence, which appears as heat
- (ii) Whitecapping
- (iii) Depth-induced wave breaking
- (iv) Bottom Friction
- (v) Non-linear wave-wave interactions (quadruplets and triads in deep water and shallow water, respectively).

It is worth noting that the non-linear interactions referred to above relate to the wave-wave interactions that dominate the evolution of the wave spectrum. In deep water quadruplets wave-wave interactions transfer wave energy from the spectral peak to lower frequencies (thus moving the peak frequency to lower values) and from the spectral peak to higher frequencies, where the energy is dissipated by whitecapping. In very shallow water triad wave-wave interactions transfer energy from lower to higher frequencies. [SWAN Manual, version 40.51 August 2006]

2.2.3 Momentum Transfer at the air-sea interface.

Momentum is transferred from the air to the sea by a frictional force known as drag. Drag resists differential movement between the media, and the amount of frictional force per unit surface contact area, which is called shear stress, τ , is felt by both of the media, which are sliding against each other.

The air within the Atmospheric Boundary Layer (ABL), which comprises the lower 2.0 km of the Troposphere, can be considered to comprise a stack of layers of air. In this case each layer of air would feel shear stress from the layers above and below it. Over the sea, the bottom layer would feel shear stress from the sea below and from the layer of air above. In turn the surface tends to be pushed along by air drag. This wind shear stress causes waves in the sea and drives ocean currents.

In the atmosphere, shear stress caused by turbulent motions is many orders of magnitude greater than that caused by molecular viscosity, and for this reason it generally called turbulent shear rather than frictional shear, and turbulent drag, rather than frictional drag. This turbulent shear is also called Reynolds Stress.

It is often easier to study the shear stress in a fluid per unit density, ρ , of the fluid, whether it be water, ρ_w , or air, ρ_a , respectively. In this case one refers to the stress as a "kinematic stress".

The kinematic stress against the sea surface is given by the symbol u^{*2} , where u^* is called the friction velocity:

$$u^{*2} = |\tau / \rho|$$

Typical values of u^* range from 0 m/sec for no wind to 0.5 m/sec and 1,0 m/sec during moderate and strong winds, respectively.

Turbulent Stress in fluid flow is proportional to wind speed squared, and it is greater over rougher surfaces. A dimensionless drag coefficient C_D relates the shear velocity to the wind speed, u_{10} , at a height of 10 m, as follows:

$$u^{*2} = C_D \times u_{10}^2$$

The surface roughness is usually quantified as an aerodynamic roughness length z_0 , which is completely independent of the heights of the roughness elements, which has a typical value for sea of $z_0 = 0.0002$ m [RB Stull, 2000]

The relationship between the drag coefficient C_D and the roughness length z_0 , for statically neutral air is given by:

$$C_D = \frac{k^2}{\ln^2(Z_R / z_0)} \quad \text{[RB Stull, 2000]}$$

Where:

- $k = 0.4$ is the von Karmen constant, and
- $Z_R = 10$ m is the reference height for the wind speed, and
- $Z_0 =$ the roughness length

Give the above C_D for the open sea is typically 1.37×10^{-3}

Drag Coefficients, which have been averaged over many observations in the open ocean at high and low wind speeds, and corrected for buoyancy effects to neutral values, CD_n , have been given in Figures 2.23 and 2.24. [GT Csanady, 2001].

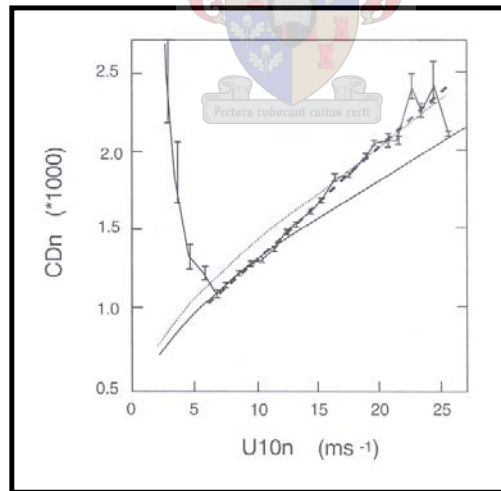


Figure 2.23: Observed Drag Coefficients in the open sea for varying wind Speeds above 6.0 m/sec. [Csanady,2001]

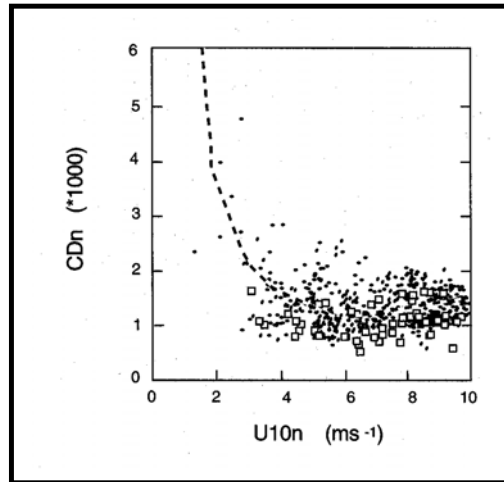


Figure 2.24: Observed Drag Coefficients in the open sea for low wind speeds [Csanady, 2001]

2.2.4 Laboratory Studies on Capillary Waves and Ripples

Laboratory observations, on the formation of capillary waves and ripples, give some insight into the water surface-wind interaction mechanisms in the wave formation process. The following laboratory observations by different authors are useful and are presented below.

It is very difficult to carry out field observations of capillary waves and ripples due to their highly irregular nature and the presence of sea waves. It is easier to observe capillary waves and ripples in the laboratory, but cognisance must be taken of the fact that the range of short waves in a wind sea starts near frequency of $\omega = 10$ radians/sec., where the celerity and wave length of a gravity wave are near 1.0 m/sec and 60 cm respectively. Shorter wind waves in the natural sea are generally three dimensional and short lived. This is not the case in the laboratory where shorter wind waves, in the order of 10 cm., can be produced with regular and parallel crests due largely to shorter fetches. Notwithstanding this problem, laboratory observations of wind waves have provided researchers with valuable information. [Csanady,2001]

The initial waves in the laboratory are short and regular, but they are unstable and they break down into chaotic wind sea and internal turbulence within 10 seconds or so. Eventually a statistically steady state, comprising short sharp-crested characteristic waves, emerges. [Csanady, 2001] Characteristic Waves in this case can be defined in terms of their phase velocity, C_p , which is equal to $\sqrt{g/k_p}$, where g is the acceleration of the gravity, and k_p is the wave number, $2\pi/L$, at the peak of the spectrum.

In a co-ordinate system, which moves with the waves, the airflow smoothly follows the undulating surface-over the waves with the lower steepness. On the other hand, the air flow separates near the crest of the steeper waves, and a “separation bubble”, comprising trapped, slowly circulating air, forms downwind of the crest as shown in Figure 2.25. A layer of high shear stress, which arches over towards the next crest, separates the bubble from the free stream above, as shown in the figure. The airflow re-attaches at the next crest so that the separation bubble occupies close to a full wavelength, with the exact length varying from one steep wave to another. The re-

attachment streamlines bends upward fairly sharply where they reach the water surface, as demonstrated by Banner and Peirson (1997), [GT Csanady, 2001]

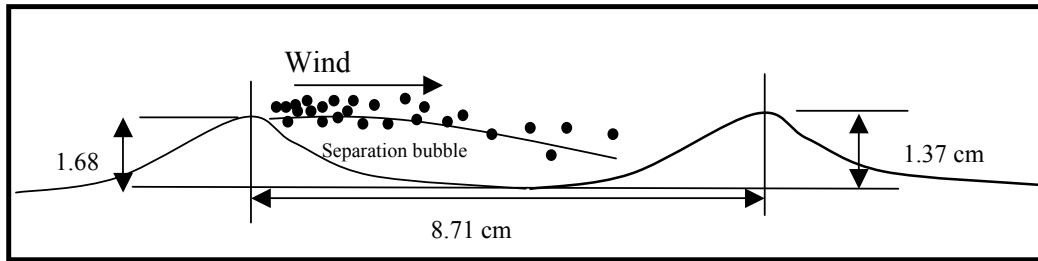


Figure 2.25: Location of the high shear layer at the outer edge of the separation bubble on a steep laboratory wave [Csanady,2001]

In addition to the mean flow pattern, described above, there is also typically a system of large eddies attached to the waves. The dimension of the eddies are of the same order of magnitude as the length of the wave and they span the entire shear flow boundary layer [Kawamura and Toba, 1988].

The eddies generate “bursts” of slow fluid upward, alternating with “sweeps” of fast fluid downward as shown in Figure 2.26. The bursts are associated with the wave crests and the sweeps with the troughs. Kawamura and Toba offer the conceptual model of the separation bubble being drained by the air flow as the steep wave originating it decays, an event they call a “big burst”. The slow fluid is displaced over the downwind crest by the wind, and the void behind it is filled by a sweep of fast moving fluid.

The net horizontal force on the wave consists of viscous shear stress and pressure force acting on the inclined surface of the wave.

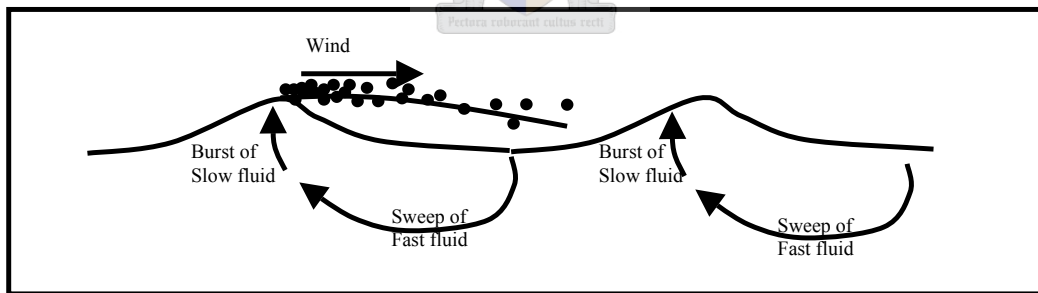


Figure 2.26: Conceptual model of Burst and Sweep flows around the Separation Bubble

The flow pattern on the air side of the steeper waves explains how forces on the windward side become as large as they do where the air flow re-attaches itself to the water surface downwind of the separation bubble. At this point the shears are intense with the shear boundary layer being very thin and with the wind velocity, outside the boundary layer, having high stream flow values. The pressure on the waves is high because the waveform has to re-direct the free shear layer through an angle of θ , which is of the order of the wave steepness. A simple conceptual model of this phenomenon is a two dimensional jet, with thickness equal to the amplitude of

the wave, impinging on the inclined solid surface of the water downstream of the separation bubble as shown in Figure 2.27.

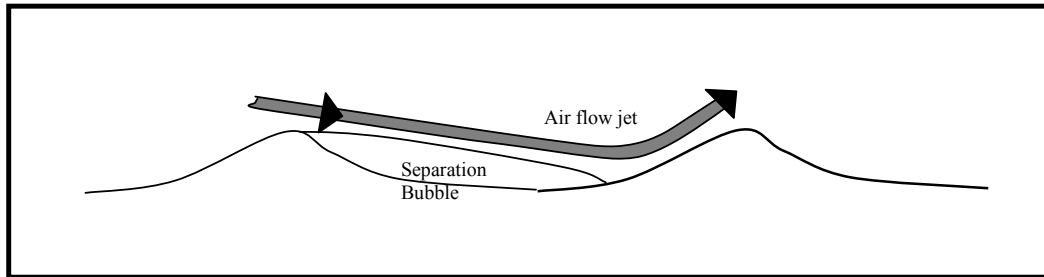


Figure 2.27: Diagram of Airflow jet reattachment downstream of a separation bubble [Csanady, 2001]

2.2.5 Sea Waves Climates

(a) General

Wave Climates are generally defined in terms of the following criteria:

- (i) Wave Height
- (ii) Wave Period, and
- (iii) Wave Direction

Wind generated sea waves are complex and incorporate many superimposed combinations of wave heights, periods and directions. If a sea state is recorded during a storm then the resulting time series will consist of random periodic fluctuations [Reeve et al, 2004]

Time series data can be analysed in either the Time Domain or the Frequency Domain, and an overview of both of these approaches is given below as background to sea state profiles which comprise the storm profiles discussed later in the study

(b) Time Domain Analysis

Wave data is normally recorded at a frequency of 2Hz for a period of 20 minutes and a typical record, made in this way by a Waverider Buoy off Slangkop, has been given in Figure 2.28.

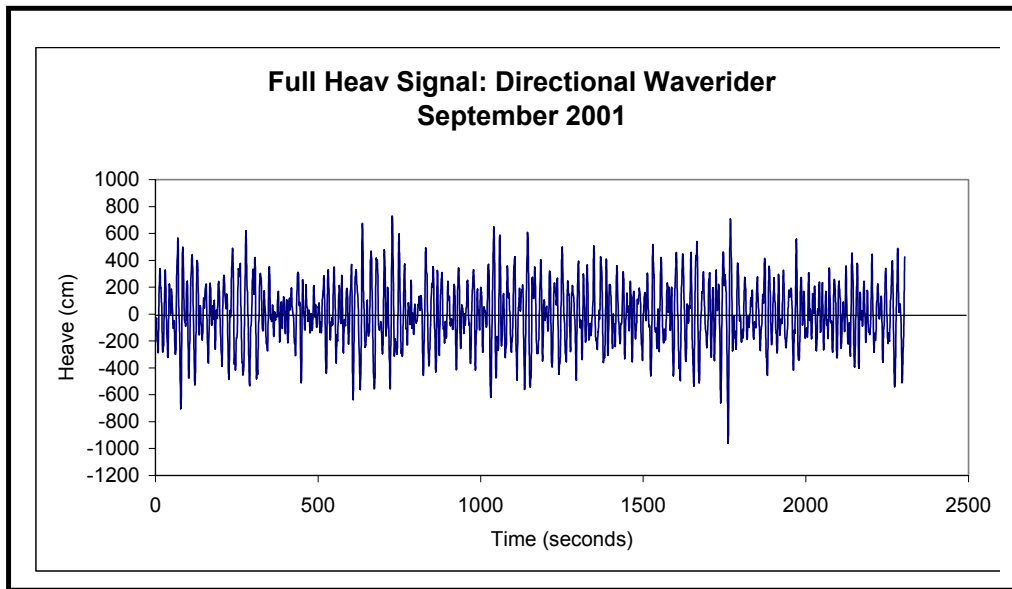


Figure 2.28: Typical 20 minute Wave Data Record off Slangkop [CSIR, 2001]

A detailed section of the above Time Series Wave Profile has been shown in Figure 2.29 below for information

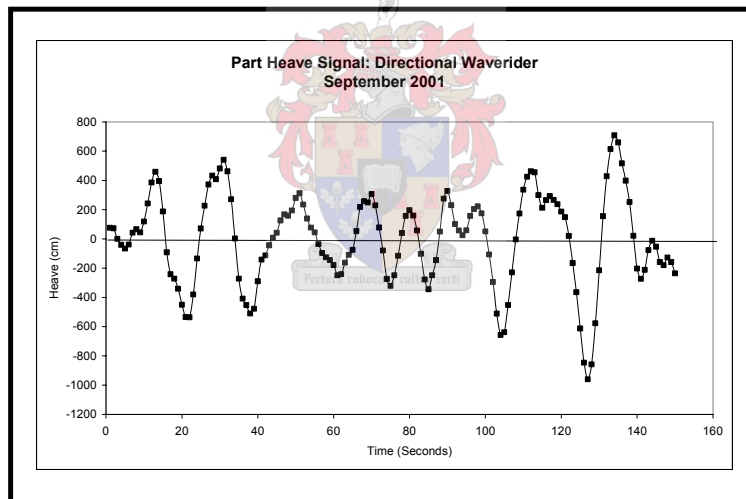


Figure 2.29: Section of Typical Time Series Wave Profile [CSIR,2001]

Most recorded wave data comes from observations of sea surface elevations above and below a fixed equilibrium level, as a time series, $\eta(t)$, at a fixed location. The standard deviation, σ , and the variance, σ^2 , of the displacements can be calculated in the normal way, and the significant wave height, H_s , is taken to be equal to $4\sqrt{\sigma^2}$.

Another important characteristic of a stationary random process in the time domain is its autocorrelation, which measures the time lag (t) over which surface elevations remain related. The autocorrelation function is defined, in this instance as $Z(t) = \overline{\eta(t_0)\eta(t_0 + t)}$ where the overbar represents the average value, and t is the lag time.

A typical auto-covariance function of the time series is shown in Figure 2.30 (a) and the peak period T_p of the series, which is equal to the lag from the beginning to the first peak, can be read off the curve.

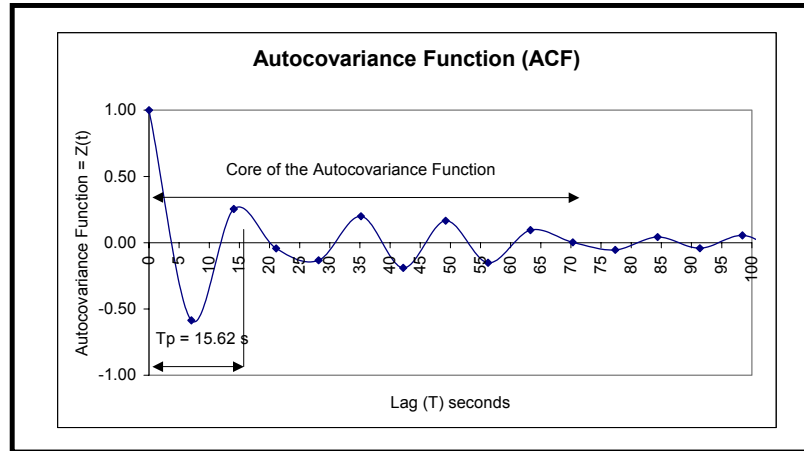


Figure 2.30(a): Typical Auto-covariance Functions of the Time Series Data

An observer of the sea will perceive dominant waves of much the same period passing a fixed location. The envelope of peaks decays on a time scale of some 4 to 5 periods, as shown in the typical normalised autocovariance function Figure 2.30 (b) for the same sample as discussed above, and this is a measure of individual wave persistence.

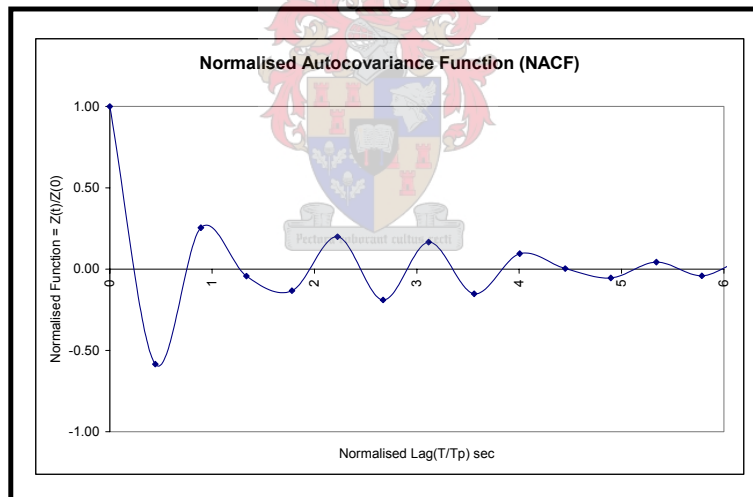


Figure 2.30 (b): Normalised Autocovariance Functions of the Time Series Data

(b) Frequency Domain Analysis

The significant wave height and peak period of a wave series can also be calculated from the wave spectrum, which is derived by using Fourier Series Transform methods. A typical wave spectrum for the Cape Point (Slangkop) wave time series given in Figure 2.28 is given in Figure 2.31.

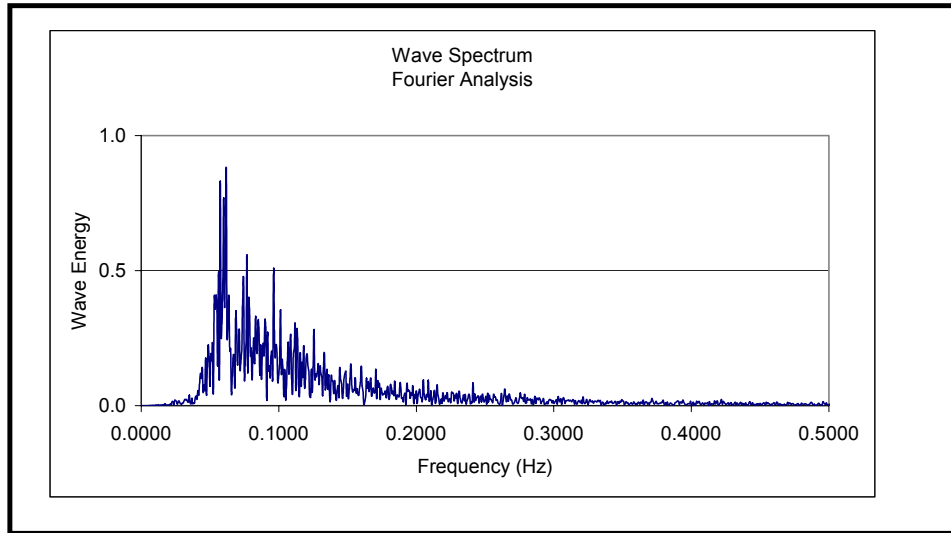


Figure 2.31: Typical Wave Spectrum, $S(f)$, showing Energy as a function of Frequency.

The significant wave height, H_{m0} , is equal to $4\sqrt{m_0}$, where m_0 is the zeroth moment equal to $\int_0^{\infty} S(f)df$, and the peak period (T_p), is the frequency with the maximum energy in the spectrum.

2.2.6 Wave Forecasting Models

The theoretical explanations, for the phenomenon of surface water wave generation, generally involve either of the following mechanisms:

- **Wave Incoherent Stochastic Forcing by random atmospheric pressure fluctuations** (Eckart 1953;Phillips 1957), or
- **Wave Coherent Forcing by wave induced atmospheric pressure fluctuations proportional to wave amplitude** (Helmholtz 1868; Kelvin 1871; Jeffreys 1925,1926, Munk 1947;Miles 1957, 1959) [Farrell et al, 2005]

The growth rate forms, but not the actual rates predicted by the above mechanisms, were incorporated together with a parameterisation of nonlinear interactions into a general prediction equation [Hasselmann, 1960]. Various empirical versions of this prediction equation were used for operational wave forecasting purposes (WAMDI, 1988).

These predictions equations incorporated the following:

- (i) a variance growth linear in time, to account for incoherent forcing unrelated to wave amplitude, and
- (ii) a variance growth exponential with time, to account for coherent forcing proportional to wave amplitude

Exponential growth rates, proceeding from coherent forcing and proportional to wave amplitude, are generally thought to be necessary to account for observed rapid rates of wave development [Farrell et al, 2005].

The well known numerical wave model SWAN (acronym for **S**imulating **W**aves **N**earshore) describes the evolution of the wave spectrum by the spectral action balance equation, which for the non-stationary mode in Cartesian co-ordinates is [SWAN, 2006] :

$$\frac{\partial}{\partial t} N + \frac{\partial}{\partial x} c_x N + \frac{\partial}{\partial y} c_y N + \frac{\partial}{\partial \sigma} c_\sigma N + \frac{\partial}{\partial \theta} c_\theta N = \frac{S(\sigma, \theta)}{\sigma}$$

The first term on the left hand side of this equation represents the rate of change of action density in time, the second and third terms represent propagation of action in geographic space (with velocities c_x and c_y in x- and y- space respectively). The fourth term represents shifting of the relative frequency due to variations in depth and currents (with propagation velocities c_σ in σ -space). The fifth term represents depth induced and current induced refraction (with propagation velocity c_θ in θ -space)

The term $S(\sigma, \theta)$ on the right hand side of the equation of the action balance equation is the source term, in terms of energy density, representing the effects of generation, dissipation, and non-linear wave-wave inter-actions):

$$S(\sigma, \theta) = S_{in}(\sigma, \theta) + S_{ds}(\sigma, \theta) + S_{nl}(\sigma, \theta)$$

The term $S_{in}(\sigma, \theta)$ in the above equation represents the generation of wave energy by wind, and models the transformation of the kinetic energy of a wind field into water wave energy and includes two terms depending on wave frequency and direction (A), and wind speed and direction (B):

$$S_{in}(\sigma, \theta) = A + B E(\sigma, \theta)$$

The expression in the term A is due to Cavaleri and Malanotte-Rizzoli [1981] with a filter to avoid growth frequencies lower than the Pierson-Moskowitz frequency [SWAN, 2006].

Two optional expressions for the coefficient B are used in the model. The first is taken from an early version of the WAM model (known as WAM Cycle 3, the WAMDI Group, 1988). This expression was originally developed by Snyder et al (1981) and it was later rescaled in terms of friction velocity, u^* , by Komen et al (1984). The drag coefficient in the expression is taken from Wu (1982) and it relates to u^* and to the driving wind speed at 10 m elevation u_{10} . The second expression for B in SWAN is taken from the most recent version of the WAM model (known as WAM Cycle 3, Komen et al 1994). This version was developed by Janssen (1991a) and it accounts for the interaction between the wind and the waves by considering the boundary layer effects and the roughness length of the sea surface.

2.3 Wave Climates

Significant patterns, or environments, of long-term sea states, which constitute wave climates, can be identified globally. Wave climates are generally associated with dominant and prevailing wind conditions, which either exist in the area, or directly impact on the area, from outside of it.

2.3.1 Major Wind Belts

The Major Wind Belts arising from the Global Weather System Components shown in Figure 2.1, and the Tri-cellular model of Atmospheric Circulation shown in Figure 2.3, have been given in Table 2.3 and are shown diagrammatically in Figure 2.32.

Table 2.3: Major Wind Belts of the World

Hemisphere	Latitude	Wind Belt
Northern Hemisphere	60° to 90° N	Polar Easterlies
	30° to 60° N	Prevailing Westerlies in the Temperate Latitudes
	0° to 30° N	North East Trade Winds
Southern Hemisphere	0° to 30° S	South East Trade Winds
	30° to 60° S	Prevailing Westerlies in the Temperate Latitudes
	60° to 90° S	Polar Easterlies

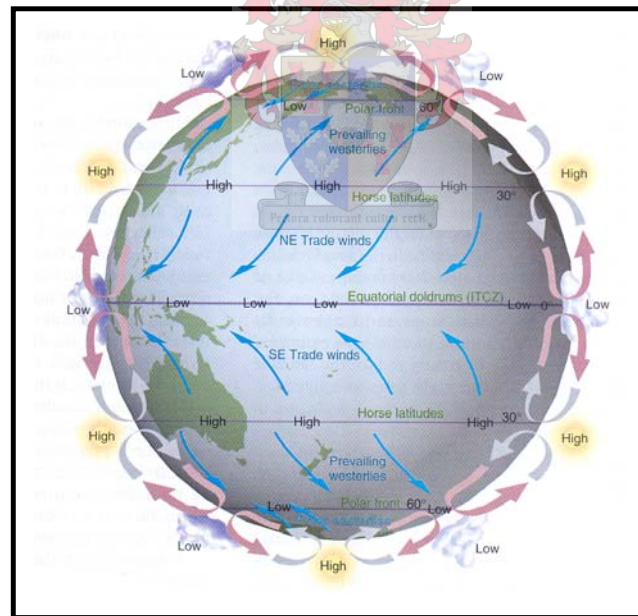


Figure 2.32: Major Wind Belts of the World [Thurman et al, 2002]

The masses of air that move across the earth’s surface from the high-pressure subtropical belts towards the equatorial low-pressure belt are known as the trade winds. If the earth did not rotate these winds would blow in a North-South Direction. In the Northern Hemisphere they curve to the right, and in the Southern Hemisphere they curve toward the left as the result of the Coriolis effect.

Some of the air that descends in the sub-tropical regions moves along the earth's surface to the higher latitudes as the prevailing Westerlies. Because of the Coriolis effect the westerlies blow from the south-west to the north-east in the Northern Hemisphere and from the north-west to the south-east in the Southern Hemisphere.

In addition to the above, air also moves away from the high-pressure polar areas to the lower latitudes, producing polar easterly wind belts [HV Thurman et al, 2002].

2.3.2 Major Wave Climates

The major wind belts and ocean climates cause the major wave climates, which have been identified globally [Woodroffe, 2002].

The largest waves are associated with the gale force winds of the sub-polar and temperate ocean climate regions. These winds are characterised by the occurrence of westerly winds and frontal activity. In the Southern Hemisphere, and particularly in the Southern Ocean, they occur in the latitudes around 60° S, and in the Northern Hemisphere they occur in the “roaring forties”, 40-60°N.

The trade wind belt is characterised by strong persistent winds, which maintain swells, in the sub-tropical and tropical ocean climate regions but which are generally rare in the doldrums of the equatorial ocean climate region.

Tropical cyclones, called Hurricanes and Typhoons in the Atlantic and Asia respectively, are significant influences on many tropical coasts but do not occur in the region 5°N – 5°S of the equator

Five broad wave environments have been recognised by Davies (1980). These are: -

- (i) Storm Wave Environments
- (ii) West Coast Swell Environments
- (iii) East Coast Swell Environments, with local wave generation and occasional tropical storms
- (iv) Monsoon Influence Environments, and
- (v) Protected or Sheltered Sea Environments

Storm Wave Environments occur where gales generate short, high-energy waves of varying direction. **West Coast Swell** occurs on coasts experiencing low long swell waves of consistent direction, but rarely experiencing storms,. **East Coast Swell** consists of rather weaker swell, amplified by local wave generation (as in the Tasman and Coral Seas off the coast of Australia), and occasional tropical storms. Areas of **Monsoon Influence** experience a reversal of principal wind and wave directions during the year. **Protected Seas** are large water bodies in which wave generation is local rather than swells from large ocean bodies [Woodroffe, 2002]. The aforementioned broad wave zones are shown in Figure 2.33, and it could be expected that the zones would vary as the seasons vary in the different hemispheres.

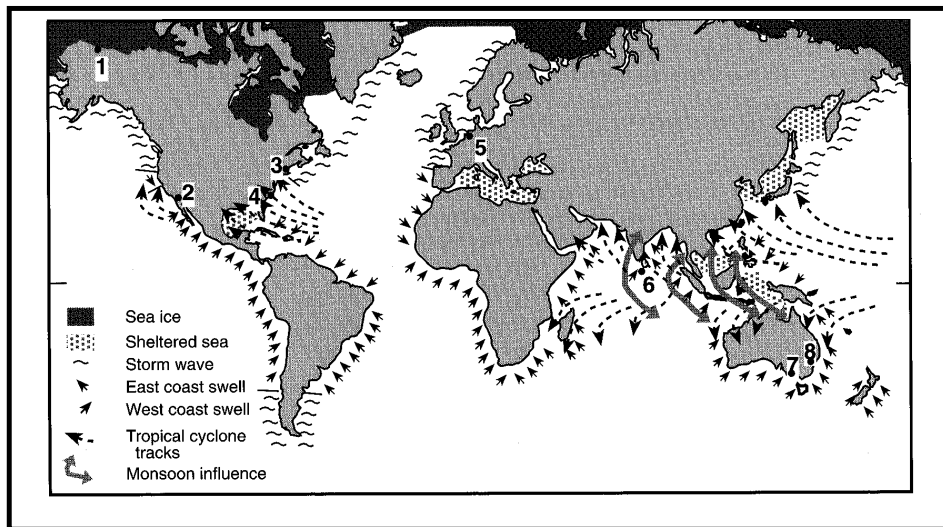


Figure 2.33: Major Wave Climates of World Coasts [Woodroffe, 2002]

2.3.3 South African Wind-Wave Climates

Having considered the above major wind-wave climates, and having reviewed the local weather conditions around the South African Coastline, which experiences a northward shift of the Southern Atlantic and Indian Ocean Anticyclones on some 6° in winter (refer to section 2.1.4), we propose that the major wave climate map prepared by Davies should be modified for the South African Coastline as shown in Figure 2.34. A similar modification to South America, Australia and New Zealand would also probably be appropriate in the Southern Hemisphere.

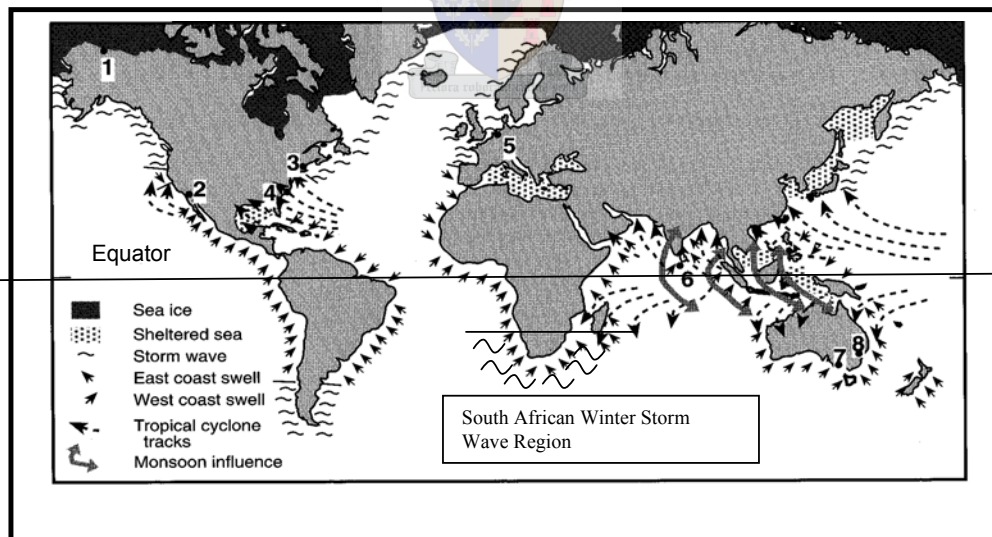


Figure 2.34: Modified Major Wave Climates of South African Coast [Woodroffe, 2002, modified]

2.4 South African Ocean Currents

Ocean currents can either reinforce or oppose sea waves in their direction of travel. These reinforcing or opposing actions can significantly affect the heights and other characteristics of the sea waves, and it is for this reason that a general overview of the currents around the South African coastline has been given in the following text for background information. A detailed study of wave-current interactions is considered to be beyond the scope of the study

2.4.1 General

It is not uncommon for waves, which are generated by the wind, to intercept currents. The interaction of waves and currents, not only change the characteristics of the waves, but at the same time they can also transform the current flow field. To evaluate the problem, one can employ one of the following approaches [Li, 1990]

- **The conservation of mass transport**, which determines the mean velocity of the current profile
- **The conservation of wave number, or the conservation of wave crest**, which determines the transformation of wave celerity, wave number or wave frequency
- **The conservation of wave energy flux or the conservation of wave action flux**, which allows calculations of wave height transformation

A detailed study of wind-wave and offshore ocean current interaction is considered to be beyond the scope of this research, however, general details relating to very large (freak) waves that occur in the area off East London have been given in Appendix A for completeness. The following text on offshore ocean currents has been included as general background for this thesis, which is based on the analysis of inshore recorded wave data.

The dominant ocean currents around the coast of South Africa comprise the following ones, which have been shown diagrammatically in Figure 2.35:

- (i) The Agulhas Current
- (ii) The South Atlantic Current (or Antarctic Circumpolar Current as it is referred to in Figure 2.35), and
- (iii) The Benguela Current

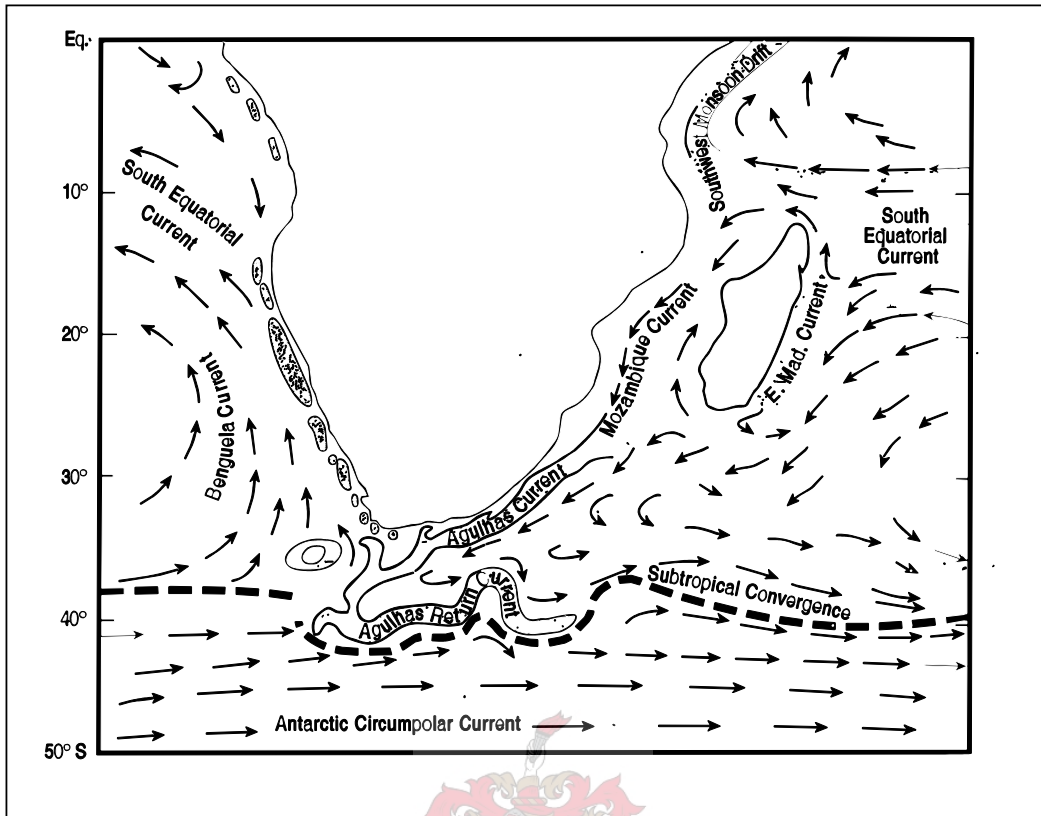


Figure 2.35: Diagrammatic layout of Dominant Ocean currents around South Africa. (The shaded areas off the west coast represent cells of upwelling of cold water in the Benguela upwelling system). [Thyson et al, 2000]

2.4.2 The Agulhas Current and Counter Current [J K Mallory, 1974]

The Agulhas Current sweeps down South Africa's southeast coast. It has its origin in the trade wind area of the Central Indian Ocean where the surface drift is known as the South Equatorial Current. This drift current impinges on the east coast of Madagascar and the coast of Mozambique, forming two stream currents, one flowing southwards down the coast of Madagascar and the other along the Mozambique coast. On reaching the southern extremity of Madagascar, the current veers across the Mozambique Channel towards the coast of Natal where it meets the Mozambique Current between Durnford Point and Durban and then flows southwards as a large oceanic river, the Agulhas Current, as shown in Figure 2.36.

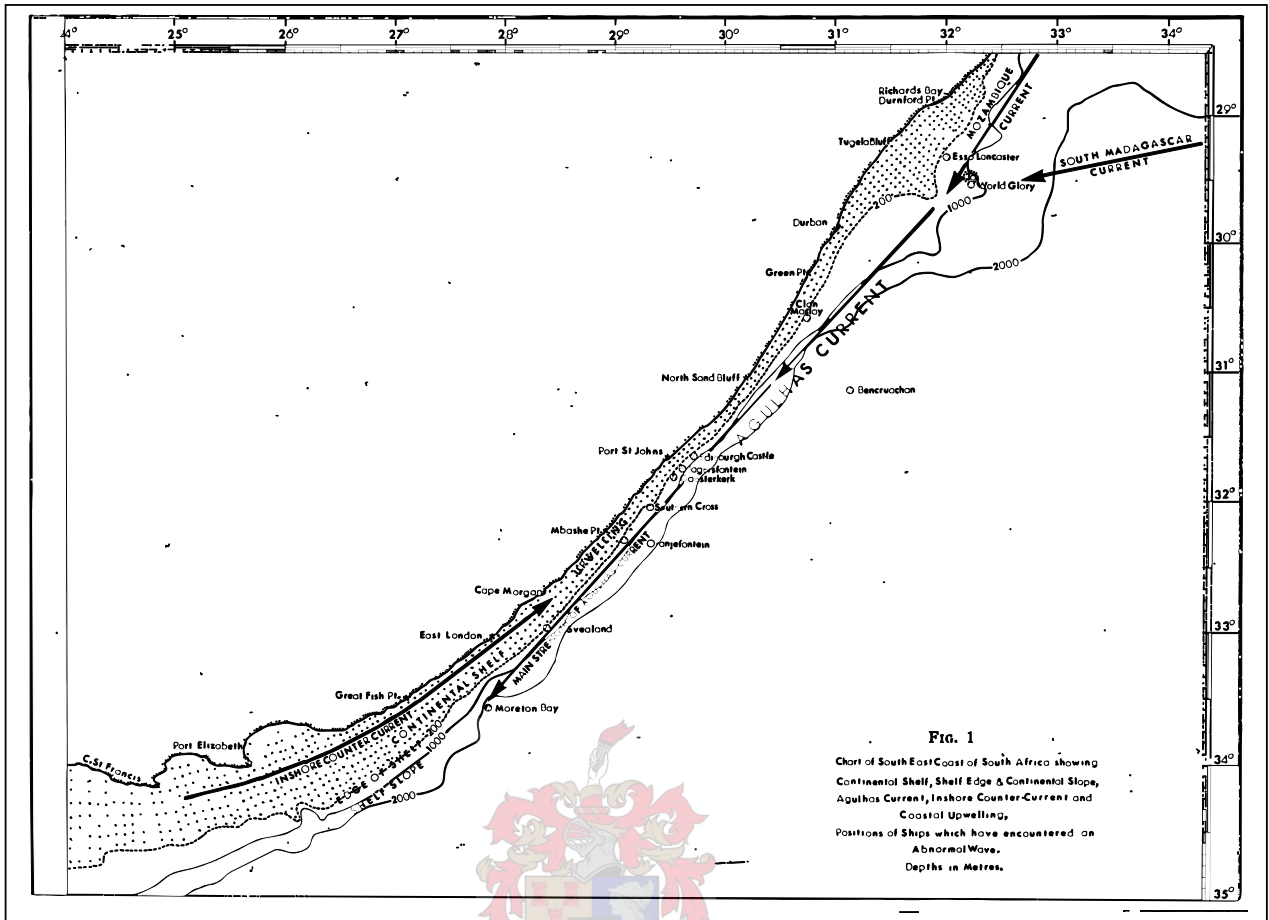


Figure 2.36: Layout showing the Agulhas current in the East Coast Swell Region [Mallory, 1974]

The course of this “river” is greatly influenced by the submarine topography due to the depth to which the core of the current penetrates, i.e. over 305 m. The main core of the current is, generally speaking, confined to the seaward side of the continental shelf because it runs deeper than the edge of the continental shelf and because the shelf slope is so steep in the area between Durban and East London. Given this situation and the fact that the current is a western boundary current, it attains its maximum velocity just seawards of this shelf edge where speeds of 4 to 5 knots are experienced between Port St. Johns and East London. The current is strongest during the southern summer and autumn when the NE Monsoon is blowing in the Arabian Sea ensuring a maximum flow through the Mozambique Channel. The width of the Agulhas Current varies from 90 km to 165 km.

The Agulhas Current continues to flow in a South Westerly direction beyond Port Elizabeth, but it changes characteristics with a divergence from the coast and the onset of downstream meanders between its main direction of flow and the coast. This situation changes beyond the Agulhas Bank where the current retroflects, under the influence of the eastward flowing South Atlantic current, to meander in an eastward direction as the Agulhas return current. This situation is shown diagrammatically in Figure 2.37.

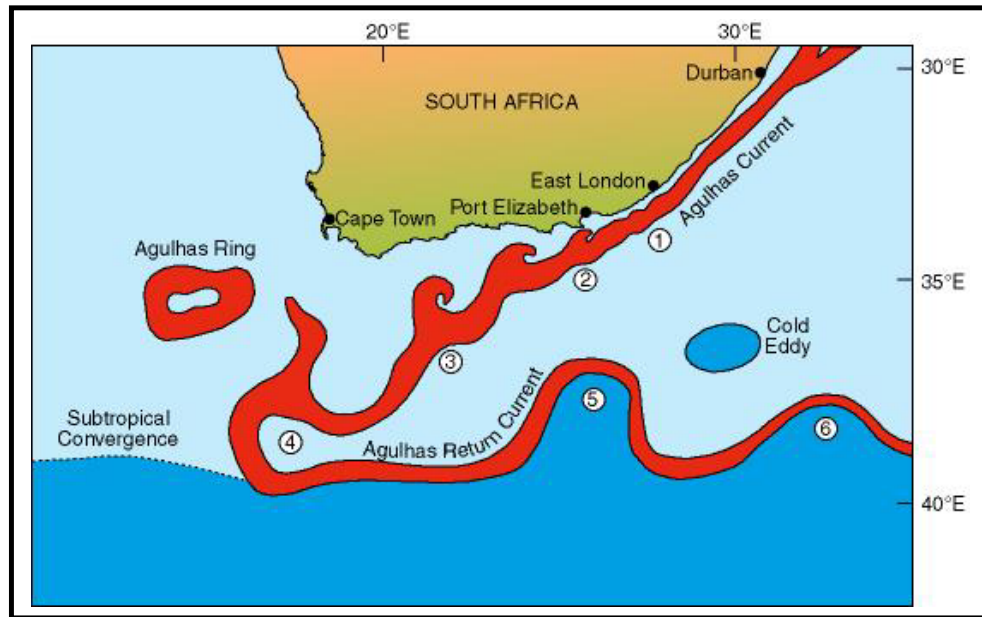


Figure 2.37: Large Scale circulation of the Agulhas Current system, showing (1) the end of the narrow current channel; (2) the divergence of the current axis from the coast; (3) the downstream meanders; (4) the retroflexion of the current; (5) and (6) the downstream meanders of the Agulhas Return Current (Diagram reproduced and altered from Boebel et al., 2003) [Lutjeharms and van Ballegooyen, 1984]

A satellite image of the retroflexion is shown in Figure 2.38.

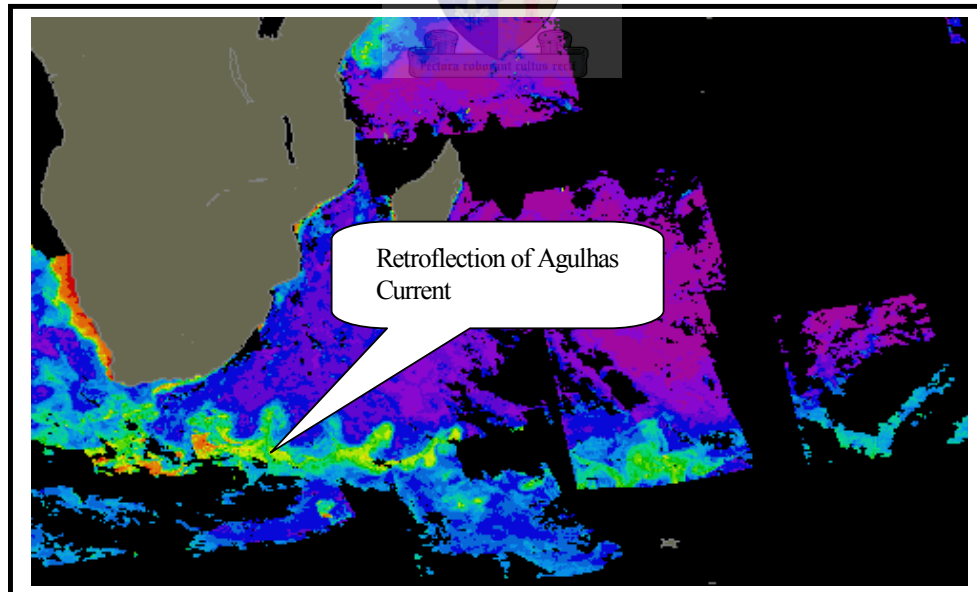


Figure 2.38: Satellite image of Agulhas Retroflexion

According to Mallory (1974) the Agulhas current is associated with an inshore counter current, which is caused by the passage of a cold front along the southern and eastern coastline and which flows in an easterly to north easterly direction at about 1 to 2 knots, as shown in Figure 2.36. This counter current flows close inshore, within about 3 to 4 miles of the coast and hence inside the southward flowing Agulhas Current. It begins to flow about six hours prior to the passage of the cold front and is probably caused by a combination of the wind-driven surface current, an ingress of the West Wind Drift, a retroreflection of the Agulhas Current south of Mossel Bay and a gradient current due to the lowering of the atmospheric pressure as the depression moves eastwards, and hence the raising of mean sea level.

One other feature on this coast has to be noted. Prior to the passage of a cold front, the wind on the coast is usually from the ENE to NE with a force of 6 to 7 for 24 hours or more. This wind acts on the surface water on the continental shelf which, being subject to Coriolis force, moves away from the coast, resulting in upwelling occurring close inshore. At the same time sea level in the vicinity of the 100-fathom (200 m) line is raised thus creating a gradient, which tends to increase the velocity of the Agulhas Current along the edge of the continental shelf [Mallory, 1974].

2.4.3 The South Atlantic Current [Boebel et al, 1998]

The near surface South Atlantic Current (SAC) flows eastward across the Atlantic at approximately 40°S. Situated near or at the Subtropical Convergence, it represents the southern rim of the subtropical circular current system. The deep SAC feeds into the Cape Basin from the southwest after crossing the Mid-Atlantic Ridge. Close to the prime meridian the SAC probably divides (Garzoli and Gordon, 1996) into an eastward branch and a northward branch. The northward branch is believed to supply the re-circulation of the anticyclonic subtropical circulation, but the transport in either branch is not known. The eastward flow passes to the south of the Cape Agulhas at about 40°S, continuing into the Indian Ocean.

2.4.4 The Benguela Current [Boebel et al, 1998]

The Benguela Current is the broad northward flow adjacent to southwestern Africa that forms the eastern limb of the South Atlantic subtropical circular current system as shown in Figure 2.35. Through its northward extension, it becomes the key conduit by which the upper layer water from the South Atlantic and the Indian Ocean flows across the equator. Bordering this current on its landward side is a coastal upwelling region, which is shown in red colour, off the South West African Coastline in Figure 2.38, and which supports the local pelagic fisheries.

The Benguela Current flows steadily near the continental shelf but has a transient flow due to the embedded Agulhas ring, shown in Figure 2.35, on the western side of the current [Garzoli and Gordon, 1996]. Agulhas rings are known to occasionally interact with the coastal upwelling regime.

The upper Benguela Current's origin and variability was recently studied in the Benguela Sources and Transport Experiment (BEST) (Garzoli et al., 1996). Of a mean Benguela Current transport of $13 \times 10^6 \text{ m}^3/\text{s}$ at 30°S between the shelf and Walvis Ridge, 50% is derived from the Central Atlantic, 25% comes from the Indian Ocean and the remainder is a blend of Agulhas Current water and tropical Atlantic water. Analysis of three years of geostrophic transport indicates that the mean Benguela Current transport does not change interannually by more than 20%. The primary interannual variability appears to be caused by variations in the sources from which the Benguela Current gains its waters.

Agulhas rings are an integral part of the hydrographic elements southwest of the Cape Agulhas. The statistical properties of the eddy field originating at the Agulhas retroflection have recently been the object of intensive studies (Lutjeharms, 1996). Once detached from the Retroflection loop, these energetic rings rapidly lose their high temperature contrast with the atmosphere and the embedding water masses.

2.5 Summary of Literature Survey

The above literature survey provides a general background on Atmospheric Weather, Sea Waves, Wave Climates and Offshore Ocean Currents insofar as they relate to Sea Storms.

The thread that runs through the survey is that of the transfer of energy initiated by the temperature differences that cause pressure differences in the atmosphere. This phenomenon causes the atmospheric weather and air movements, which influence the different wave climate regions in the world, and around the South African Coastline.

The air movements follow the synoptic patterns and can cause sea storms by one or a combination of the following mechanisms, at the air-sea interface:

- (i) Momentum Transfer across the interface
- (ii) Instability of the air and sea boundaries at the interface
- (iii) Partial Sheltering of the wave form from air movements
- (iv) Rough turbulence at the interface

Wind wave characteristics can be significantly affected by the ocean currents with which they interact. This interaction is generally more significant in the case of offshore, deep sea, ocean currents and details of its effects on sea storms is considered to be beyond the scope of this research.



3. AVAILABLE WEATHER AND SEA STATE DATA AT SELECTED RECORDING STATIONS ON THE SOUTH AFRICAN COASTLINE

It is generally accepted that Sea Storms, comprising high waves with long wavelengths and high peak periods are caused by Atmospheric Storm Weather, comprising high winds with low clouds and heavy rains. This study compares the frequency of occurrence of weather types and synoptic patterns, on the basis of their production of heavy rainfall, with that of sea storms in given sea areas, to identify which atmospheric types cause the sea storms.

3.1 Meteorological Weather Data

3.1.1 Synoptic Charts

Typical synoptic charts of the different sea areas, as prepared by the South African Weather Services, have been analysed to determine the following for the atmospheric storms that cause the sea storms:

- (i) The Locations of the Storms
- (ii) The Directions of travel of the Storms
- (iii) The Speed of travel of the Storms

Typical synoptic charts of the areas have been included in section 2.1.

3.1.2 Weather Deviations and Synoptic Patterns

The different weather deviations and synoptic patterns, which are considered to influence storms around the South African Coastline, have been discussed in section 2.1, and their monthly frequencies of occurrence, based on rainfall intensity, have been determined by Vowinckel (1956) and Taljaard (1982) [Thyson et al, 2000].

The above data has been used in this study to derive annual frequencies of occurrence of the weather types and synoptic patterns, which are given in Table 3. These frequencies of occurrence have then been compared with the annual frequencies of occurrences of the sea storm around the South African Coastline, to identify which weather types and synoptic patterns cause the sea storms.

Table 3.1: Annual Frequencies of Occurrence of Weather Types and Synoptic Patterns affecting the South African Coastline [Thyson et al, 2000 modified].

Synoptic Pattern	Month of Year											
	Jan	Feb	Mar	Apr	May	Jun	Jul	Aug	Sep	Oct	Nov	Dec
Continental High	4%	4%	4%	5%	8%	16%	16%	15%	14%	8%	4%	2%
Cold Snaps	0%	0%	0%	8%	11%	11%	14%	22%	16%	8%	8%	3%
Cut-off Low	1%	4%	6%	10%	11%	6%	5%	11%	13%	10%	12%	10%
Easterly Wave	13%	11%	11%	12%	9%	4%	4%	7%	5%	6%	8%	9%
Westerly Low	16%	9%	22%	8%	3%	3%	3%	3%	8%	13%	11%	3%

3.2 Wave and Wind Data Sets

This research is based on the analysis of wave data sets from the Port Nolloth, Cape Point and Durban Areas. Wave and Wind data sets have been obtained from the FA Platform on the Agulhas Bank. The locations of these stations have been given in Figure 3.1, together with the respective depths of water at their locations, and the details of the data sets have been recorded in Table 3.2

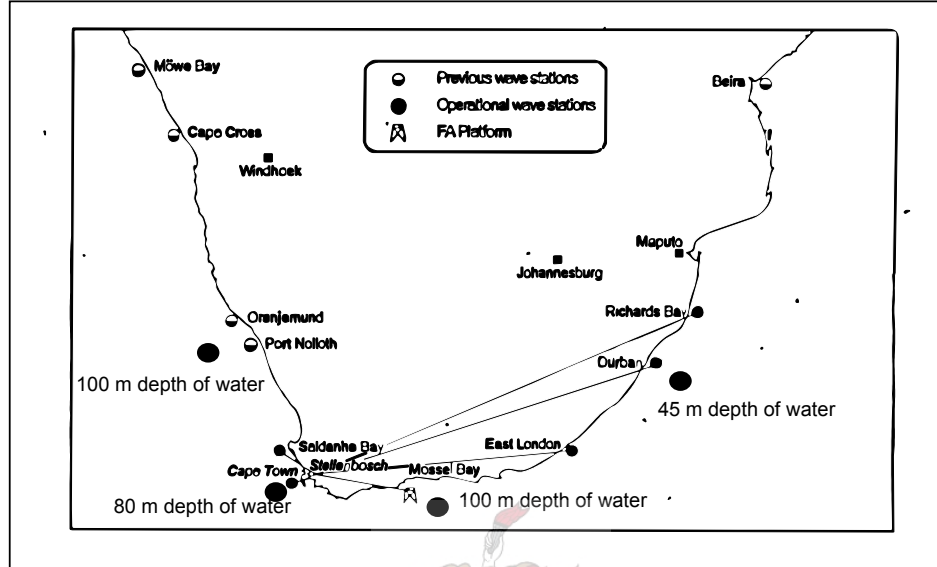


Figure 3.1: Location of Wave Recording Stations with their Water Depths

Table 3.2: Details of Analysed Wave Data

Location	Type of Data	Description of Data	Overall Period of Data
Port Nolloth Area	Waves	3 Hourly H_s and T_p	8 th April 1987 to 31 st August 1996
Cape Point	Waves	3 hourly H_s and T_p	1 st July 2000 to 30 June 2006
Agulhas Bank (FA Platform)	Waves	1 hourly H_s and T_z	1 st January 1998 to 31 st December 2003
	Wind	1 hourly maximum and average speeds, and directions	
Durban (Coopers Light)	Waves	3 Hourly H_s and T_p	11 th August 1992 to 31 st October 2001

The recorded data is inevitably not fully complete due to certain values in the record not being recorded as the result of instrument malfunction. Missing data has been interpolated between known values, on the basis of linear regression, when the period has not exceeded 6 values, whether they be 1 hour or 3 hours. However, when the period of missing data has exceeded this limit, no data for the malfunctioning period has been used in the analysis.

The periods of wave data coverage, and percentages of recovery, for the Port Nolloth, Agulhas Bank and Durban Areas are presented below, in Figure and Table format, for the respective areas. The Cape Point data set covered the period from 1 July 2000 to 30 June 2006 and included 16 019 records. This number was compared with the number of possible records, which was 17 520, and it was found that the set was 91.4% complete. This is considered to be very acceptable.

3.2.1 Port Nolloth Area

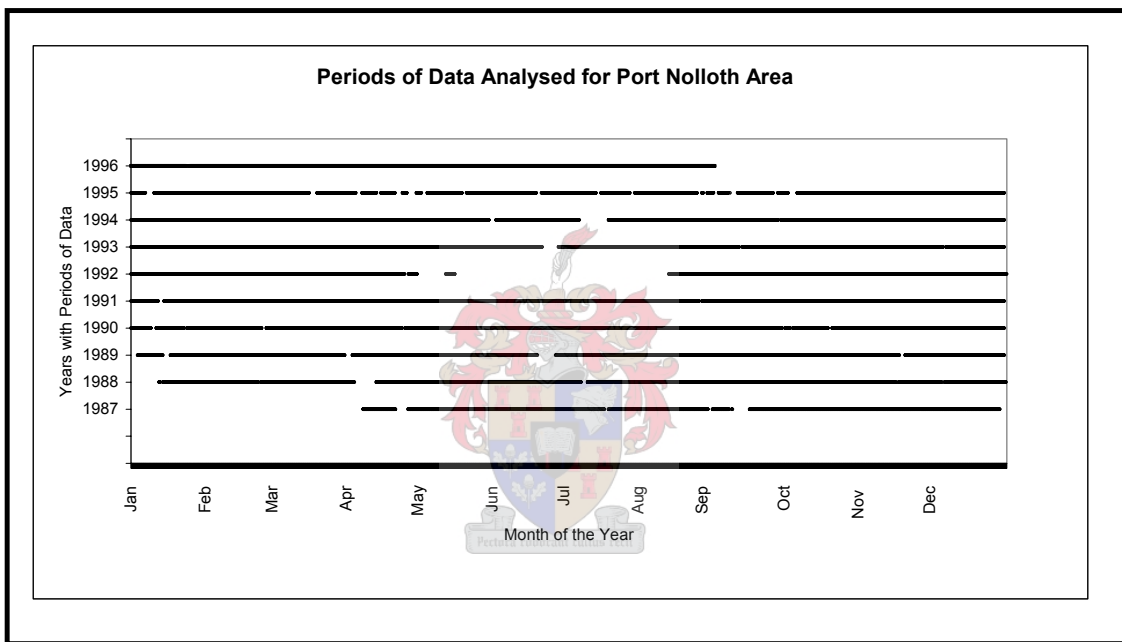


Figure 3.2: Annual Periods of Data Analysed from the Port Nolloth Area

Table 3.3: Periods of data Analysed, and percentages of recovery, for the Port Nolloth Area

Season	Summer			Autumn			Winter			Spring			Total Records	% age records	Remarks
Months	Dec	Jan	Feb	Mar	Apr	May	Jun	Jul	Aug	Sep	Oct	Nov			
Days / m	31	31	28	31	30	31	30	31	31	30	31	30			
Max Records /m	248	248	224	248	240	248	240	248	248	240	248	240	2920		
Years	Records collected														
1987	233	0	0	0	143	248	240	235	233	174	248	240	1994	68%	Not a full year
1988	233	145	223	248	167	248	240	227	248	240	248	231	2698	92%	
1989	248	201	224	243	220	248	179	248	248	240	248	221	2768	95%	
1990	248	222	209	248	231	248	240	248	248	233	224	240	2839	97%	
1991	248	229	224	248	240	248	240	248	239	240	248	240	2892	99%	
1992	248	248	232	248	216	31	0	154	240	248	240	240	2105	72%	
1993	239	248	224	248	240	248	186	248	248	230	248	240	2847	98%	
1994	248	248	224	248	240	237	228	151	248	231	248	240	2791	96%	
1995	248	220	224	222	151	214	223	216	221	178	218	240	2575	88%	
1996	0	237	232	248	240	248	240	248	248	0	0	0	1941	66%	Not a full year
Monthly Ave. for full year	245	220	223	244	213	215	192	198	232	229	241	237			
% of monthly max	99%	89%	100%	98%	89%	87%	80%	80%	93%	95%	97%	99%			
% of Seasonal max	96%			91%			84%			97%					

3.2.2 Agulhas Bank Area

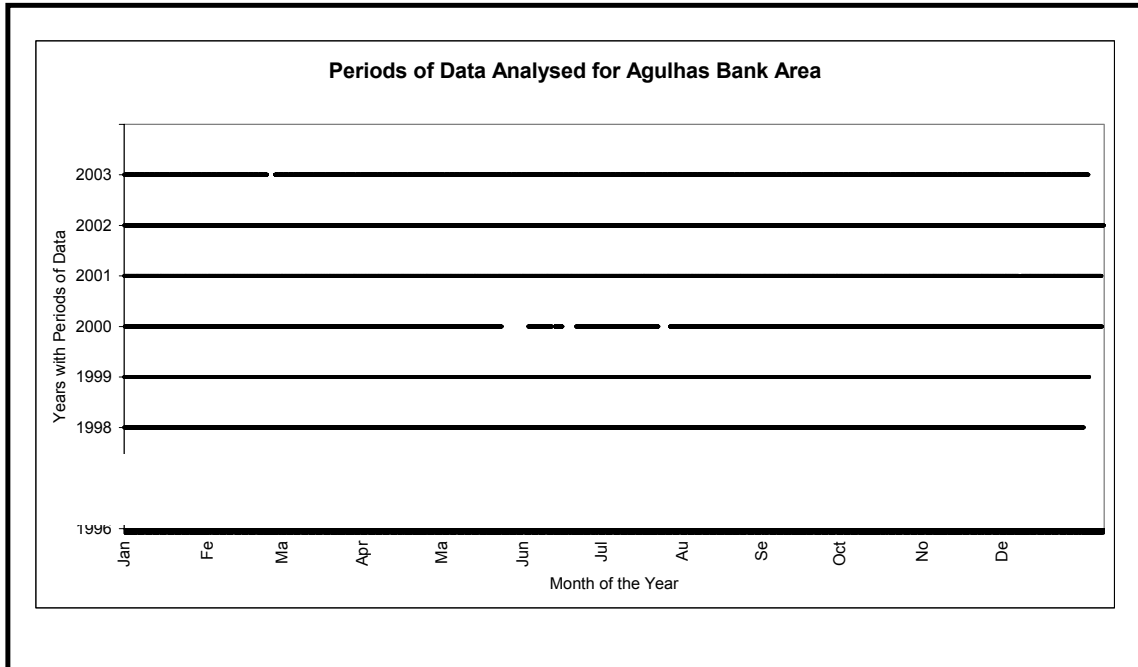


Figure 3.3: Annual Periods of Data Analysed for the Agulhas Bank Area

Table 3.4: Periods of Data Analysed, and percentages of recovery, for the Agulhas Bank Area

Season	Summer			Autumn			Winter			Spring			Total Records	% age records
Months	Dec	Jan	Feb	Mar	Apr	May	Jun	Jul	Aug	Sep	Oct	Nov		
Days / m	31	31	28	31	30	31	30	31	31	30	31	30		
Max Records /m	744	744	672	744	720	744	720	744	744	720	744	720	8760	
Years	Records collected													
1998	734	748	668	723	709	729	704	726	712	700	741	714	8608	98%
1999	728	731	668	744	709	729	704	730	733	700	728	709	8613	98%
2000	746	742	684	742	702	513	568	645	745	722	752	721	8282	95%
2001	719	745	681	745	725	741	719	730	755	720	746	716	8742	100%
2002	743	743	681	745	725	748	720	744	754	720	746	720	8789	100%
2003	743	745	602	745	725	749	720	622	744	720	746	720	8581	98%
Monthly Ave. for full y	735.5	742.3	664	740.7	715.8	701.5	689.2	700	740.5	714	743	716.7		
% of monthly max	99%	100%	99%	100%	99%	94%	96%	94%	100%	99%	100%	100%		
% of Seasonal max	99%			98%			96%			100%				

3.2.3 Durban Area

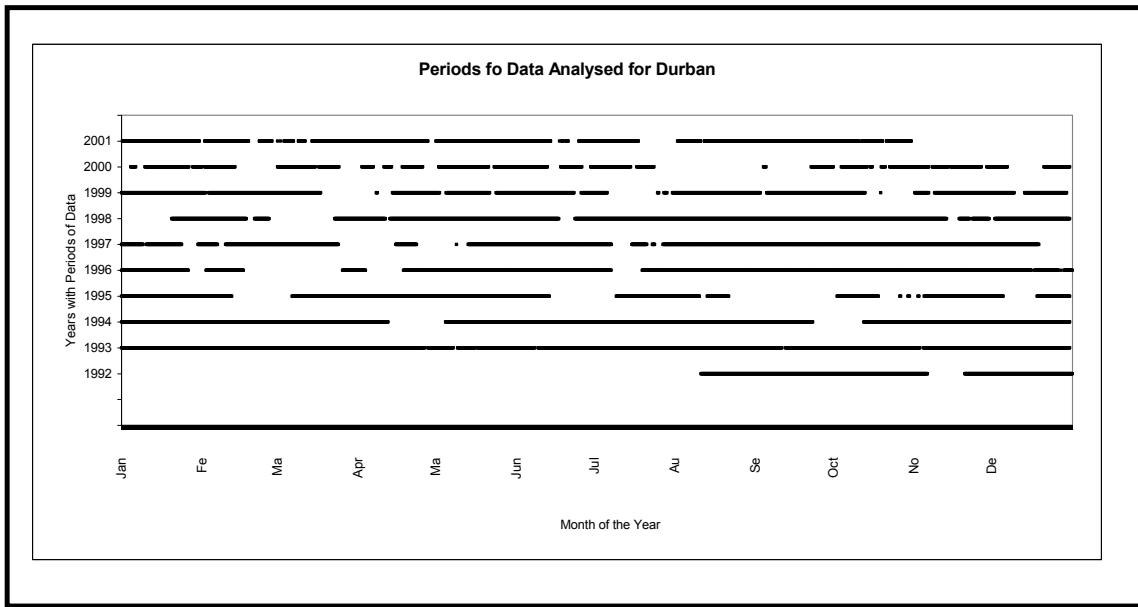


Figure 3.4: Annual Periods of Data Analysed for the Durban Area

Table 3.5: Periods of Data Analysed, and percentages of recovery, for the Durban Area

Season	Summer			Autumn			Winter			Spring			Total Records	% age records	Remarks
	Dec	Jan	Feb	Mar	Apr	May	Jun	Jul	Aug	Sep	Oct	Nov			
Months	31	31	28	31	30	31	30	31	31	30	31	30			
Days / m	248	248	224	248	240	248	240	248	248	240	248	240			
Max Records /m	248	248	224	248	240	248	240	248	248	240	248	240			
Years	Records collected														
1992	248	0	0	0	0	0	0	0	168	240	248	126	1030	35%	Not a full year
1993	248	248	224	248	231	230	231	248	248	230	248	230	2864	98%	
1994	248	248	224	248	101	211	240	248	248	185	147	240	2588	89%	
1995	144	248	92	195	240	248	110	173	151	0	138	205	1944	67%	
1996	224	206	116	48	124	248	240	153	248	240	248	240	2335	80%	
1997	153	190	200	196	65	142	240	145	248	240	248	240	2307	79%	
1998	231	94	183	64	227	248	191	248	248	240	248	195	2417	83%	
1999	208	248	215	142	130	210	219	63	248	222	107	213	2225	76%	
2000	128	181	94	180	124	224	174	166	0	78	175	207	1731	59%	
2001	0	238	170	188	224	240	169	144	222	240	229	0	2064	71%	Not a full year
Monthly Ave. for full	198	208	169	165	155	220	206	181	205	179	195	221			
% of monthly max	80%	84%	75%	67%	65%	89%	86%	73%	83%	75%	79%	92%			
% of Seasonal max	80%			73%			80%			82%					

4 ANALYSIS OF DATA

The data, which has been described in section 3, has been analysed in this section in order to compare frequencies of occurrence of weather types and sea storm events, and to compare wave height statistics between different sea areas, and to identify sea storm parameters and processes.

4.1 Weather Types and Local Synoptic Patterns around the South African Coastline

4.1.1 Annual Distribution of Weather Types and Synoptic Patterns causing Atmospheric Storms

The different Weather Types and Local Synoptic Patterns causing atmospheric storms around the South African Coastline have been discussed in Section 2.1.5 above.

The weather types and synoptic patterns which have been identified, by inspection and by the comparison of weather and sea storm frequencies in the different areas, as affecting the Port Nolloth, the Agulhas Bank and the Durban Areas are given in Table 4.1. Their frequencies of occurrence, which have been recorded in Table 3.1 have been combined and plotted for the West Coast, the South Coast and the East Coast Regions in Figure 4.1. These frequencies of occurrence will be compared with those of the sea storms in the different Regions, later in this section.

Table 4.1: Grouped Weather Types and Synoptic Patterns effecting sea storms around the South African Coastline

Part of South African Coastline	Type of Weather and/or Synoptic Patterns which could influence Sea Storms in the Area
Port Nolloth Area	Westerly Low (WL), Westerly Wave and Cold Snap (WW & CS) Cut Off Low (CoL)
Agulhas Bank Area, including the Cape Coast.	Continental High (CH) Westerly Wave and Cold Snap (WW & CS), Cut-off Low (CoL)
Durban Area	Westerly Wave and Cold Snap (WW & CS) Cut-off Lows (CoL), Easterly Wave (EW)

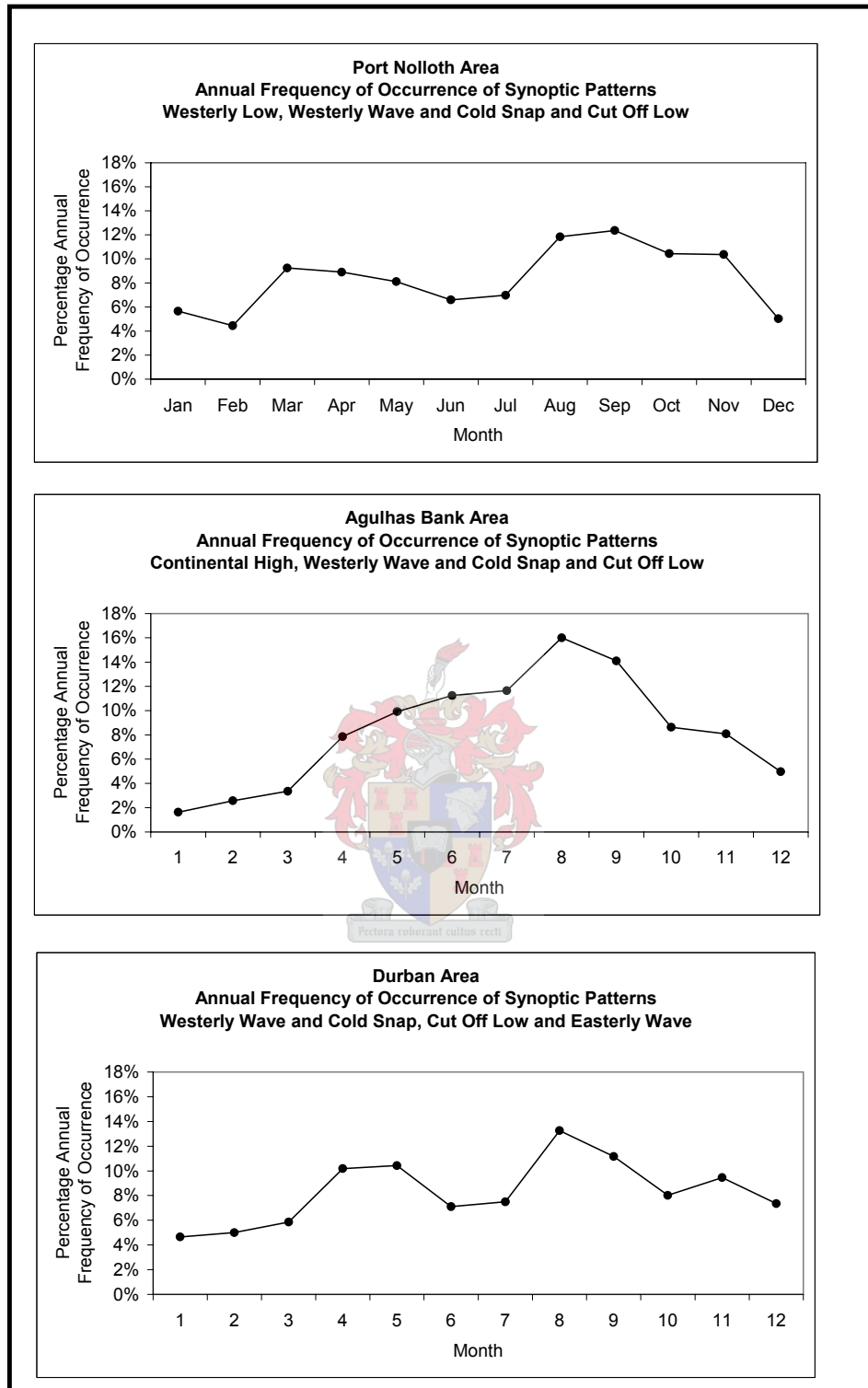


Figure 4.1: Graphs of Combined Regional Weather Types and Synoptic Patterns.

4.1.2 Regional Wind and Wave Directions

(a) Regional Wind Directions

The FA Platform, on the Agulhas Bank, is the only location where wind direction data is collected at the same site as wave data. This wind direction data, for the year 1998, has been analysed to determine the frequencies of occurrence of the wind from different directions and they have been plotted in the Polar Diagram in Figure 4.2.

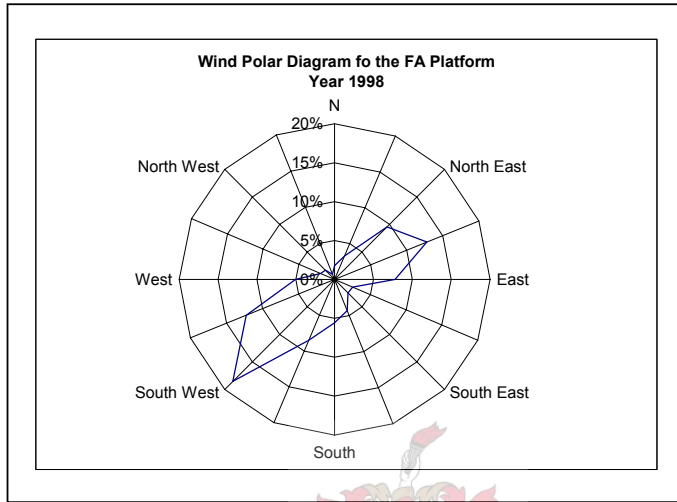


Figure 4.2 Wind Direction Polar Diagram for the FA Platform for the Year 1998

(b) Regional Wave Directions

Wave Directions around the South African Coast, based on Visual Estimates from Voluntary Observing Ships, have been shown in Figure 4.3

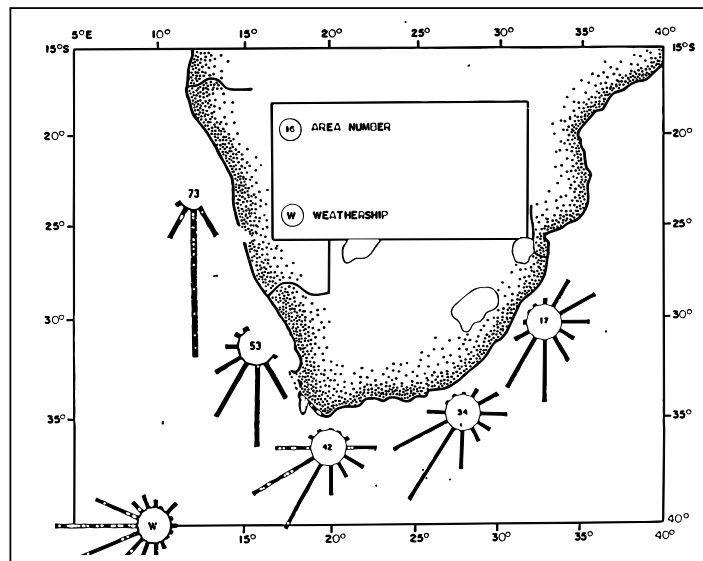


Figure 4.3 Wave Direction Distributions [Rossouw, 1989]

The Direction Distributions for the given areas have been extracted from the Tables in Swart and Serdyn (1981).

There is a good correlation between the dominant South West wind direction in the Agulhas Bank Area (Figure 4.2) and the dominant South South West wave direction for this area (Area 42 in Figure 4.3)

4.2 Statistical Analysis of Wave Heights

4.2.1 General

The following significant wave height parameters have been considered to represent the sea states and define the Wave Climates in the different sea areas around South Africa and they have been used to classify and compare the Regions:

- The Frequency of Occurrence of H_{m0} values.
- The Probability of Exceedance of H_{m0} values.
- 1 in 20 year, 1 in 50 year and 1 in 100 year H_{m0} values, based on the Extreme I Distribution, with $\hat{\alpha} = (\text{Sample Average} - 0.5772 \beta)$ and

$$\beta = \sqrt{6x \text{Variance} / \pi^2} \text{ [J Rossouw, 1989]}$$

The tails in the first two of the above distributions have been cut-off in the graphical representations for presentation purposes, but the full samples have been included in the analysis of the extreme values for H_{m0} in the different areas.

The wave data in the different areas has been analysed to determine the required significant wave height parameters representing the sea states in the region, and the following information has been given below graphically:

- Frequency of Occurrence Distributions of H_{m0}
- Probability of Exceedance Graphs of H_{m0}
- Percentage of Exceedance Data and a Fitted Extreme 1 Distribution curve.

4.2.2 Port Nolloth

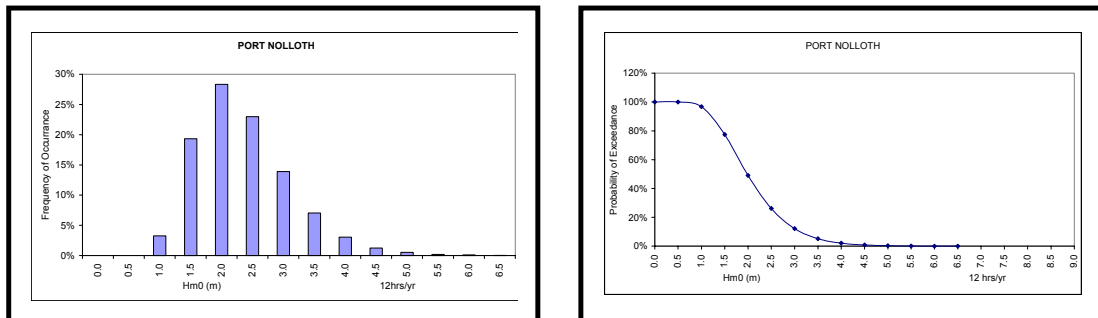


Figure 4.4 (a): Frequency of Occurrence and Probability of Exceedance and Percentage of Exceedance of H_{m0} – Port Nolloth

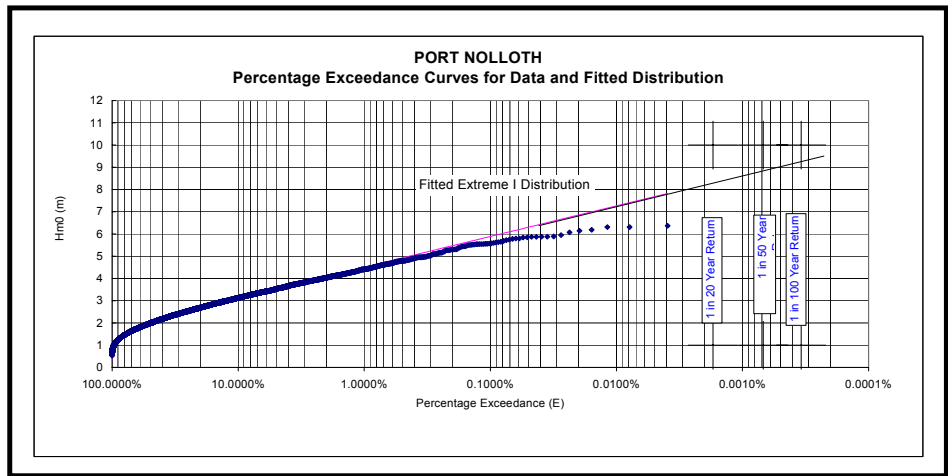


Figure 4.4 (b): Percentage Exceedance Data with a Fitted Distribution Curve for H_{m0} – Port Nolloth

4.2.3 Cape Point Area

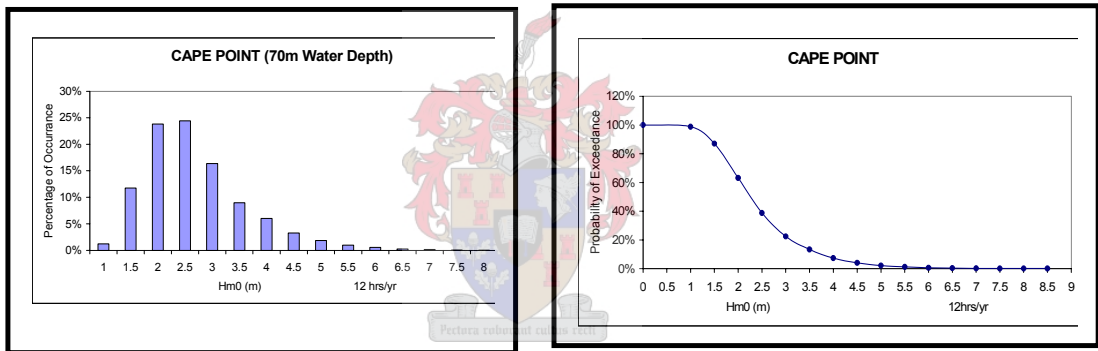


Figure 4.5 (a): Frequency of Occurrence and Probability of Exceedance and Percentage of Exceedance of H_{m0} – Cape Point

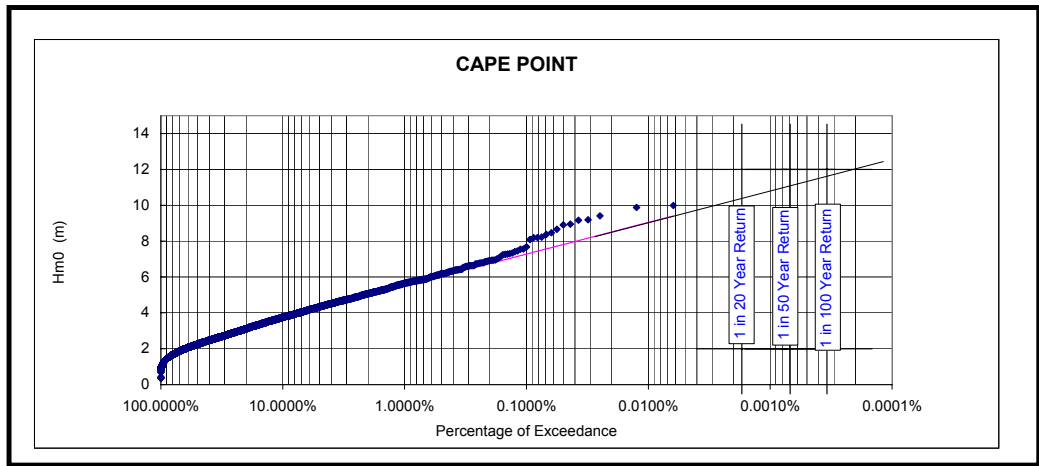


Figure 4.5 (b): Percentage Exceedance Data with a Fitted Distribution Curve for H_{m0} – Cape Point

4.2.4 Agulhas Bank Area

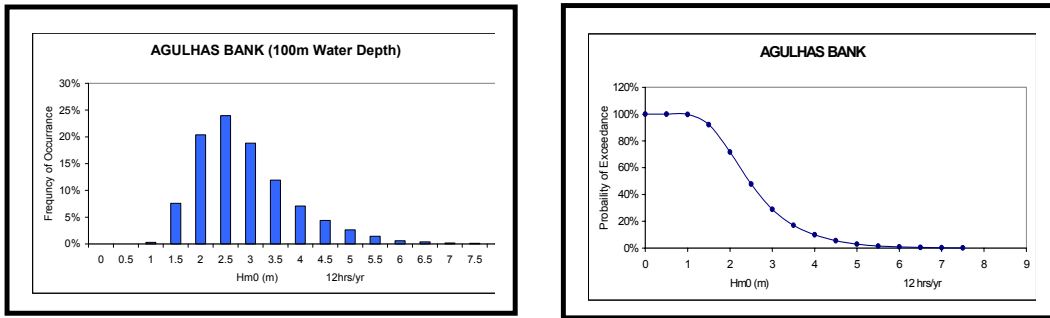


Figure 4.6 (a): Frequency of Occurrence and Probability of exceedance and percentage of Exceedance of H_{m0} . – Agulhas Bank

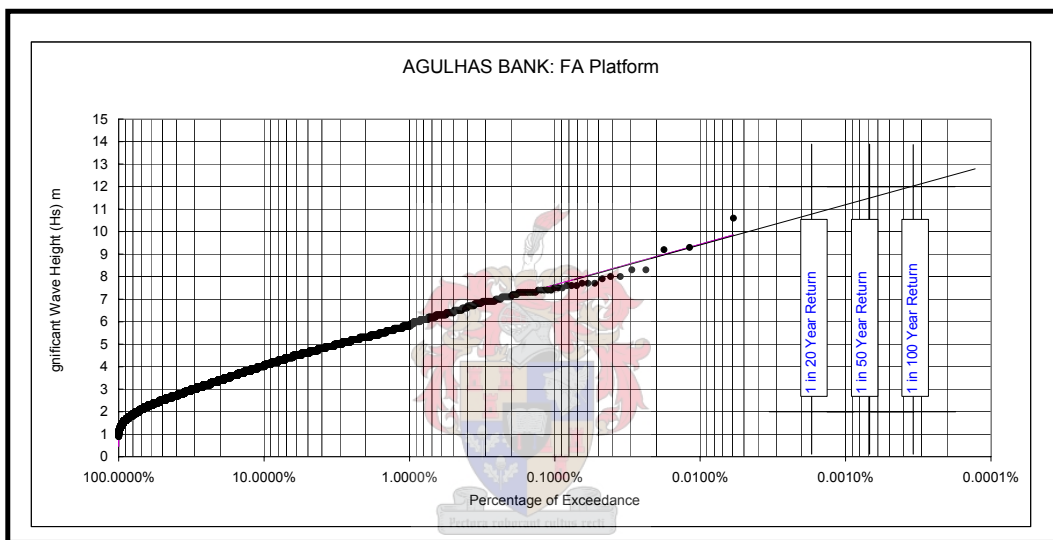


Figure 4.6 (b): Percentage Exceedance Data and fitted Distribution Curve for H_{m0} . – Agulhas Bank

4.3.5 Durban Area.

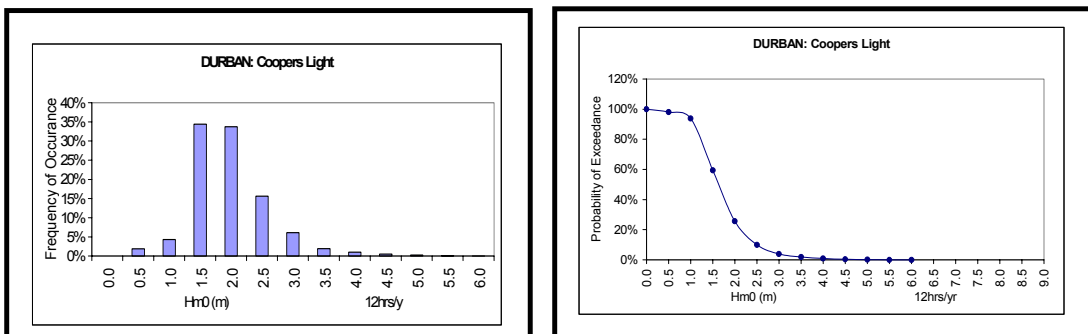


Figure 4.7 (a): Frequency of Occurrence and Probability of Exceedance and percentage of Exceedance of H_{m0} - Durban.

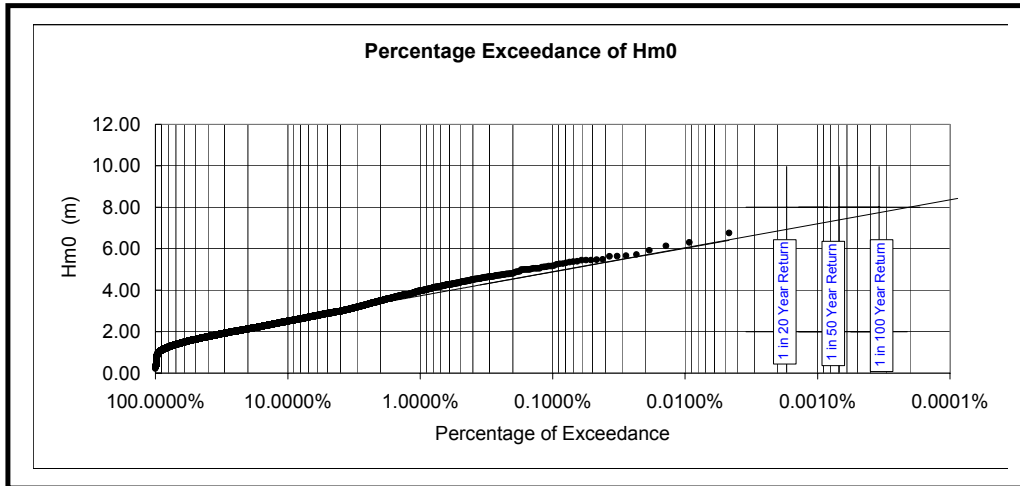


Figure 4.7 (b): Percentage Exceedance Data and Fitted Distribution Curve for Hm0- Durban

4.2.6 Combined Frequency of Occurrence and Probability of Exceedance Curves for H_{m0} for the different coastal areas

Comparative Frequency of Occurrence and Probability of Exceedance Curves for the Different Representative Sea Storm Areas are given in Figures 4.8 and 4.9 respectively. It can be seen that the sea states in the different areas are significantly different, and this is considered to be due to the different wave climates and weather patterns in the areas. The differences could also be caused, to a degree, by the fact that the wave heights are recorded in different water depths, where local conditions could be different, but this has been considered to be a second order effect in this study.

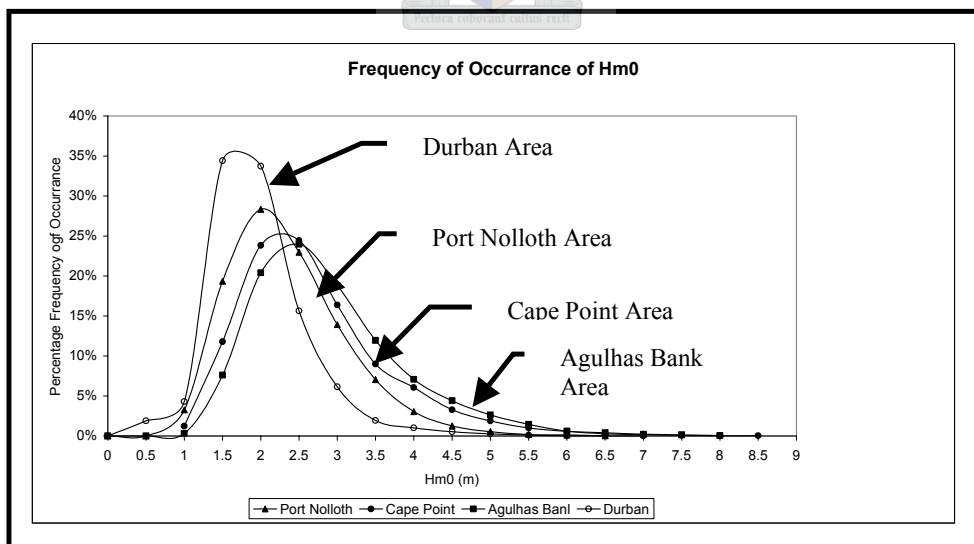


Figure 4.8: Combined Probability of Exceedance Curves for H_{m0} for the Different Areas

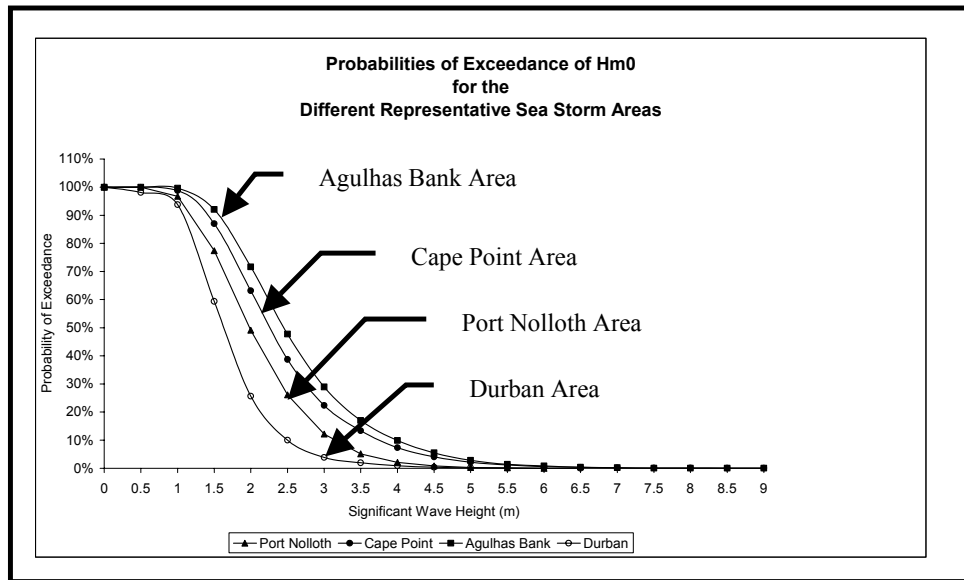


Figure 4.9: Combined Probability of Exceedance Curves for H_{m0} for the Different Areas.

4.3 Analysis of Sea Storms

4.3.1 Definition of Sea Storms and Sea Storm Parameters

(a) General

Sea Storms are non-stationary processes comprised of a series of sea states with varying wave spectra and significant wave heights. Storms are normally analysed in the short term, on the basis of either the statistical properties of the water surface displacements or the spectral properties of the waves, to derive a significant wave height (H_s or H_{m0}). Storms are analysed on a long-term basis by either the statistical analysis of the distribution of the significant wave heights or quasi-deterministic methods, to determine extreme values.

Sea Storms are created by the transfer of kinetic energy, from the movement of the air above the surface of the sea, to a combination of potential and kinetic energy within the sea itself. The velocity of the air over the surface of the sea during a storm has two components consisting of:

- The velocity of the weather system causing the atmospheric storm, such as a cold front feature, and
- The velocity of the air moving from high to low pressure areas within the surface atmosphere over the sea

Cold front features can be clearly seen in satellite images of the earth's surface as the result of the cloud cover footprint associated with these features. Typical features are presented in Figure 4.10, and they can be correlated with surface air pressure diagrams and drawn on synoptic charts, as given in Figure 4.11.

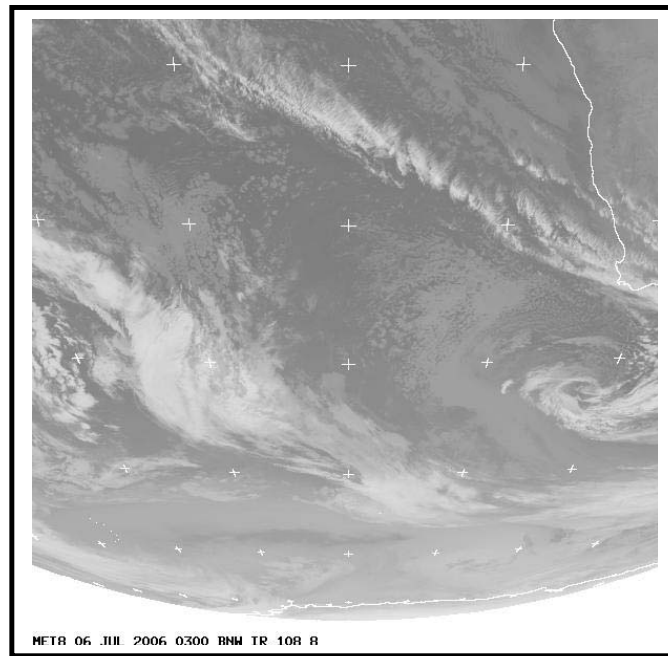


Figure 4.10: Satellite Image of the West and Part-Southern Coast of South Africa, showing typical Cold Front cloud features

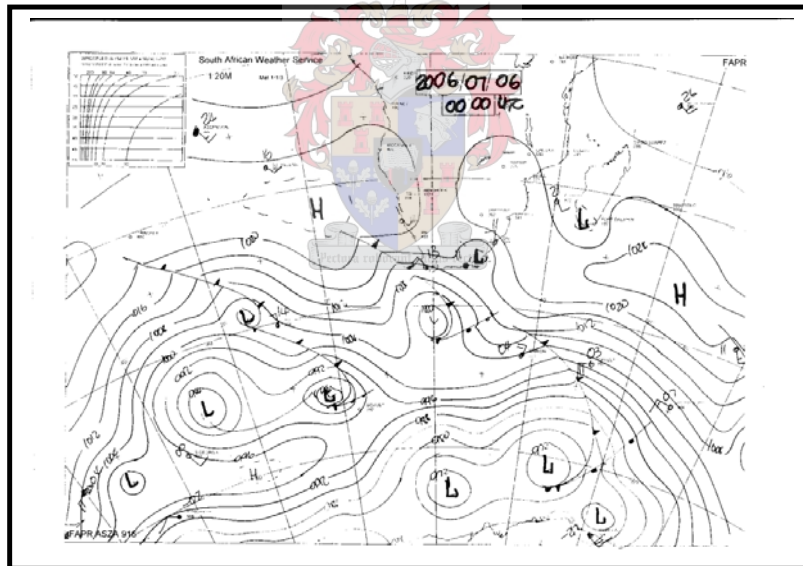


Figure 4.11: Synoptic Chart of the of the same area shown in the satellite image in Figure 3.16

(b) Definition of a Sea Storm

The term “storm” is very generally used to refer to a high energy event, and a sea storm is generally defined in terms of wind force as follows:

“A Storm occurs when wind forces exceed 8 on the Beaufort scale”.

A Wind force of 8 on the Beaufort scale corresponds to an average wind speed of 17.2 m/sec.

Boccotti (2000) has defined a sea storm as “a sequence of sea states in which the significant wave height exceeds the fixed threshold of $1.5 \times H_{s(ave)}$ and does not fall below this threshold for a continuous time interval greater than 12 hours”, where $H_{s(ave)}$ is the mean annual significant wave height on the examined site.

Based on this definition, the South African Sea Storm is defined as follows:

“a sequence of sea states in which the significant wave height exceeds the fixed threshold of $1.5 \times H_{s(ave)}$ for at least one continuous time interval greater than 12 hours, during a period when the sea states have a significant wave height greater than the storm threshold value of $H_{s(ave)}$ ”, where $H_{s(ave)}$ is the mean annual significant wave height on the examined site.

The difference between the first and the second of the above definitions is that the second one allows for the fact that a sequence of sea states can fall below the fixed threshold for a significant period of time (>12 hours) before exceeding it again in a single storm, as for the 1st storm in Figure 4.12.

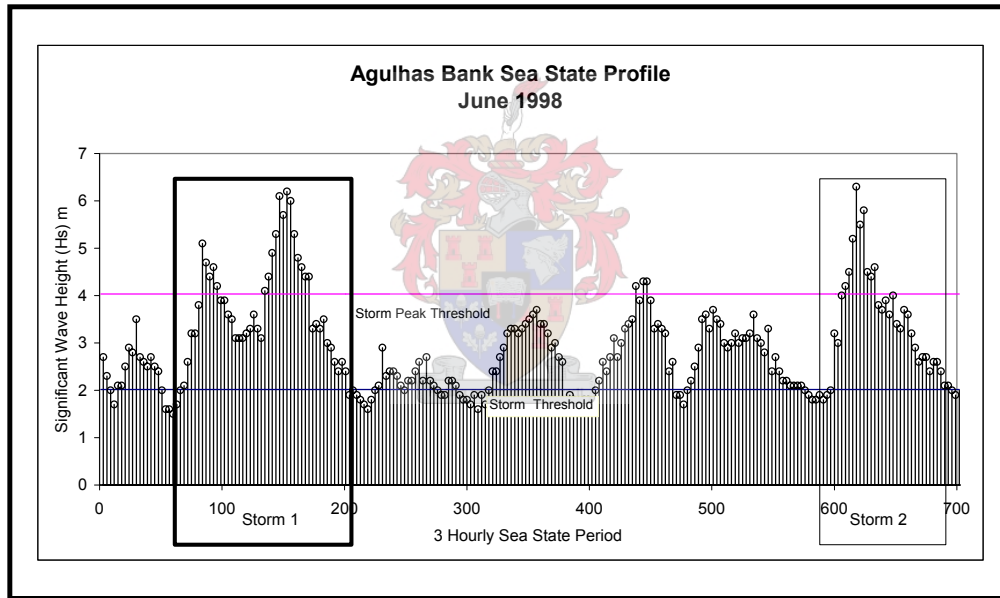


Figure 4.12: Two typical South African Sea Storm Profiles

It has been found to be necessary to modify Boccotti’s definition of a storm, to define a South African Storm, due to types of sea states that are encountered around the South African coastline. These sea states are caused by weather patterns with generally sustained high winds, which blow over long fetches (in the order of 900km) for significant periods of time (in the order of 2 to 4 days). The aforementioned “generally sustained high wind” conditions are subject to some degree of perturbation about a high average value, and this can result in typical multiple peaks during the sea storms.

(c) Sea Storm Parameters

The following parameters which will be used to characterise sea storms, will be derived from the recorded Sea State Data, being the 3-hourly Significant Wave Heights (H_s) and the Wave Periods, whether they be the peak periods (T_p) or the Zero Crossing Periods (T_z):

- **Storm Peak Threshold (SPT)** equal to 1.5 x the annual average significant wave height for the site of the Storm” [Boccotti, 2000]
- **The Storm Threshold (ST)** equal to the annual Average H_{m0} value for the area
- **The Storm Peak Duration (SPD)** equal to the time that the sea state exceeds the Storm Peak Threshold, provided that it is greater than a 12 hour continuous, and does not fall below this threshold, before rising again, for a continuous period of less than 12 hours
- **The Storm Duration (SD)** is defined as “the time that the sea state exceeds the Storm Threshold, with at least one Storm Peak in the period”
- **The Maximum Storm Intensity ($H_{m0(max)}$)** equal to the significant wave of the highest sea state during the storm
- **The Peak Period (T_p)** is the Wave Spectral Peak Period = $1/f_p$

(d) Sea Storm Wave Peak Periods (T_p)

(i) General Peak Wave Periods

The distribution of General Deep Water Peak Wave Periods (T_p) in the Port Nolloth, Slangkop (Cape Point), Agulhas Bank and Richards Bay Areas has been given in Table 4.2. The data is taken from research work reported on by Rossouw (1989). The data given in Table 4.2 is given graphically in Figure 4.13

Table 4.2: Distribution of General Peak Wave Periods (T_p) [Rossouw (J), 1989].

Wave Period T_p (Seconds)	Sea Area around South Africa and Percentage Frequency of Occurrence			
	Port Nolloth	Slangkop	Agulhas Bank	Richards Bay
5.22	0.33	0.68	0.45	2.95
5.51	0.11	0.18	0.04	1.09
5.82	0.44	0.32	0.14	1.05
6.17	0.50	0.49	0.51	1.12
6.56	0.77	0.77	0.49	1.86
7.01	0.61	1.22	1.46	3.06
7.53	1.10	1.31	2.13	3.99
8.13	1.49	1.72	2.82	5.70
8.83	3.03	3.56	4.83	9.23
9.66	8.63	8.70	8.61	11.96
10.67	19.78	19.16	18.56	12.79
11.91	32.01	29.81	28.03	17.27
13.47	24.24	23.00	22.50	20.12
15.52	6.45	7.88	8.06	7.21
18.29	0.50	1.14	1.18	0.70
22.26	0.00	0.06	0.18	0.17

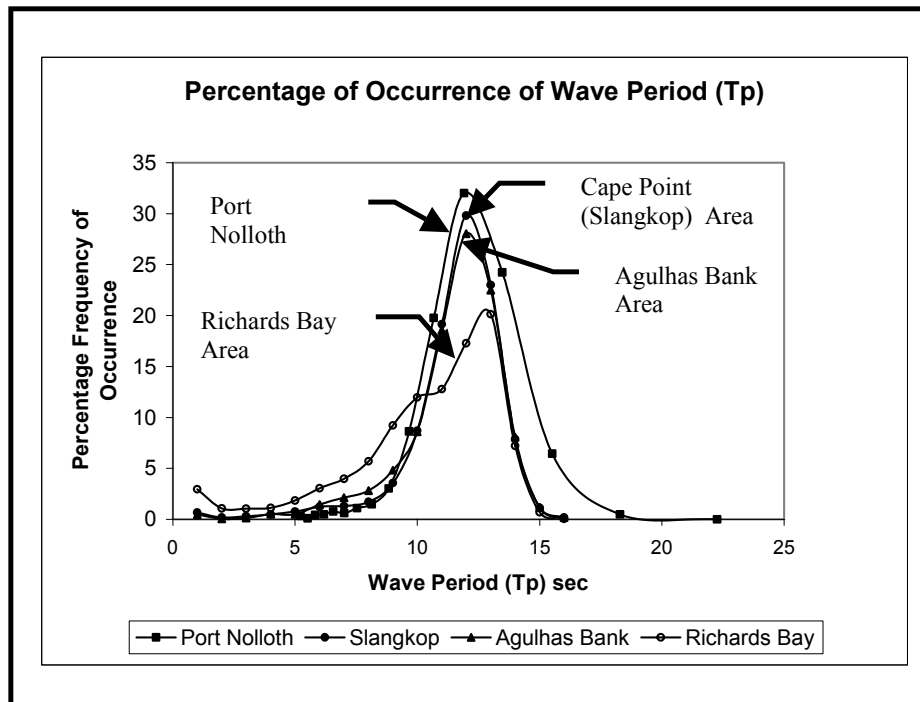


Figure 4.13: Percentage Frequency of Occurrence of General Deep Water Peak Wave Periods (Tp)

(ii) Storm Wave Peak Periods (Tp)

The storm events in the Port Nolloth, Agulhas Bank and Durban Sea Areas, around the South African Coast have been analysed to determine the Average Peak Periods (\bar{T}_p) for the events, and the findings have been summarised in the Table 4.3 together with remarks relating to the swell component of the wave spectra:

Table 4.3: Average Peak Wave Periods (\bar{T}_p) for storms in the different Areas around the South African Coast

Sea Storm Area	Average Peak Wave Periods (\bar{T}_p)	Remarks
Port Nolloth Area	12.8 sec.	High Swell Component
Agulhas Bank Area	11.1 sec.	Significant Swell Component
Durban Area	9.7 sec	Smaller Swell Component

4.3.2 The offshore storm process

The following stages in the development of atmospheric and sea storms have been identified off the southern coastline of South Africa, in the Agulhas Bank area, where meteorological data have been collected together with sea state data and they are considered to comprise, what we call, an offshore storm process. This process comprises the following sequence of events:

- (i) The **alignment of the wind** to a more or less constant direction, which is sustained for a significant period of time.
- (ii) The **increasing of the wind speed** until it reaches a speed where it exceeds the celerity of the wave group in the sea, and a wind sea develops.
- (iii) **The increasing of sea state intensities**, as reflected by significant wave heights, to the point where they exceed the storm threshold, which is equal to the average H_{m0} value for the area, which marks the beginning of the sea storm.
- (iv) **The continued increasing of sea state**, as reflected by significant wave heights, to the point where it exceeds 1.5 x the annual average significant wave in the area, for a continuous period of not less than 12 hours.
- (v) The **peaking of the wind speed**, after which it starts to fall as the atmospheric storm overtakes the sea storm.
- (vi) The **peaking of sea state**, after which it starts to decay.
- (vii) The **continued decay of the wind speed** until it falls below the celerity of the wave group in the sea, and the wind sea changes to a swell.
- (viii) The **continued decay of the sea state** to a point where it falls below the storm threshold value and this marks the end of the sea storm

The following elements have been plotted for a sea storm on the Agulhas Bank in January 1988 in Figure 4.14 to illustrate the offshore storm process:

- (i) The significant wave heights of 3 hourly sea states (H_s)
- (ii) The wind direction in degrees true north
- (iii) The average wind speed times 10, for the purposes of incorporating it into the graph
- (iv) The wave group celerity times 10, for the purposes of incorporating it into the graph.

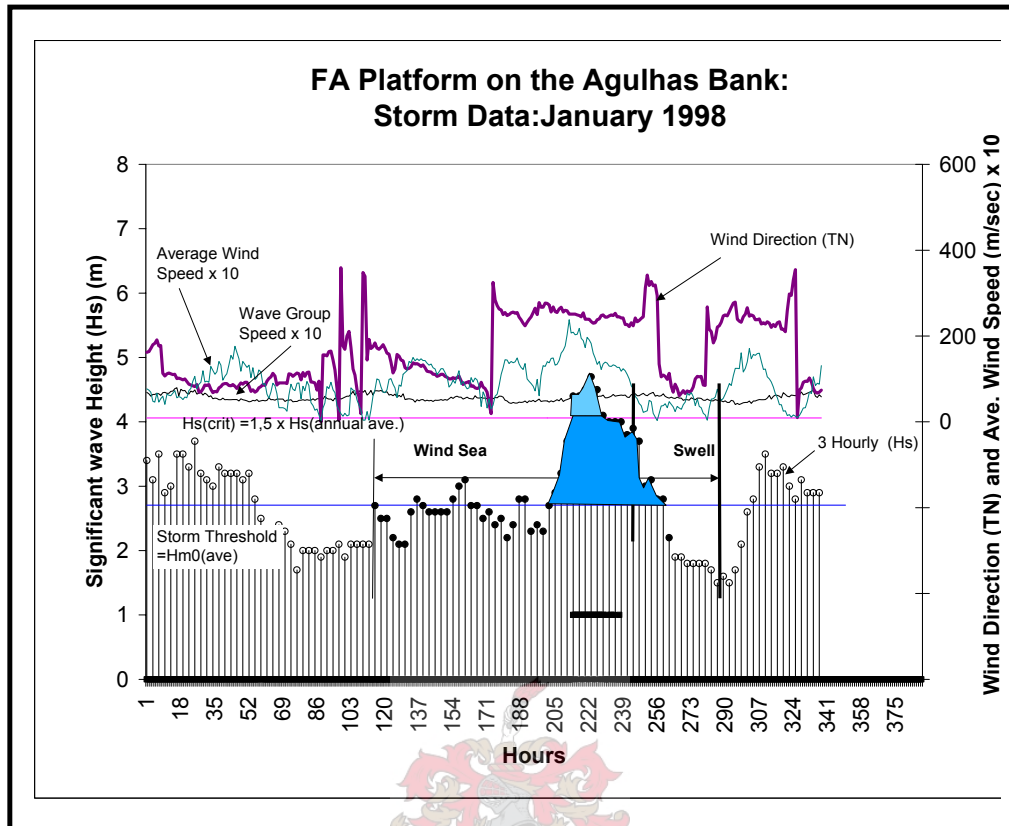


Figure 4.14: Graph showing profile of a Typical Storm off the Southern Coast of South Africa

The profile for the second storm on the Agulhas Bank Area in June 1998 has been given in Figure 4.15 and similar graphs to that shown in the figure, for other storms on the Agulhas bank have been given in Appendix B.

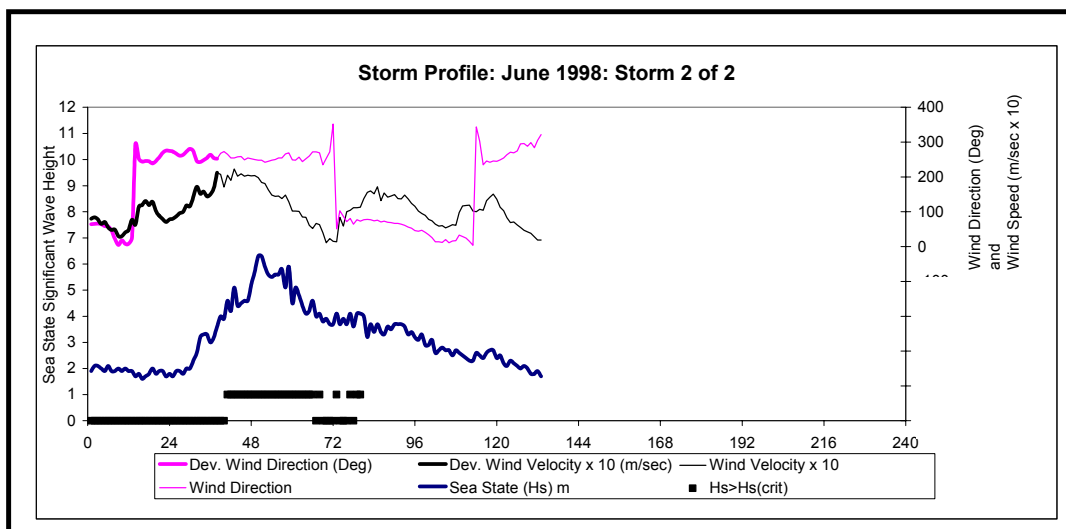


Figure 4.15: The profile for the second storm on the Agulhas Bank Area in June 1998

The cold front features, which are often associated with atmospheric storms off the southern coast of South Africa, move from west to east at typical speeds of 10 m/sec (36 km/hr) to 20m/sec (72 km per hour). Typical daily movements of cold front features off the southern coast of South Africa are given in Figures 4.16 (a), (b) and (c)

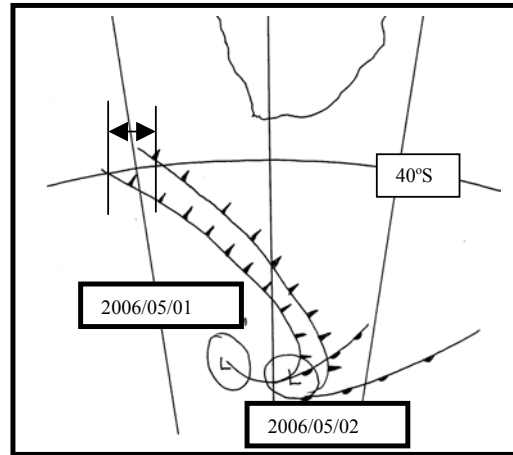


Figure 4.16 (a): Cold Front movement from 2006/05/01 to 2006/05/02.

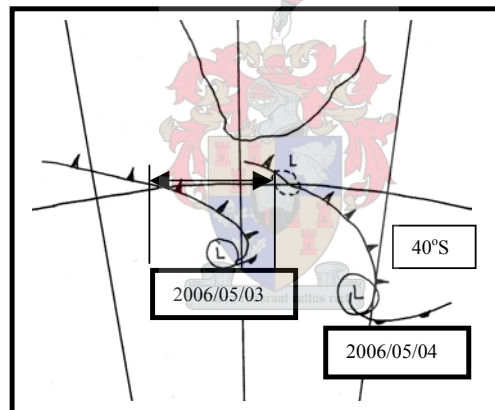


Figure 4.16 (b): Cold Front movement from 2006/05/03 to 2006/05/04.

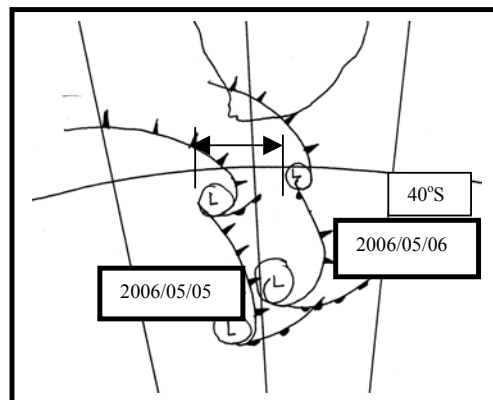


Figure 4.16 (c): Cold Front movement from 2006/05/05 to 2006/05/06.

Strong winds, with high wind velocities cause sea states, which comprise of high waves with long periods and high wave group celerities. More often than not, the strong winds, which cause the Sea Storms, as outlined above occur during an Atmospheric Storm together with clouds and rain.

An analysis of the 1998 meteorological and wave data for the Agulhas Bank Area, which is plotted in Appendix B, shows that:

- (i) the **largest waves** in the 1998 sea storms all lag the highest wind speeds during the storm by periods of between 4 hours and 43 hours, with an average of 19 hours.
- (ii) Typical **average wind speeds**, which cause sea storms in the Agulhas Bank area have been found to range from about 5 m/sec (18 km/hr) to about 30 m/sec (110 km/hr).
- (iii) Typical **wave group celerities** of the storms, based on average zero crossing periods (T_z) of about 10 seconds, range from about 6 m/sec (20 km/hr) to about 10 m/sec (35 km/hr).
- (iv) Typical **atmospheric storm speeds** in the Agulhas Bank area range from about 10 m/sec (36 km/hr) to about 17 m/sec (61 km/hr).

Given the above the atmospheric storms, which create the sea storms, will overtake the waves they create in the sea. This means that the largest waves in a sea storm will arrive at a given location in the sea after the local wind speed has reached a maximum and started to fall. An example of this phenomenon is illustrated using the typical, averaged, 1998 data, is given below:

- Given: 1 A Typical Sea Storm Development Period is 66 hours.
2. The average lag time of the Maximum Sea State after the Peak Wind Speed is 19 hours.
 3. Typical Storm Wave Group Celerities are 7,9 m/sec.
- Then:
1. The time taken for the atmospheric storm to develop and overtake a sea storm at a given location is 66 hours minus 19 hours = 47 hours.
 2. The ratio of the Atmospheric Storm Development Time to the Sea Storm Development Time = $47 / 66 = 0,71$.
 3. The Atmospheric Storm Speed = $1 / 0,71 \times$ the Storm Wave Group Celerity, which equals $1,4 \times 7,9 = 11,0$ m/sec.

The measured atmospheric storm speeds, as identified in Figures 4.16 (a), (b) and (c) range from 9,8 m/sec to 16,7 m/sec (which confirms the figures in the example above).

4.3.3 Storm Passage Variations in relation to a fixed position

(a) General Southern Hemisphere Details.

The major events that can be anticipated to occur during a typical storm moving from the west to the east over a fixed location on the south coast in the southern hemisphere include:

- **Change in wind direction**, from offshore to onshore
- **Change in wind speed**
- **Change in sea state** from a calm sea, to a swell, to a wind sea and back to a calm sea, with consequential rises and falls of wave height
- **Change in Barometric Pressure** from high pressure, to low pressure and back to a high pressure, with resulting set-downs and surge

The majority of the waves that comprise high seas and sea storms are generated by cyclonic storms in the atmosphere. These cyclonic storms are characterised by the upward movement of air, which diverges from surface low-pressure zones (as shown diagrammatically in section 2.1.5), and which rotates clockwise in the southern hemisphere and counter-clockwise in the northern hemisphere.

Atmospheric storms generally move more slowly than the longest waves that they generate with the result that these waves travel out of the generating area, in front of the storm. Waves within the generating area are called seas while those, which have moved out ahead, are called swells.

The area encompassed by the cyclone can be divided into four quadrants. The most dangerous quadrant is the one in which the storms forward movement adds to the orbital wind velocity

High seas and sea storms are often a combination of local wind sea waves from one direction and swells from another.

Waves from a storm at a site may be superimposed on the swells running ahead of another storm that is still hundreds of kilometres away. The result of this situation is usually a confused sea with occasional pyramidal waves and troughs.

A schematic generalised representation of a storm passage on the south coast of the Southern Hemisphere land mass showing the variation in wind direction, wind speed, wave height and surge characteristics have been given in Figure 4.17.

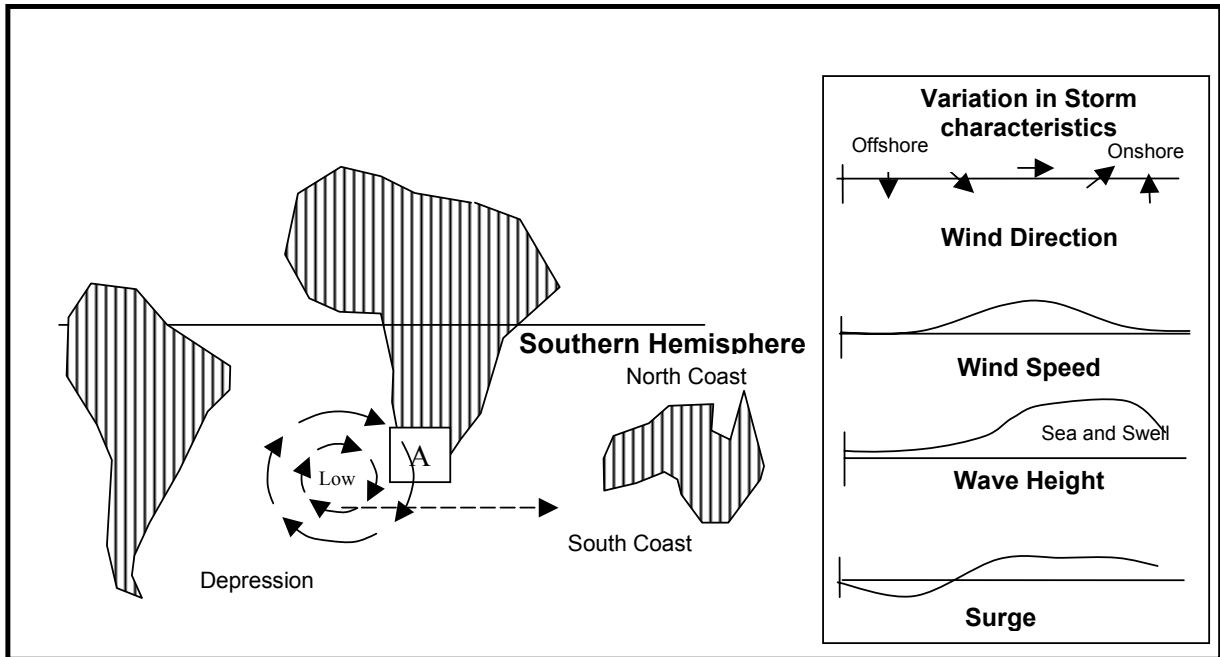


Figure 4.17: Schematic generalised representation of a storm passage on the south coast of the Southern Hemisphere land mass, showing the variation in wind direction, wind speed, wave height and surge characteristics. [After CD Woodroffe, 2002]

(b) Agulhas Bank Area Details

An analysis of the wind direction, wind speed, wave height and synoptic chart data for the Agulhas Bank Area leads one to the conclusion that a typical sea storm in the area can be broken down into the following three stages which are shown diagrammatically in Figure 4.18:

- STAGE 1: The wind direction becomes aligned around a mean value which remains more or less constant during the development stage of the sea storm.
- STAGE 2: The wind speed starts to increase soon after the commencement of the alignment of the wind direction referred to above.
- STAGE 3: The sea state increases from a calm sea, with $H_s < 2$ before the commencement of stage 1, under the effect of the increased wind speed in stage 2, to a peak value caused by a combination of the wind sea and swell sea effects.

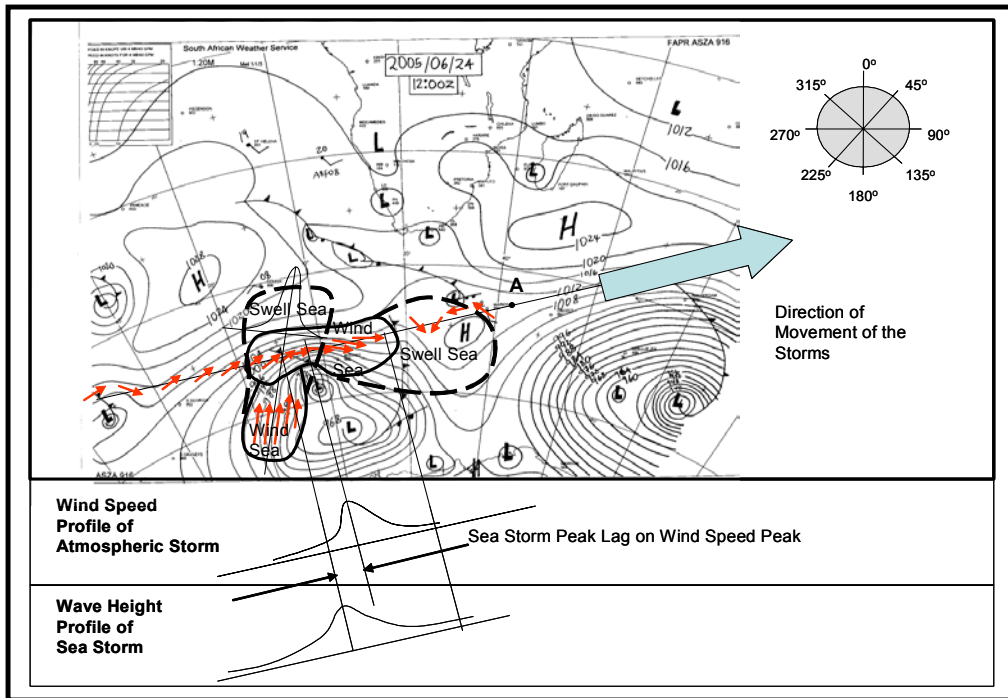


Figure 4.18: Storm Cycle Diagram

The changes in wind direction along the axis of the atmospheric storm movement has been shown diagrammatically in Figure 4.19

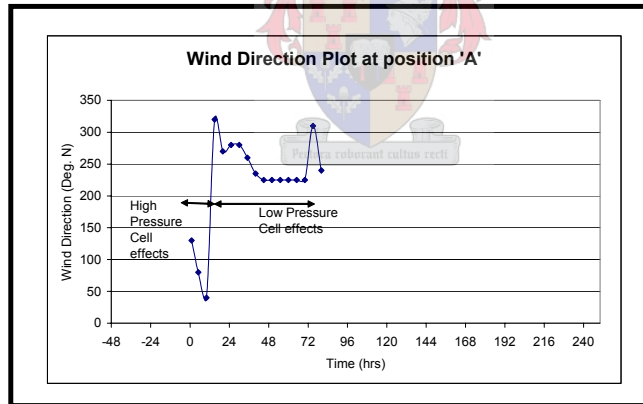


Figure 4.19: Illustrative plot of wind Directions at 'A'

4.3.4 Annual Frequencies of Sea Storms around South Africa

The annual frequencies of the sea storms on a monthly basis, in the different representative areas around South Africa, have been calculated and are presented in the graphs in Figure 4.20 below:

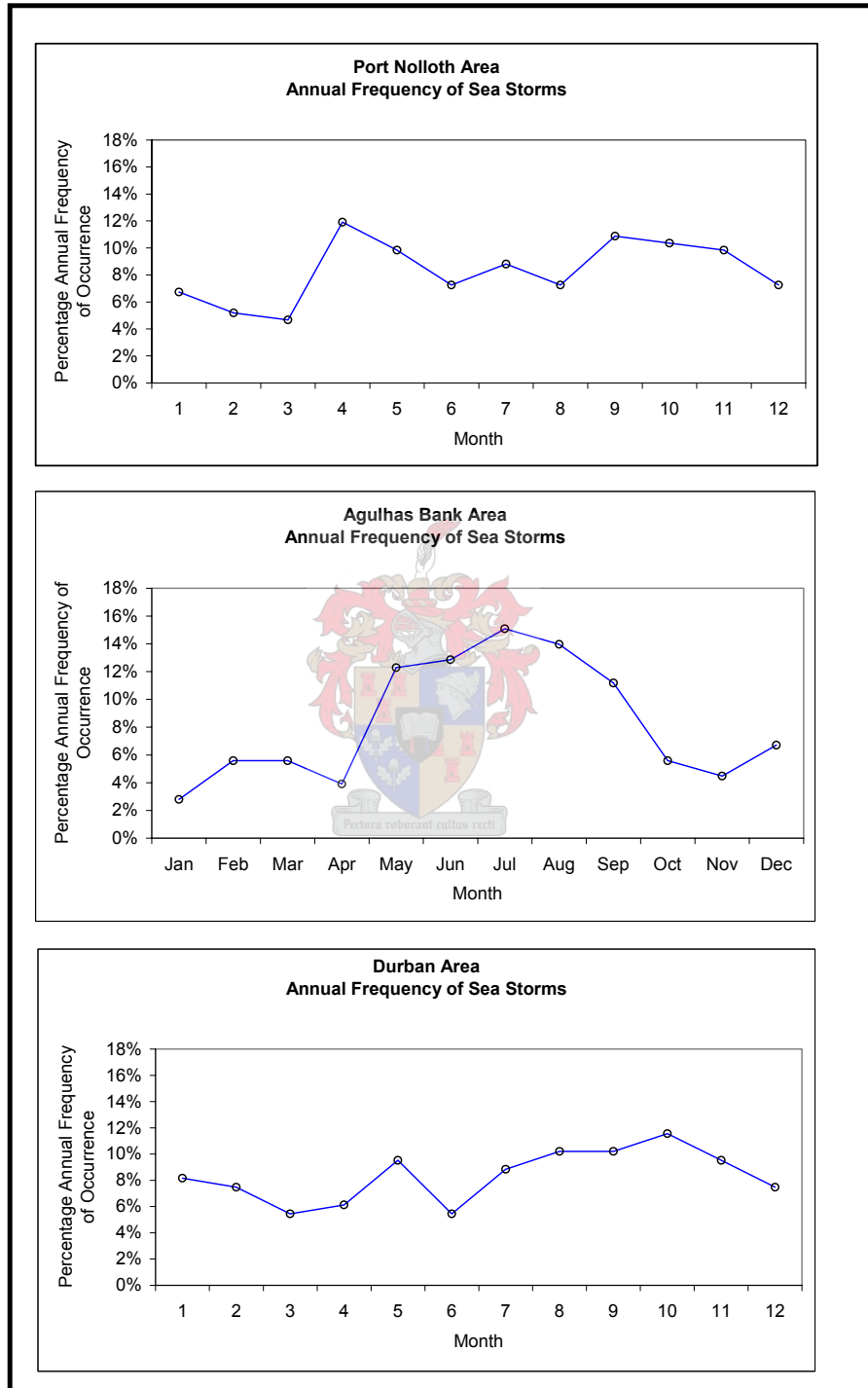


Figure 4.20: Graphs of the Annual Frequencies of the Sea Storms, in the different representative areas around South Africa

4.3.5 Sea Storm profile

The profile of a sea storm can be defined as “the intensity of the sea states above the storm threshold level for the duration of the storm,” that is until the sea state intensity falls below the storm threshold level. The sea state intensity is defined by the significant wave height of the sea state for the period in question. Typical sea state periods, or recording intervals, are 1 hour or 3 hours.

A typical sea storm profile diagram, incorporating the above parameters, based on the sea storm intensity above the storm threshold level, has been given in Figure 4.21.

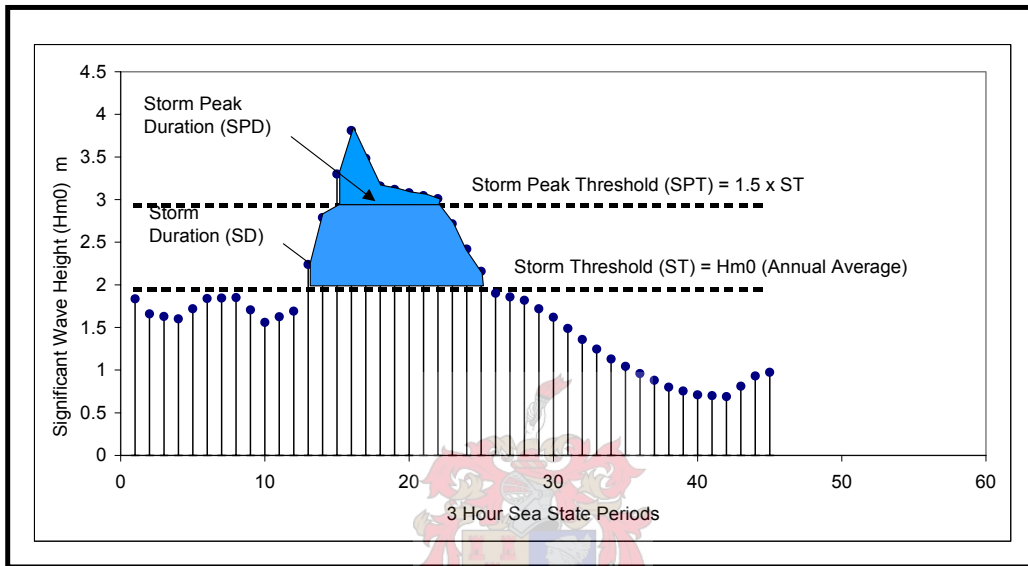


Figure 4.21: Storm Parameter Diagram

Sea State Profiles in the Agulhas Bank Area for each month of 1998, have been given in Figure 4.22. The profiles are based on the Significant Wave heights on the sea state periods, and the storm peak durations have been marked in the figures.

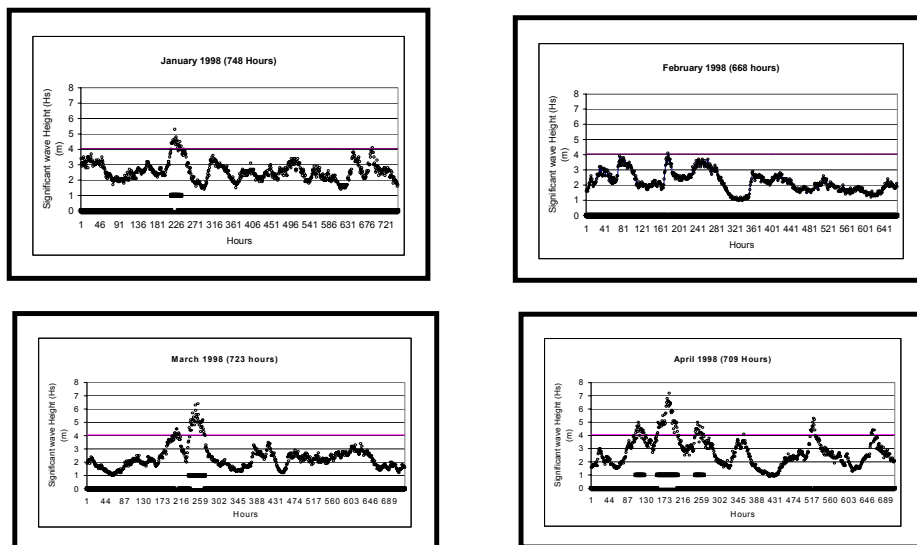


Figure 4.22: Typical Monthly Sea State Profiles for the Agulhas Bank Area 1998

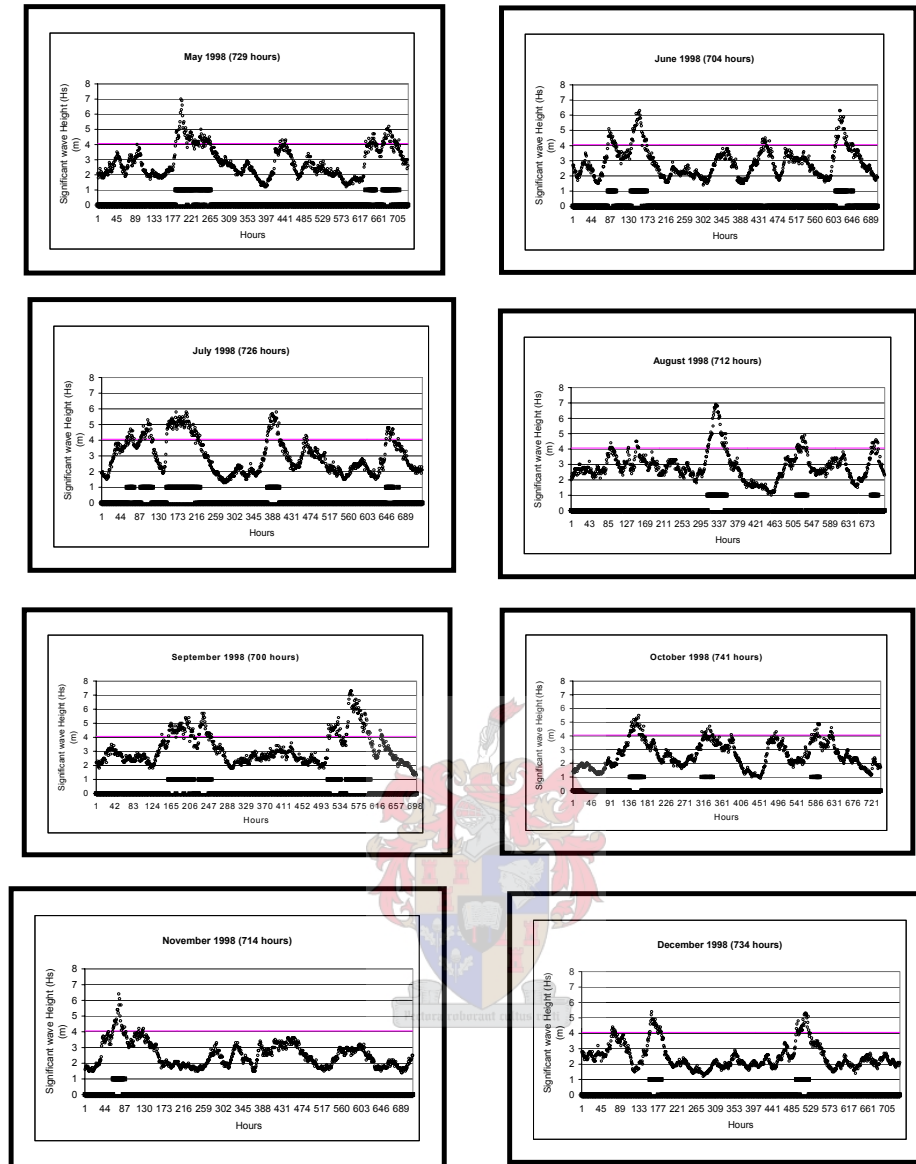


Figure 4.22 (continued): Typical Monthly Sea State Profiles for the Agulhas Bank Area 1998

4.3.6 South African Area Sea State and Sea Storm Profiles

Typical Sea State Profiles for the different Representative Areas around the South African Coast have been given in Figures 4.23 to 4.26. The different profiles, as defined by H_{m0} values and the storm durations, can be identified by inspection. The H_{m0} sea state values in the Figures have been recorded at 3 hourly intervals.

(a) Port Nolloth Area

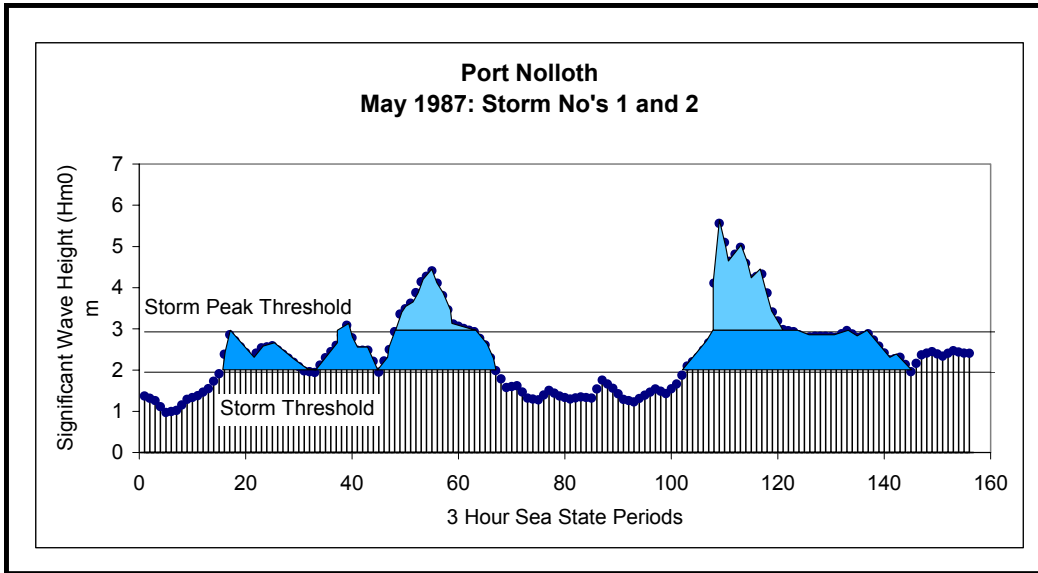


Figure 4.23: Typical Monthly Sea State Profile for the Port Nolloth Area with storms shown shaded.

(b) Cape Point Area

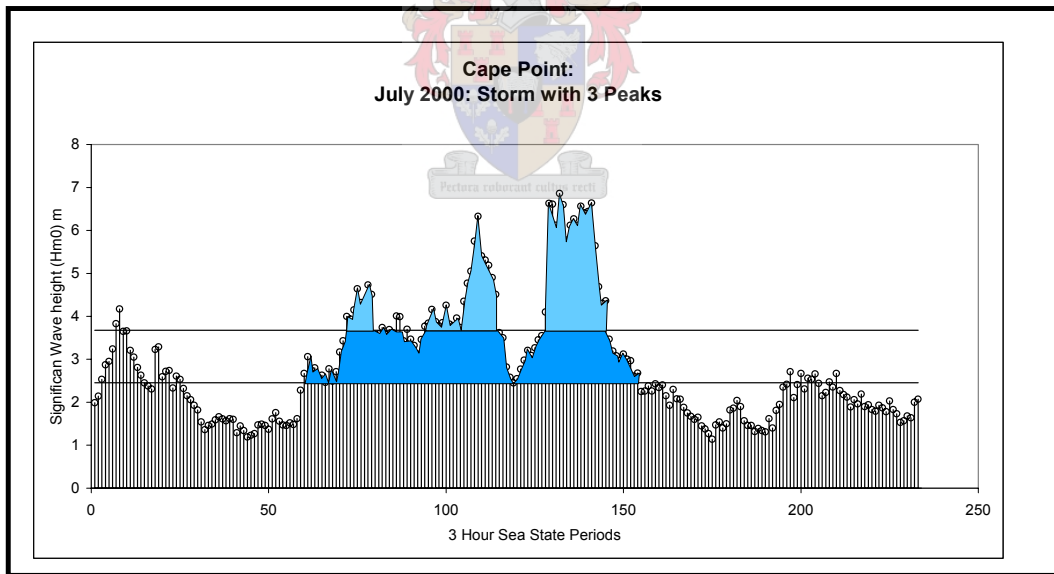


Figure 4.24: Typical Monthly Sea State Profile for the Cape Point Area with storm shown shaded

(c) Agulhas Bank Area

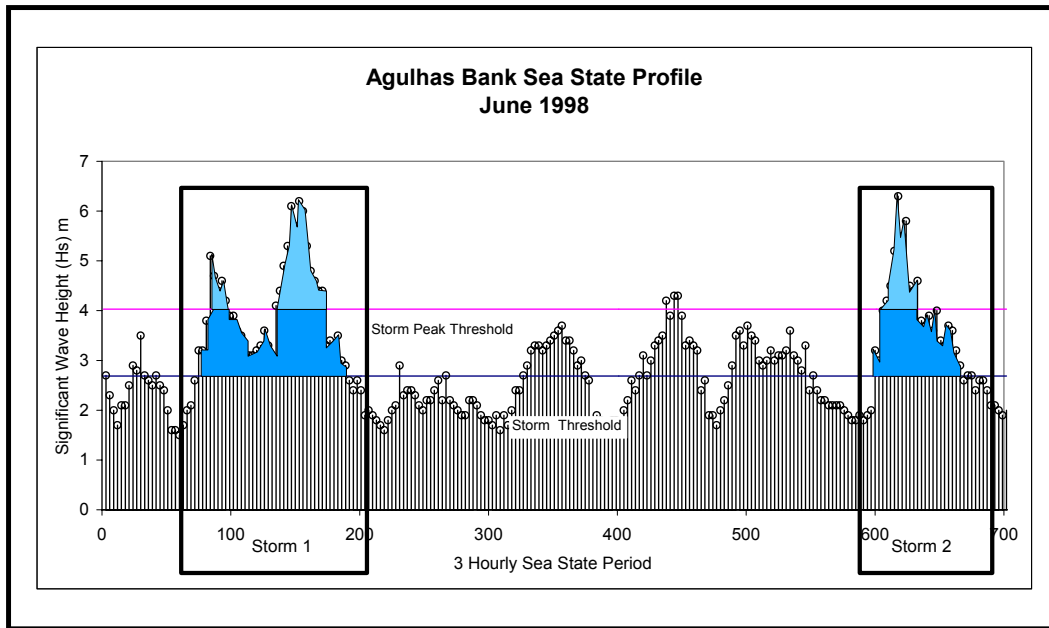


Figure 4.25: Typical Monthly Sea State Profile for the Agulhas Bank Area

(d) Durban Area

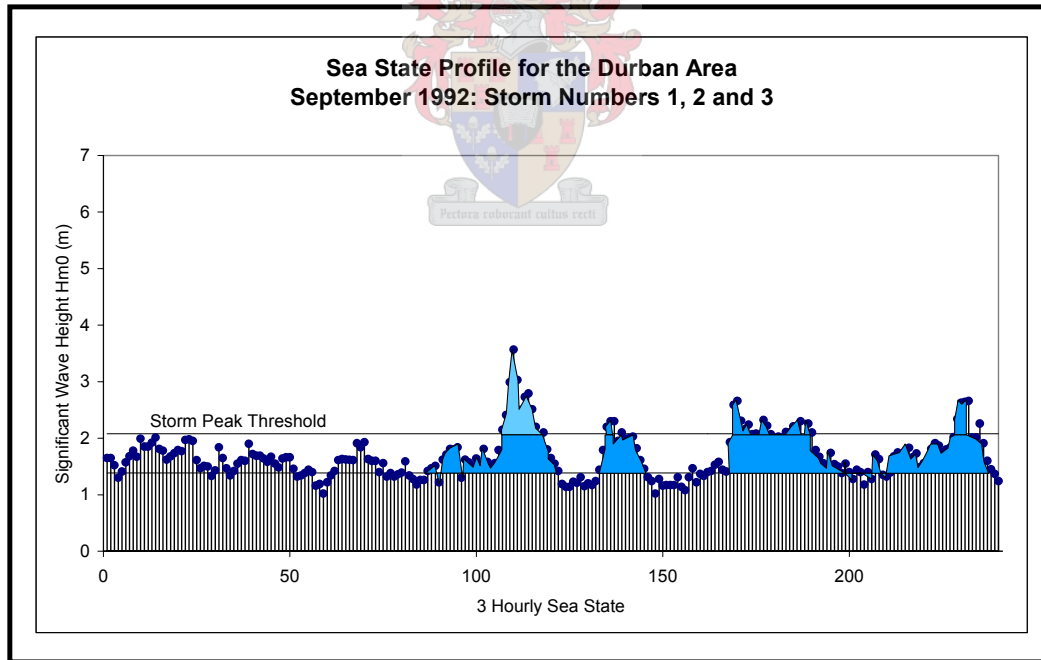


Figure 4.26: Typical Monthly Sea State Profile for the Durban Area

4.3.7 Wave Energy and Energy Flux

(a) General Considerations

The energy of a wave has its genesis in differential solar energy (heat), which causes air to move from areas of high pressure to areas of low pressure, as described in section 2.1 on Atmospheric Weather. This air mass transfer phenomenon causes the build up of kinetic energy in the atmosphere and its transfer to the sea, over which the wind blows, in the form of potential energy, kinetic energy and surface tension energy.

The surface tension component of the transferred energy can be considered to be small, and negligible, when compared with the levels of potential and kinetic energy, which have equal values.

The energy contained in a gravity wave is referred to in terms of the total energy per unit area of the surface, or per meter length of the wave crest length, if the wavelength, L , is known.

The Potential Energy (E_p) per m of wave crest length for Airy waves, which are linear waves, equals the Kinetic Energy (E_k) per m of wave crest length and is equal to:

$$E_p = E_k = \frac{\rho_w g H^2 L}{16} \text{ Joules/m}$$

Hence the total energy E per m for regular waves is given by:

$$\bar{E} = E_p + E_k = \frac{\rho_w g H^2 L}{8} \text{ Joules/m}$$

The total average energy per unit surface area for regular waves, termed the *specific energy* or *energy density* is given by:

$$\bar{E} = \frac{E}{L} = \frac{\rho_w g H^2}{8} \text{ Joules/m}^2$$

[CEM, 2004]

For irregular waves, the total wave energy (\bar{E}) in Joules per square meter is related to the variance of the sea surface displacement η by the following equation:

$$\bar{E} = \rho_w g \langle \eta^2 \rangle \text{ Joules/m}^2$$

where ρ_w is the water density, g is gravity, and the brackets denote a time or space average [RH Stewart, 2005].

The significant wave height, based on spectral analysis methods, is given by the following formula for a narrow range of wave frequencies [CEM, 2004]:

$$H_s \approx H_{m0} = 4 \times \langle \eta^2 \rangle^{.5}$$

where $\langle \eta^2 \rangle^{.5}$ is the standard deviation of the surface displacement.

Given the above,

$$\langle \eta^2 \rangle = H_{m0}^2/16, \text{ and}$$

$$\bar{E} = \rho_w g \times H_{m0}^2/16 \text{ Joules/m}^2$$

(b) Energy Flux (WEF) Equation

Energy in the ocean is transferred from one point to another by gravity waves, which represent the flow of energy rather than the flow of water. In deep water, where waves move vertically, the lateral movement of water is very nominal, but the lateral transfer of energy is significant.

Wave energy levels change over periods of hours to days, in response to either local wind conditions or the arrival of swell from storms some distance away, [G Hagerman, 2001]

Wave Energy Flux J (also referred to as Wave Power \bar{P}) is the rate at which energy is transmitted in the direction of wave propagation across a vertical plane perpendicular to the direction of wave advance and extending down the entire depth [CEM 2004]

Generally J or \bar{P} can be taken as being equal to $\bar{E} \times C_g$, where \bar{E} is the energy density and C_g is the wave group velocity (or celerity). The following wave energy flux equations apply to deep and shallow water:

(i) Deep Water Case ($d > L/2$): $\bar{P}_0 = \bar{E}_0 \times 0.5 \times C_0$ Joules/sec/m,

Where: d = Water depth
 L = Wave Length
 C₀ = deep water wave celerity, and

(ii) Shallow Water Case ($d < 0.14L$): $\bar{P} = \bar{E} \times C$ Joules/sec/m,

Where: C = wave celerity [CEM 2004]

It has been found that Wave Energy Flux, J, (or Wave Power \bar{P}) can be determined in accordance with the following equation [G Hagerman, 2001]:

$$\bar{P} = 0.5 \times H_{m0}^2 T_p \text{ kW/m of wave crest}$$

The multiplier of 0.5 in the above equation approximates to the actual multiplier, which depends on the shape of the wave spectrum. Studies have shown that this multiplier could typically range from 0.45 to 0.65, and a value of 0.5 is an appropriately conservative approximation. [G Hagerman, 2001]

The peak period, T_p in the above equation is often replaced with T_e , which is the wave energy period, and which can be defined in terms of the moments of the energy spectrum as $T_e = \frac{m_{-1}}{m_0}$. There are many possible definitions of a typical wave period for a mixed population of waves and, notwithstanding the fact that T_e is the most

relevant for wave power, T_p has been used in this study. The ratio $\frac{T_p}{T_e}$ can vary from 1,2 to 1,4, depending on the Power Operator Spreading Index. [Technical Report prepared by the European Marine Energy Centre, 2004].

(c) Storm Energy (SE)

If one considers that a storm is comprised of a series of sea states, which have representative significant wave heights and periods and therefore Energy Flux, then one could derive a Storm Energy by multiplying the Wave Energy Flux/m² for each sea state times the duration of the relevant sea states and summing the total for a given storm.

$$SE = 0.5 \times 3 (N) \times \sum_{n=1}^N H_{m0(n)}^2 T_{p(n)} \text{ kWh/m of wave crest length}$$

where,

- N = Number of 3 hour sea state intervals with $H_{m0} > \text{Storm Threshold}$
- H_{m0} = Significant Wave Height of each Sea State Interval
- T_p = Average Period for the Duration of the Sea State Interval

Consider the storm included in the sea state profile in Figure 4.27.

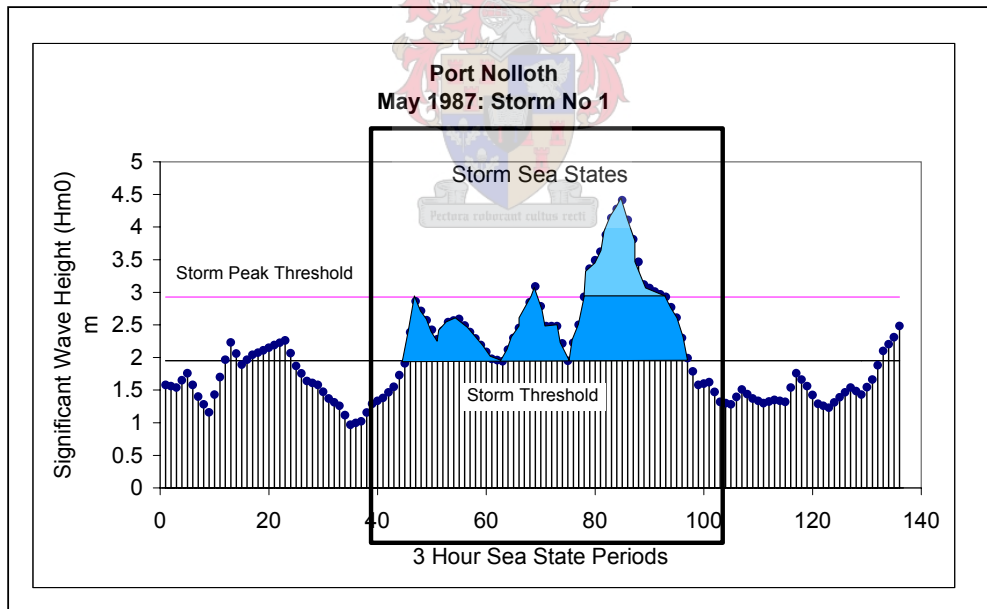


Figure 4.27: Typical Sea State Profile incorporating a single Storm

A typical calculation of storm energy flux for the storm in Figure 4.18 has been given in Appendix C.

4.3.8 Equivalent Wave Energy (EWE) Storm Profiles

(a) Individual (EWE) Storm Profiles

An **Equivalent Wave Energy (EWE) Storm Profile** for individual storms can be derived on the basis that:

- (i) The **Maximum Storm Intensity**, or Maximum Significant Wave Height, $(H_{m0})_{max}$ of the EWE Storm is the same as the Maximum Storm Intensity for the actual storm.
- (ii) The **Storm Threshold** for the EWE Storm would be the same as that of the actual storm
- (iii) The **Storm energy Flux (SEF)** for the EWE Storm would be the same as that for the actual storm.
- (iv) The **Duration** of the EWE Storm could be calculated on the basis of (iii) above.

The process for calculating the EWE Storm profile has been summarised below:

- (i) Analyse the statistical values of the Sea Surface Displacement Data to derive H_{m0} for selected Sea State Periods.
- (ii) Determine the Storm Threshold Level, which is equal to the Annual Average Significant Wave Height in the Area.
- (iii) Determine the Storm Peak Threshold level, which is 1,5 x the Storm Threshold.
- (iv) Check whether or not that the Storm Peak Threshold is exceeded for more than a 12-hour continuous period: if yes, the profile is a storm otherwise it is not.
- (v) Calculate the Sea State Wave Energy Levels
= $0.5 \times H_{m0}^2 \times T_p \times \text{Sea State Duration}$.
- (vi) Calculate the Storm Wave Energy, comprising the total of the Sea State Wave Energies, by adding the Sea State Wave Energy Levels for the duration of the storm.
- (vii) Calculate the EWE Storm Duration from the Actual Storm Energy, the Storm Threshold level, the Storm Intensity ($H_{m0_{max}}$) and the Average T_p value from the Actual Storm.
- (viii) Plot the EWE Storm Profile.

The above process is shown diagrammatically in Figure 4.28

The EWE Duration referred to in (vii) above is calculated by dividing the Storm Wave Energy by $0,5 \times$ the square of the average of the Storm Threshold and the Maximum Intensities \times the average peak wave period for the actual storm, as follows:

$$\text{EWE Duration} = \frac{\text{StormWaveEnergy}}{\left(0,5 \times \left(\frac{\text{MaximumStormIntensity} + \text{StormThreshold}}{2} \right)^2 \times T_p(\text{ave}) \right)}$$

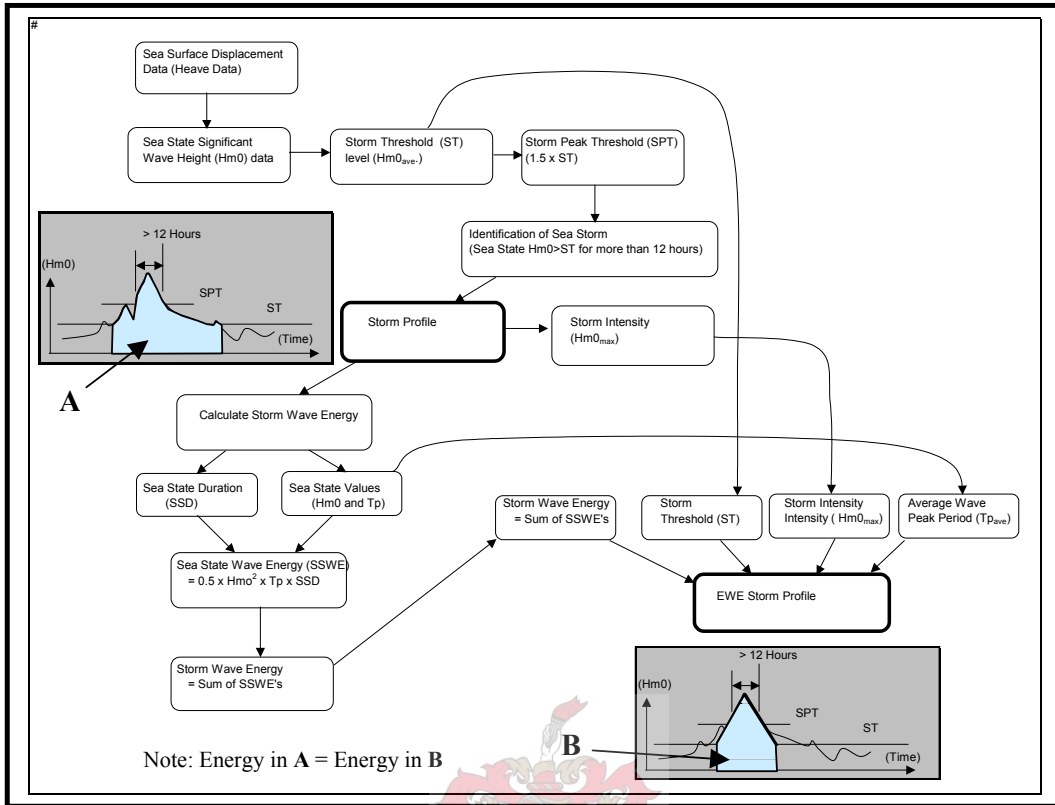


Figure 4.28: Diagrammatic Process of EWE Storm Profile Development

The calculations of the Equivalent Wave Energy (EWE) Storm Profile for the storm in Figure 4.18 has been given in Appendix D

Plots the Typical EWE Storm Profiles, with corresponding Actual Sea State Profiles, for the Port Nolloth, Cape Point, Agulhas Bank and Durban Sea Areas are given in Figures 4.29 to 4.32. The storms have been selected at random to illustrate the usefulness of the concept rather than to demonstrate the concept for the largest storms only.

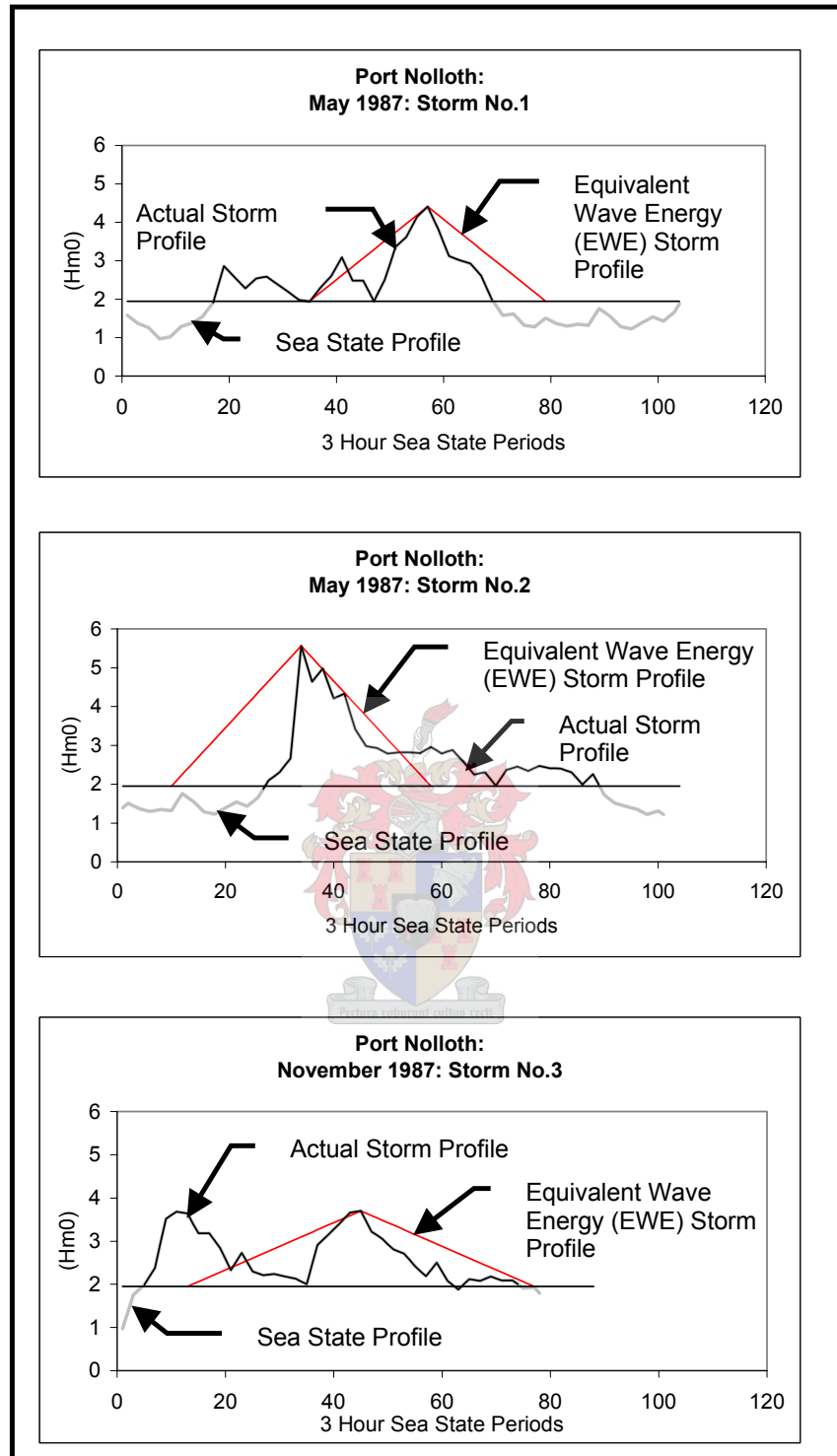


Figure 4.29: Typical Plots of Actual and Equivalent Wave Energy Storm Profiles for the Port Nolloth Area

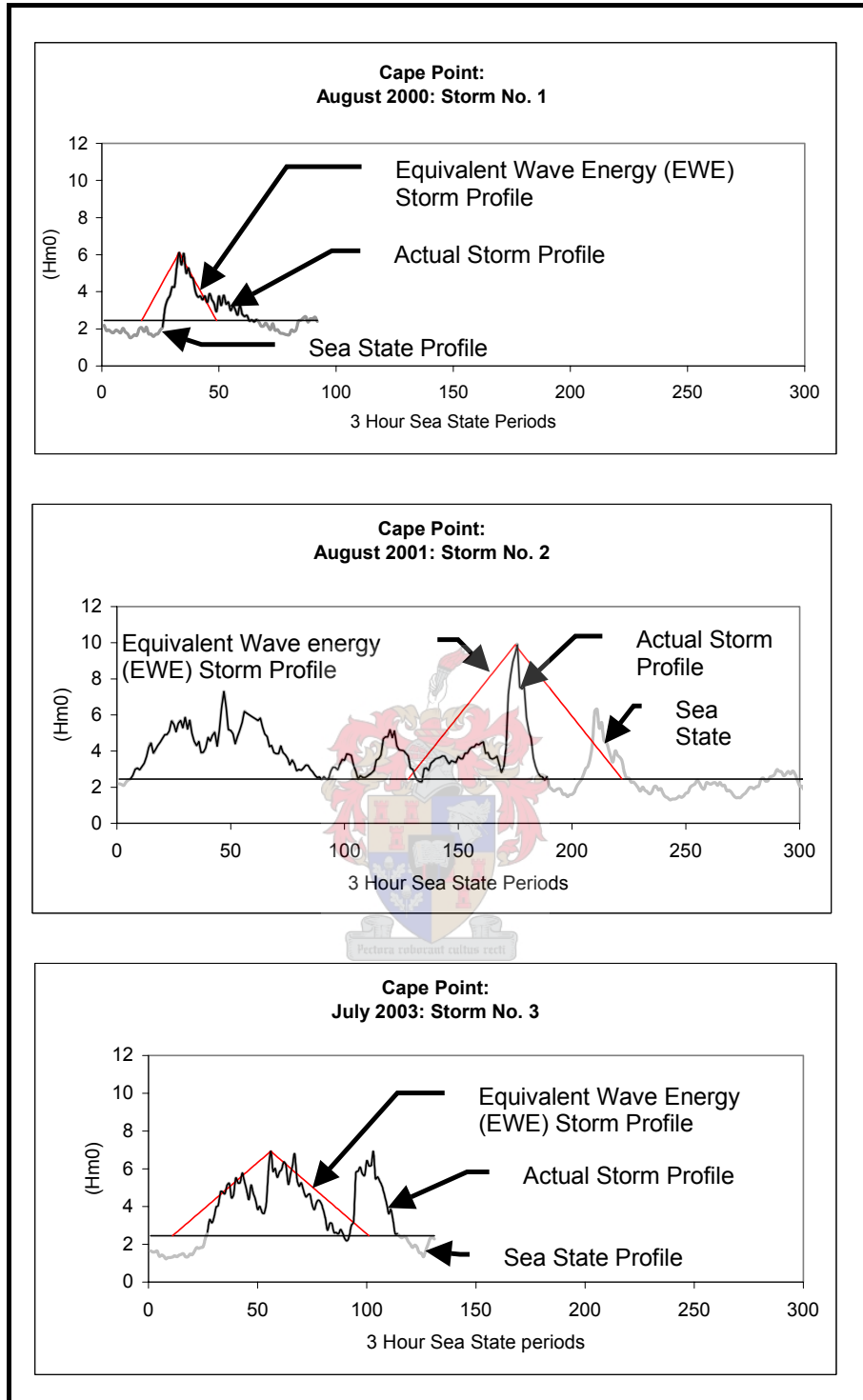


Figure 4.30: Typical Plots of Actual and Equivalent Wave Energy Storm Profiles for the Cape Point Area

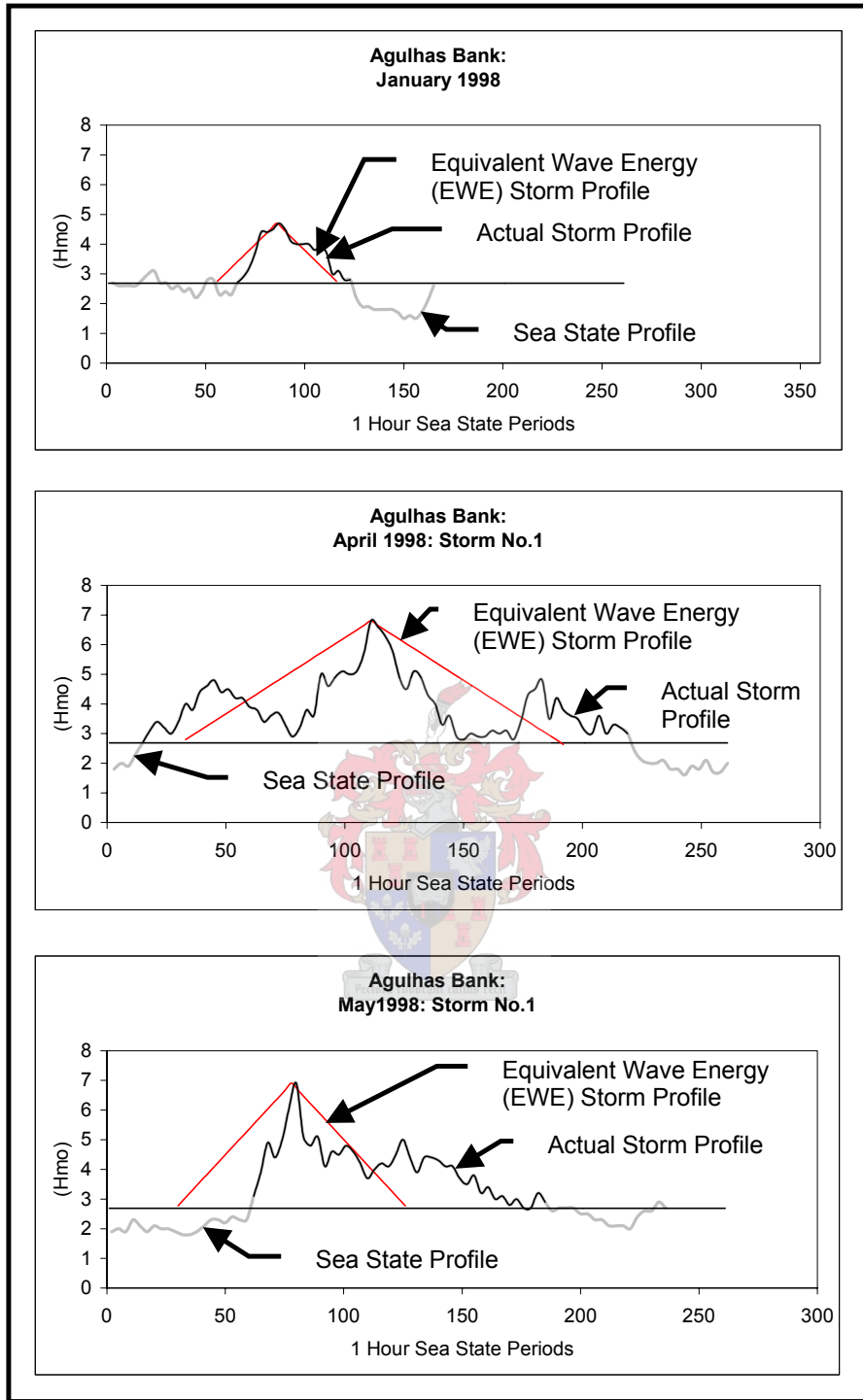


Figure 4.31: Typical Plots of Actual and Equivalent Wave Energy Storm Profiles for the Agulhas Bank Area

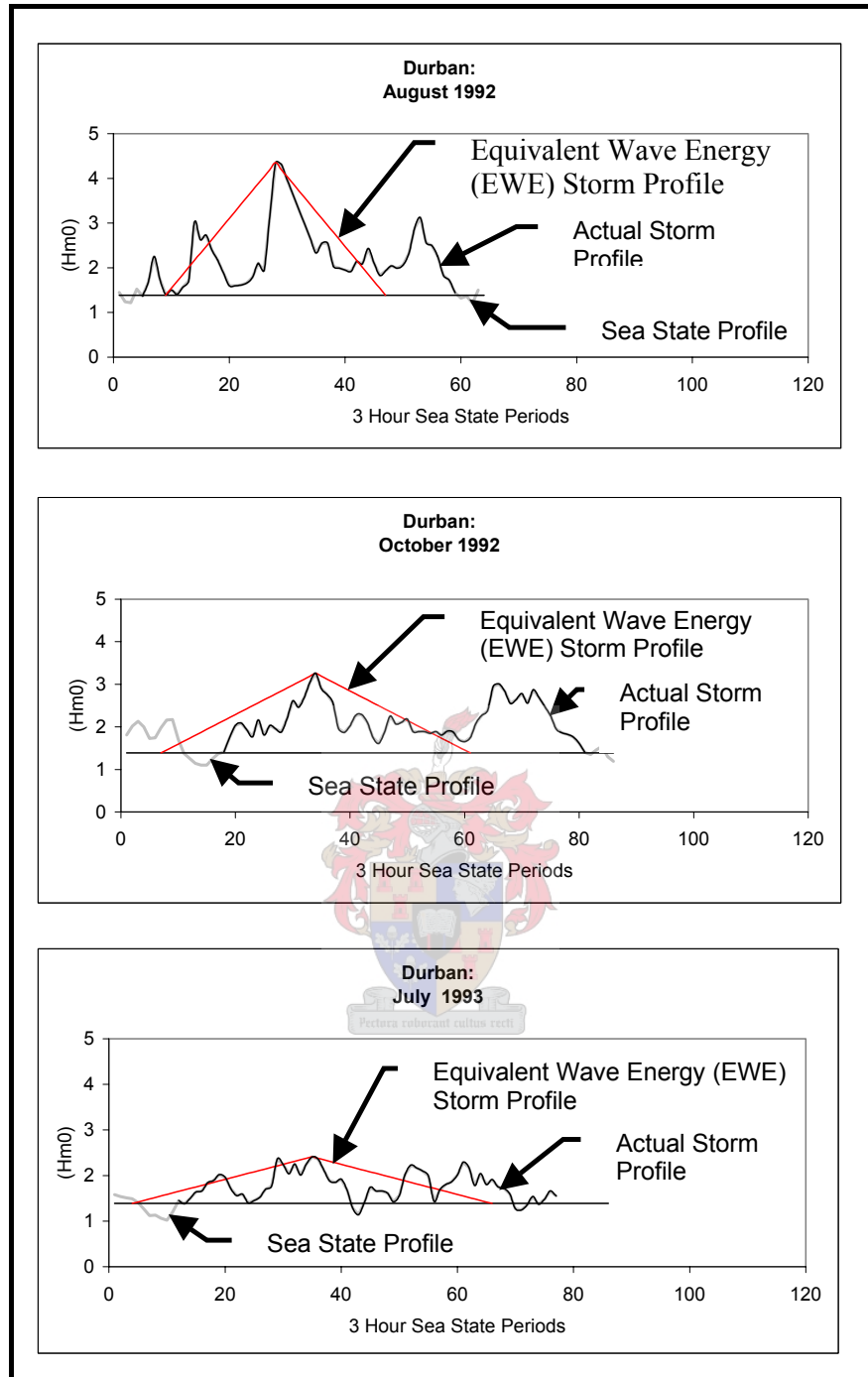


Figure 4.32: Typical Plots of Actual and Equivalent Wave Energy Storm Profiles for the Durban Area

(b) Representative Area Equivalent Wave Energy (EWE) Storm Profiles

Representative Area (EWE) Storm Profiles can be derived on the basis of Regional Average Parameters and these profiles can be used for the comparison of different sea storm regions on the basis of:

- (i) Average Storm Energy levels,
- (ii) Average Maximum Storm Intensities, and
- (iii) Storm Thresholds

Duration of EWE Storm Profile = D_{ewes}

$$D_{(ewes)} = \frac{E_{se(ave)}}{0.5x[(ST + H_{m0(max)}) / 2]^2 x T_{p(ave0)}}$$

Where:

- $E_{se(ave)}$ = Average Actual Storm Energy for the Area (kWh/m)
- $H_{m0(max)}$ = Average Maximum Storm Intensity in the Area (m)
- ST = Storm Threshold for the Area (m)
- $T_{p(ave)}$ = Average T_p for the Actual Storm Sea States for the Area

In this study, the Average Actual Storm Energy values for the different Areas is based on the analysis of 229 storms in the Port Nolloth Area, 107 storms in the Agulhas Bank Area and 152 storms in the Durban Area.

Average EWE Storm Profiles for the Port Nolloth Area, The Agulhas Bank Area and the Durban Area, based on the average energy of the sea storms in the different areas have been shown Figure 4.33.

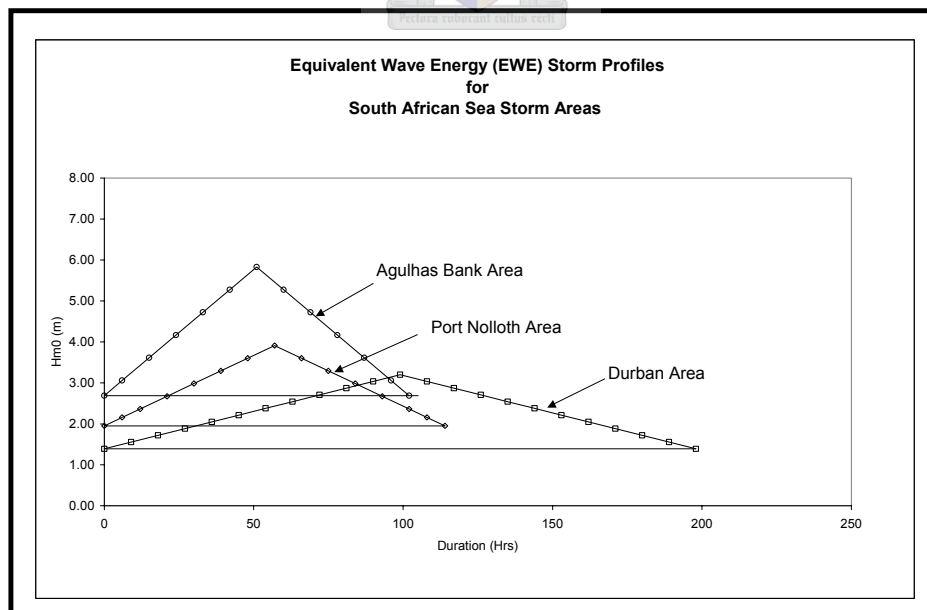
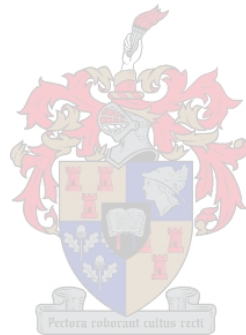


Figure 4.33: Equivalent Wave Energy (EWE) Storm Profiles for the sea storm areas around South Africa

From the profiles in Figure 4.33, it can be seen that :

- (i) Sea Storms with the highest and lowest intensities occur in the Agulhas Bank and Durban Areas respectively, and
- (ii) Sea Storms with the shortest and longest durations occur in the Agulhas Bank and Durban Areas respectively,
- (iii) Sea Storms with the highest and lowest thresholds occur in the Agulhas Bank and Durban Areas respectively,

Given the above, one can expect high energy, frequent storms with short average durations (100 hours or 4 days) in the Agulhas Bank Area, during the storm season. The next most aggressive region, from the point of view of sea storms, is the Port Nolloth area with the Durban Area being the mildest sea storm region. Notwithstanding this position it is worth noting that the sea storms in the Durban Area have the longest duration, on average. Average Sea Storm in this area last some 200 hours (or 8 days), which is twice as long as average storms in the Agulhas Bank Area.



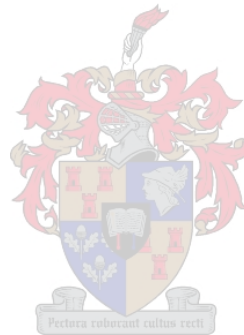
5. FINDINGS

Findings related to correlations between of sea storms and weather types, wave climates, storm frequencies, wave statistics, storm parameters and sea storm processes have been made in this section.

5.1 Correlation of Sea Storms with Weather Types and Synoptic Patterns

The synoptic patterns which influence the sea storms around the coast of South Africa have been discussed in section 2.1.5 above and the frequencies of the sea storms in the different regions is discussed in section 4.3.4 above.

Trend curves for the average occurrences of the above-mentioned weather types and sea storms have been plotted in Figure 5.1. It can be seen from the graphs that the correlation between the frequencies of the weather types, identified as causing sea storms in the different regions, and the storms themselves, is good for each of the three regions. This confirms the dependency of the sea storms on the identified weather patterns for each region.



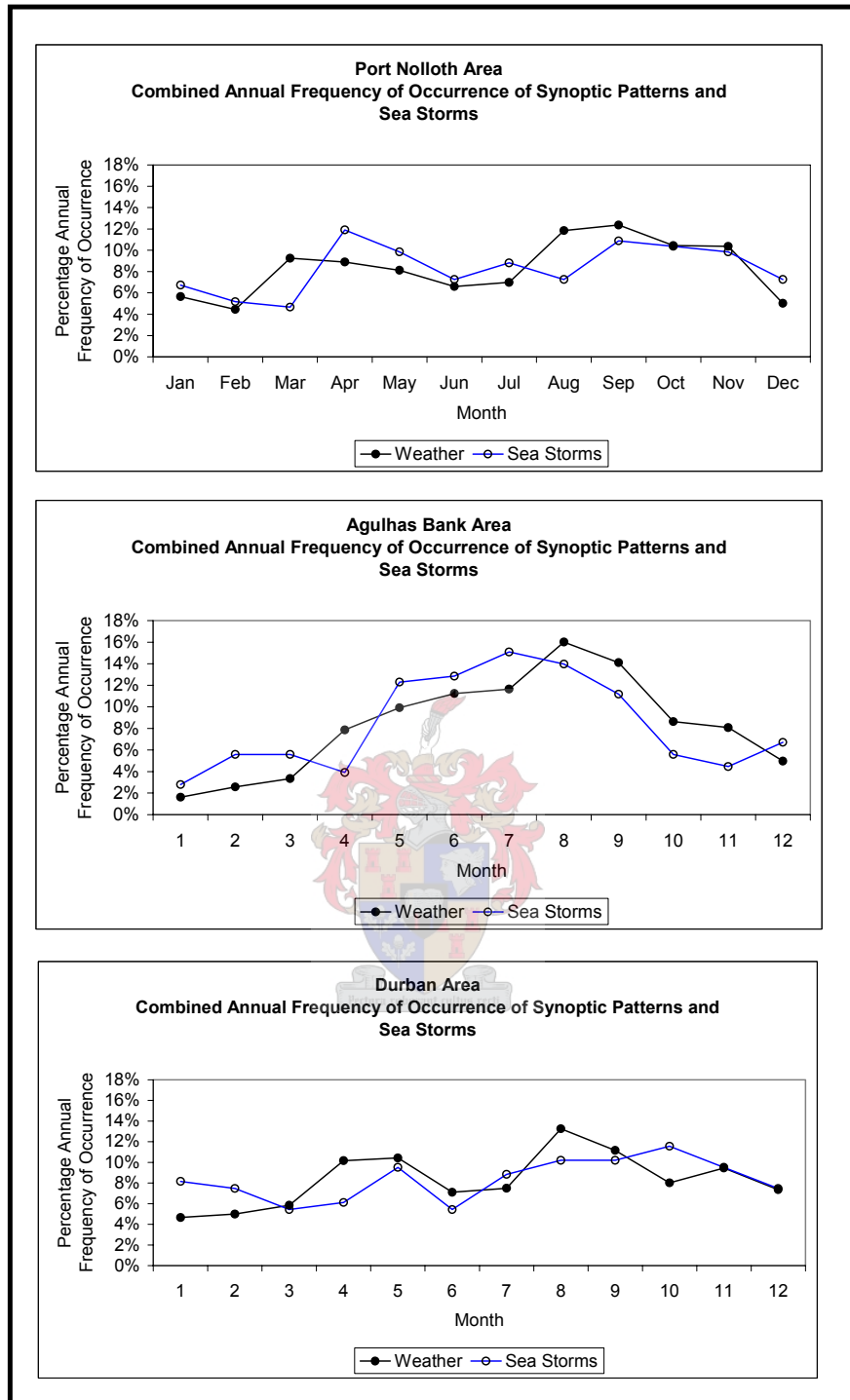


Figure 5.1: Graphs showing the monthly frequencies of occurrence of weather types and sea storms in the different areas.

5.2 Wave Statistics

The frequency of occurrence and probability of exceedance curves of the significant wave heights in the different regions is distinctly different, and this has been shown in Figures 4.8 and 4.9. The highest sea states occur in the Agulhas Bank and Cape Point Areas, with the lowest sea states, based on nearshore measurements, occurring in the Durban Area. Intermediate sea states occur in the Port Nolloth Area.

5.3 Wave Climates

The following two major wave climates, which are discussed in section 2.3.2, are found to relate to the identified South African sea storm regions:

- The West Coast Swell wave climate
- The East Coast Swell wave climate

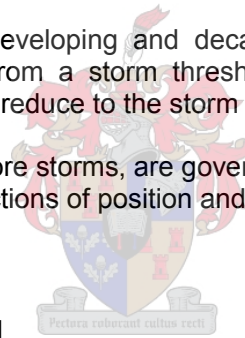
In addition to these already generally accepted major wave climates, another one referred to as the South African Winter Storm Wave Climate (refer to section 2.3.3), is considered to be applicable in winter, when there is a northerly shift in the wind belts.

5.4 Sea Storm Processes

Sea storms pass through a developing and decaying stage associated with the increasing of the sea states from a storm threshold value to a maximum storm intensity value, after which they reduce to the storm threshold value and below.

The above processes, for offshore storms, are governed and effected by the following factors, which are functions of position and time along the path of the atmospheric storm:

- Wind direction
- Wind Speed
- Atmospheric Storm Speed
- Sea Wave Celerity.



In shallow water, sea storm processes are governed by the above factors, as well as water depth, bathymetry and sheltering effects.

The Sea Storm has a profile which develops with time, which can be represented by the intensity of the sea states above the storm threshold level, and which can be reduced to an Equivalent Wave Energy Storm Profile for comparison purposes

All of the above concepts are illustrated in the diagram of the Offshore Storm Process in Figure 5.2.

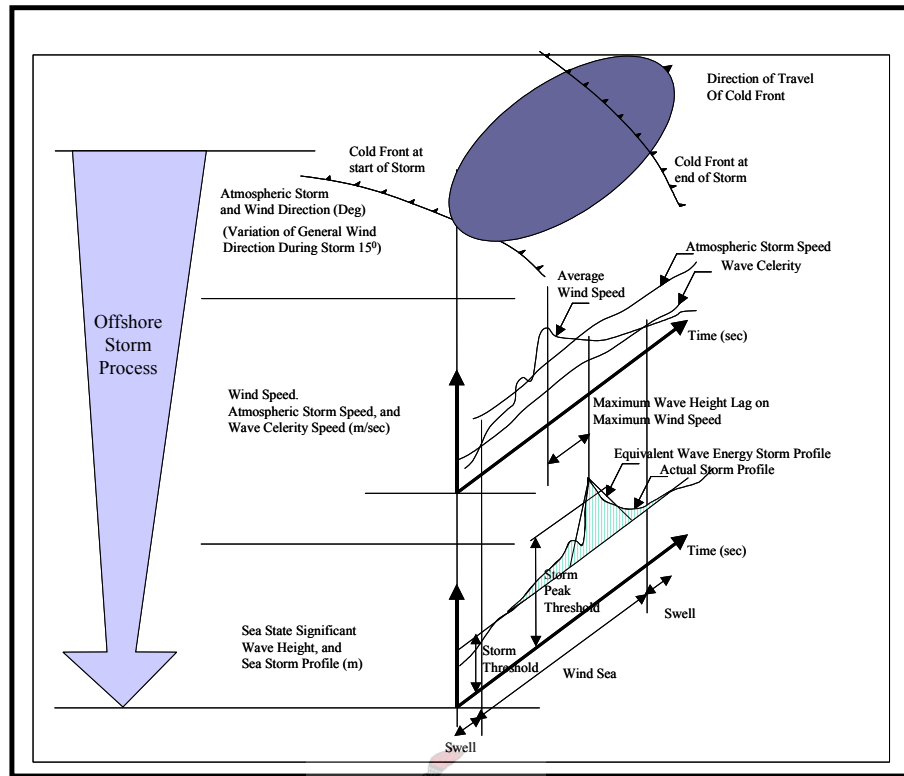


Figure 5.2: Diagram illustrating Offshore Storm Process

5.5 Storm Frequencies

The average monthly occurrences, of the storms in the different regions, have been shown in the graph in Figure 5.3.

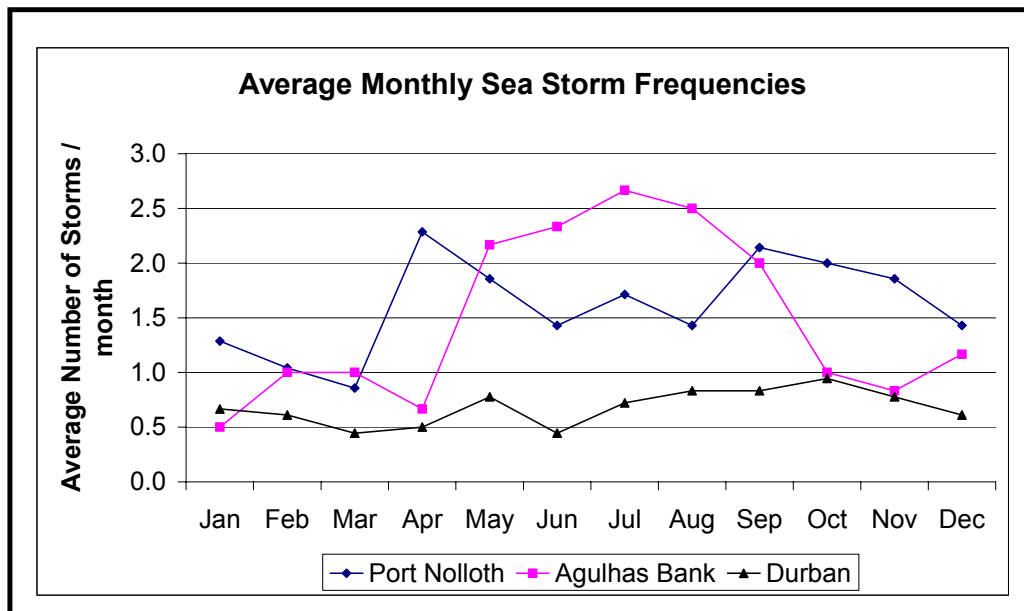


Figure 5.3: Average monthly occurrences, of the storms in the different regions

It can be seen that the distributions of the storms are clearly different for each of the identified regions. The highest average number of 2.6 storms per month occurs in the South African South Coast Region (Agulhas bank Area) in July. The second highest number of sea storms, in the amount of 2.3 on average, occurs in the South African West Coast Region (Port Nolloth Area) in April, during one of its two peaks. The other peak in this Region occurs in September with some 2.2 storms on average. The South African East Coast Region (Durban Area) has a single annual peak average of approximately 1 (one) storm in October.

5.6 Sea Storm Thresholds, Maximum Intensities and Storm Wave Peak Periods.

The average sea storm thresholds, maximum average intensities, and peak storm wave periods, which occur during sea storms in the different regions are distinctly different and have been shown in Table 5.1 below.

Table 5.1: Storm Thresholds, Average Maximum Storm Intensities, and the Average Storm Wave Peak periods

Criteria	South African West Coast Region	South African South Coast Region	South African East Coast Region
Storm Thresholds (Average H_{m0})	1.96m	2.69	1.39
Average Maximum Storm Intensities	3.91 m	5.83 m	3.2 m
Average Storm Wave Peak Periods (T_p)	12.8 sec	11.1 sec	9.7 sec

5.7 Storm Wave Energy Levels

The average Storm Wave Energy levels that occur during the sea storms in the different regions are quite different as shown in Table 5.2

Table 5.2: Average Storm Energy levels

Criteria	South African West Coast Region	South African South Coast Region	South African East Coast Region
Average Storm Wave Energy	6031 kWh/m	9703 kWh/m	5021 kWh/m

The highest and lowest energy storms occur in the South African South Coast and South African East Coast Regions respectively, with intermediate wave energy storms occurring in the South African West Coast Region.

The Equivalent Wave Energy sea storm profiles, which are discussed in section 4.3.8 above are distinctly different and have been shown in Figure 4.33.

5.8 Characteristics of Sea Storms

Sea Storms around the South African coast can be characterised on the basis of the following parameters:

- (i) Storm Thresholds
- (ii) Maximum Intensities
- (iii) Storm Durations
- (iv) Wave Energy Levels

The above parameters can all be incorporated into the Equivalent Wave Energy Storm Profile for any given storm. This provides the opportunity for any given storm to be compared with another storm in the same region or elsewhere, on an objective scientific basis in terms of Energy Level, Storm Threshold, Maximum Intensity and Duration.

Average EWE Storm Profiles for the South African Sea Storm Regions have been given in Figure 5.4

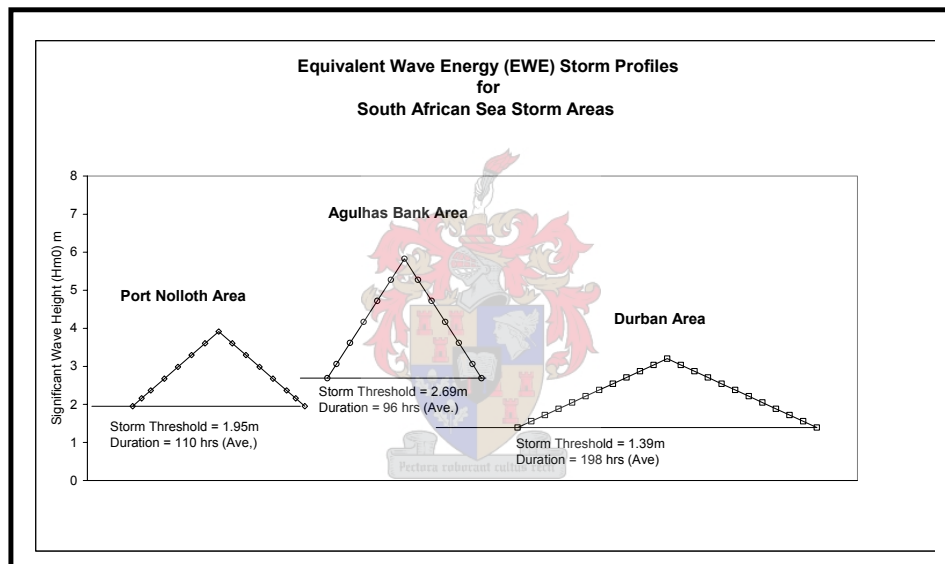


Figure 5.4: Average EWE Storm Profiles for the South African Sea Storm Regions

The different EWE Storm Profiles have different degrees of “steepness” which can be measured in terms of the ratio of the Maximum Storm Intensity less the Storm Threshold, in meters, divided by the Equivalent Storm Duration, in days. This ratio for the average EWE Storm Profiles in the different regions around the South African Coast are given in Table 5.3.

Table 5.3: Steepness ratios for Regional EWE Storms

Storm Area	Port Nolloth Area	Agulhas Bank Area	Durban Area
Steepness Ratio	$\frac{3.9-2.0}{4.58} = 0.42$	$\frac{5.8-2.7}{4.00} = 0.78$	$\frac{3.20-1.4}{8.25} = 0.22$

The steepness ratios are considered to be an indication of risk for the given storm. An EWE Storm, with a high steepness ratio, will generally cause more damage than one with a low steepness ratio as the Energy of the former storm event is delivered at a higher rate.

In general, actual storm durations will always exceed the duration of the EWE Storm profile. This is because actual storms do not usually have uniform development and decay slopes. Given this situation the ratio of Actual Storm Durations / EWE Storm Durations can vary from 1.0 to 2.0, depending on the development and decay slopes of the actual storms. Storm Duration Ratios for the Actual and EWE Storm Profiles in Figures 4.29 to 4.32 have been given in Table 5.4



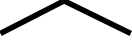
Table 5.4: Storm Duration Ratios

Storm Description		Storm Duration Ratio $= \frac{\text{ActualStormDuration}}{\text{EWEStormDuration}}$	Average Ratios for Sea Areas
Port Nolloth Area	May 1987:Storm No. 1	1.3	1.3
	May 1987: Storm No. 2	1.3	
	November 1987:Storm No. 3	1.2	
Cape Point Area	August 2000: Storm No. 1	1.7	1.4
	August 2001: Storm No. 2.	2.0*	
	July 2003: Storm No. 3	1.1	
Agulhas Bank Area	January 1998	1.0	1.2
	April 1998: Storm No. 1	1.3	
	May 1998: Storm No. 1	1.4	
Durban Area	August 1992	1.6	1.3
	October 1992	1.3	
	July 1993	1.1	

* Denotes high value due to extreme maximum storm intensity.

The above characteristics of South African Sea Storms have been summarised in Table 5.5.

Table 5.5: Characteristics of South African Sea Storms

Storm Area			Port Nolloth Area	Agulhas Bank Area	Durban Area
Synoptic Pattern causing Sea Storms			West Coast Low	Westerly Wave and Cold Snap	East Coast Low
			Cut-off-Low		
				Continental High	
Major Wave Climates			West Coast Swell	South Coast Winter Storm	East Coast Swell
Frequency of Storms	Peaks / Year	Number of Peaks	2	1	1
		Month/s of Occurrence	April and September	July	October
	Peak Number of storms / month		2.2 to 2.3	2.6	1.0
Sea State Parameters (Hs)	Frequency of Occurrence	Max. Occurring Hs	1.8m	2.4m	1.4
		Probability of Exceedance	55%	51%	70%
	1:100 Year Significant Wave Height		9.3m	12.1m	7.7m
Storm Parameters	Storm Threshold (ST)		2.0m	2.7m	1.4m
	Average Maximum Intensity		3.9m	5.8m	3.2m
	Average Storm Wave Peak Period (Tp)		12.8 sec	11.1 sec	9.7 sec
	Ave Storm Duration		110 hours	97 hours	198 hours
	Average Storm Energy Level		6031 kW/m	9703 kW/m	5021 kW/m
EWE Storm Profile (Sea State Intensity > Storm Threshold)	Profile				
	Steepness Ratio: $\frac{\text{Max Intensity}-\text{ST}}{\text{Duration}}$ (m/days)		$\frac{3.9-2.0}{4.58} = 0.42$	$\frac{5.8-2.7}{4.00} = 0.78$	$\frac{3.20-1.4}{8.25} = 0.22$

5.9 Proposed Sea Storm Regions

Based on the information derived from the available data, it appears that the South African coastline can be divided into three Sea Storm Regions. The Regions are based on the **Weather Types and Synoptic Patterns** that cause the weather in the regions as well as their **Wave Statistics** and their **Storm Processes and Characteristics**. The following regions are proposed:

- (i) The South African West Coast (SAWC) Region
- (ii) The South African South Coast (SASC) Region
- (iii) The South African East Coast (SAEC) Region

The above regions have been shown in Figure 5.5 and they conform very closely to the METAREA VII coastal regions shown in Figure 5.6.

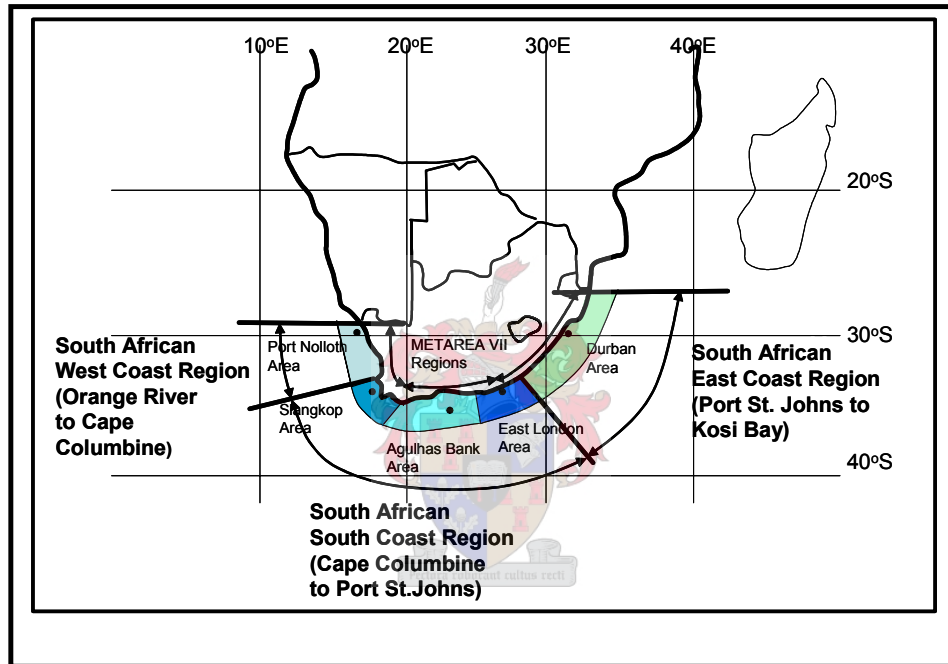


Figure 5.5: South African Sea Storm Regions

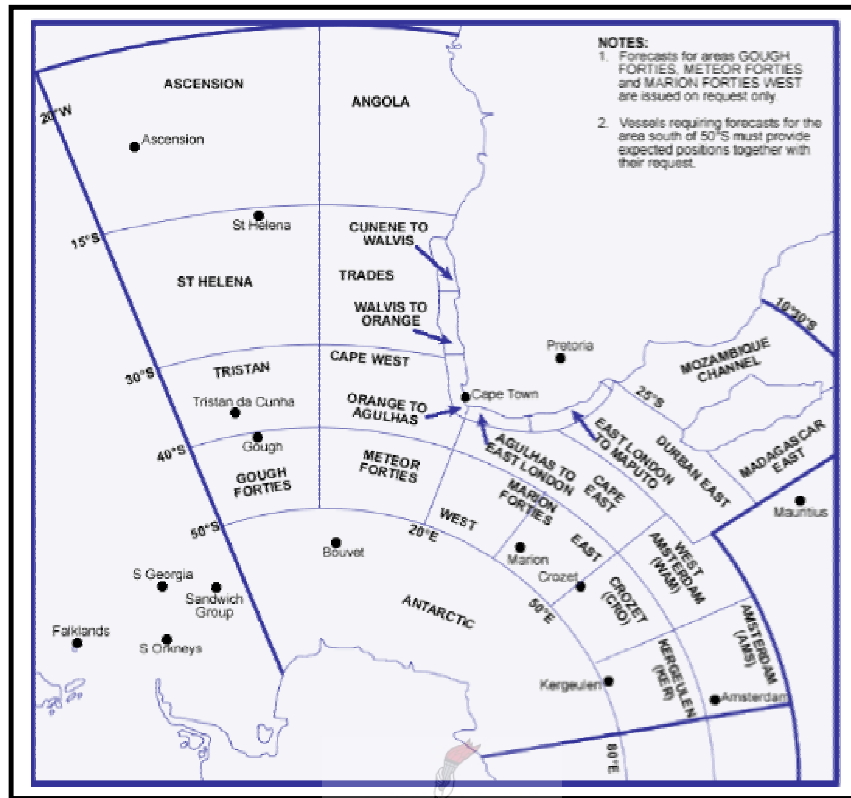


Figure 5.6: Marine METAREA VII [SA Weather Services]



6. SUMMARY AND CONCLUSIONS

Sea Storms are high-energy events of finite duration, which effect Ships at sea, Offshore Structures, Coastal Engineering Structures, Coastal Engineering Construction Works and Natural Coastlines.

Waves, arising from sea storms, are probably the most significant hydraulic parameter in the Design and Risk Management Process, and an understanding of storm events, as well as the ability to mitigate their negative impacts, are important aspects of Coastal Engineering.

Significant factors, which govern the impact of Sea Storm, include the following: -

- (i) Their intensity
- (ii) Their duration,
- (iii) Their frequency of occurrence, and
- (iv) Their Energy Level.

Storm durations affect the construction stages of a Coastal Engineering Project more than Permanent Works due to the fact that they can cause:

- (i) Damage to exposed, vulnerable, construction faces, and
- (ii) Increased downtime periods,

The frequency of occurrence of storms also affects construction stages more than Permanent Works, due to the fact that a second and third storm, occurring soon after an earlier one, can compound damage from the earlier storm/s, which may not have been fully repaired at the time.

Sea Storms are non-stationary processes comprised of a series of sea states with varying wave spectra and significant wave heights. Storms are normally analysed in the short term, on the basis of either the statistical properties of the water surface displacements or the spectral properties of the waves, to derive a significant wave height (H_s), and on a long term basis by either the statistical analysis of the distribution of the significant wave heights or quasi-deterministic methods, to determine extreme values.

Sea Storms are created by the transfer of kinetic energy, from the movement of the air above the surface of the sea, to a combination of potential and kinetic energy within the sea itself. The velocity of the air over the surface of the sea during a storm has two components consisting of:

- (i) The velocity of the weather system causing the atmospheric storm, such as low pressure systems, and
- (ii) The velocity of the air moving from high to low pressure areas within the weather system, over the sea

The following stages in the development of atmospheric and sea storms have been identified off the southern coastline of South Africa, in the Agulhas Bank area, where meteorological data has been collected together with sea state data, and they are considered to comprise, what we call, an offshore storm process. This process can be characterised by the following sequence of events:

- (i) The **alignment of the wind**
- (ii) The **increasing of the wind speed** until it reaches a speed where it exceeds the celerity of the wave group in the sea, and a wind sea develops.
- (iii) **The increasing of sea state intensities**, as reflected by significant wave heights, to the point where they exceed the storm threshold equal to the annual average significant wave height for the area, which marks the beginning of the sea storm.
- (iv) **The continued increasing of sea state**, as reflected by significant wave heights, to the point where it exceeds 1.5 x the annual average significant wave in the area, for a continuous period of not less than 12 hours.
- (v) The **peaking of the wind speed**, after which it starts to fall as the atmospheric storm overtakes the sea storm.
- (vi) The **peaking of sea state**, after which it starts to decay.
- (vii) The **continued decay of the wind speed** until it falls below the celerity of the wave group in the sea, and the wind sea changes to a swell.
- (viii) The **continued decay of the sea state** to a point where it falls below the storm threshold value, marking the end of the sea storm.

Typical **average wind speeds**, which cause sea storms in the Agulhas Bank area have been found to range from about 5 m/sec (18 km/hr) to about 30 m/sec (110 km/hr).

Typical **wave group celerities** of the storms, based on average zero crossing periods (T_z) of about 7 seconds to 12 seconds, range from about 6 m/sec (20 km/hr), to 10 m/sec (36 km/hr).

Typical **atmospheric storm speeds** in the Agulhas Bank area range from about 10 m/sec (36 km/hr) to 17 m/sec (61 km/hr).

Given the above, the atmospheric storms, which create the sea storms, will overtake the waves they create in the sea. This means that the largest waves in a sea storm will arrive at a given location in the sea after the local wind speed has reached a maximum and started to fall.

A sea storm is generally defined in terms of wind speed as follows:

“A Storm occurs when wind forces exceed 8 on the Beaufort scale”.

A Wind force of 8 on the Beaufort scale corresponds to a average wind speed of about 17 m/sec.

Boccotti (2000) has defined a sea storm as “a sequence of sea states in which the significant wave height exceeds the fixed threshold of $1.5 \times H_{S(ave)}$ and does not fall below this threshold for a continuous time interval greater than 12 hours”, where $H_{S(ave)}$ is the mean annual significant wave height on the examined site.

In this study a modified definition is proposed for South African Sea Storms as follows:

“a sequence of sea states in which the significant wave height exceeds the fixed threshold of $1.5 \times H_{s(ave)}$ for at least one continuous time interval greater than 12 hours, during a period when the sea states have a significant wave height greater than the storm threshold value of $H_{s(ave)}$ ”, where $H_{s(ave)}$ is the mean annual significant wave height on the examined site.

The difference between the first and the second of the above definitions is that the second one allows for the fact that a sequence of sea states can fall below the fixed threshold for a significant period of time (>12 hours) before exceeding it again in a single storm.

It has been found to be necessary to modify Boccotti's definition of a storm, to define a South African Storm, due to types of sea states that are encountered around the South African coastline. These sea states are caused by weather patterns with generally sustained high winds, which blow over long fetches (in the order of 900km) for significant periods of time (in the order of 2 to 4 days). The aforementioned “generally sustained high wind” conditions are subject to some degree of variation about a high average value, and this can result in typical multiple peaks during the sea storms.

The profile of a sea storm on the South African Coastline can be defined as “the intensity of the sea states above the storm threshold level for the duration of the storm”, that is until the sea state intensity falls below the storm threshold level. The sea state intensity is defined by the maximum significant wave height of the sea state for the period in question. Typical sea state recording intervals are 1 hour or 3 hours.

The energy of a wave has its genesis in differential solar energy (heat), which causes air to move from areas of high pressure to areas of low pressure in a circular manner due to the Coriolis effect. This air mass transfer phenomenon causes the build up of kinetic energy in the atmosphere and its transfer to the sea, over which the wind blows, in the form of potential energy, kinetic energy and surface tension energy.

The surface tension component of the transferred energy can be considered to be small, and negligible, when compared with the levels of potential and kinetic energy, which have values of the same magnitude.

Energy in the ocean is transferred from one point to another by gravity waves, which represent the flow of energy rather than the flow of water. In deep water, where waves cause cyclical vertical water level variations with orbital water molecule movements, the lateral net movement of water is minimal, but the lateral transfer of energy is significant.

If one considers that a storm is comprised of a series of sea states, which have representative significant wave heights and periods and therefore Energy Flux, then one could derive a Storm Energy Flux by multiplying the Wave Energy Flux per meter length of wave crest, for each sea state, times the duration of the relevant sea state and summing the total for a given storm.

In this thesis, an **Equivalent Wave Energy (EWE) Storm Profile** for individual storms has been derived on the basis that:

- i. The **Maximum Storm Intensity**, or Maximum Significant Wave Height, $(H_{m0})_{\max}$ of the EWE Storm is the same as the Maximum Storm Intensity for the actual storm.
- ii. The **Storm Threshold** for the EWE Storm would be the same as that of the actual storm
- iii. The **Storm energy Flux (SEF)** for the EWE Storm would be the same as that for the actual storm.
- iv. The **Duration** of the EWE Storm could be calculated on the basis of (i), (ii) and (iii) above, assuming a symmetric, triangular “Capital Lambda” (Λ), shaped linear profile for the EWE Storm.

This research adds to the background “Body of Knowledge” relating to the character of the sea storms in the Regions around South Africa.

The following five main conclusions evolved from this study:

- (i) The occurrence of Sea Storms can be correlated with the occurrence of Atmospheric Weather Types and Synoptic Patterns,
- (ii) Characteristic Wave Statistics can be derived for Sea Storm Areas from selected recording stations,
- (iii) Sea Storm Processes, including recorded wind and wave parameters associated with the storms, can be identified and characterised,
- (iv) Equivalent Wave Energy (EWE) Storm Profiles can be derived from actual sea storm profiles and used as the basis for the comparison of storm events.
- (v) Based on the above, the South African Coastline can be divided into the following three Sea Storm Regions:
 - a) The South African West Coast (SAWC) Region
 - b) The South African South Coast (SASC) Region
 - c) The South African East Coast (SAEC) Region

More research could be carried out on the determination of a Storm Prediction Model, which could be developed for the different regions, on the basis of generating wind characteristics, to facilitate planning and engineering activities in them.

K R MacHutchon

REFERENCES

Boccotti P, 2000. **“Wave Mechanics for Ocean Engineering”** a Book published by Elsevier Science

Boebel O, 1998. **“South Atlantic Currents”**, Notes on the KAPEX (Cape of Good Hope Experiment) Project

Coastal Engineering Manual (CEM), US Army Corp of Engineers, 2004

Csanady GT, 2001. **“Air-Sea Interaction: Laws and Mechanisms”**, a Book published by Cambridge University Press.

EMEC Standard, 2004. **“Performance Assessment for Open Wave Energy Conversion Systems in Open Sea Test Facilities”** a standard published by the European Marine Energy Centre, Orkney, UK.

Farrell BF and Ioannou, 2005. **“Generalised Stability Analysis of Wind Generated Surface Water Waves”**, a Technical Paper under consideration for publication in Journal Fluid Mechanics.

Gerwick BC, 2000 **“Construction of Marine and Offshore Structures”**, a Book published by CRC Press LLC

Hagerman G, 2001. **“Southern New England Wave Energy Resource Potential”** a Technical Paper presented at the Building Energy 2001 conference in Boston in March 2001

Herbich JB, 1990. **“Handbook of Coastal and Ocean Engineering: Volume 1: Wave Phenomena and Coastal Structures”**, a Book published by Gulf Publishing Company

Jone ISF, 200. **“ Wind Stress over the Ocean”**, a Book published by Cambridge University Press

Lavranov IV, 2003. **“Wind-Waves in the Ocean: Dynamics and Numerical Simulations”**, a Book published by Springer

Mallory JK, 1974. **“Abnormal Waves on the South East Coast of South Africa”**, a Technical Paper published in the International Hydrographic review Vol. L1. No 2. J

Reeve D et al, 2004. **“Coastal Engineering Processes - Theory and Design Practice”** a Book published by Spon Press

Reynolds R, 2004 **“Philips Guide to Weather”**, a Book published by a Division of the Octopus Publishing Group Ltd

Rossouw J, 1989 **“Design waves for the South African Coastline”**, a PHD Thesis at the University of Stellenbosch.

Russell RCH et al, 1954. **“Waves and Tides”**, a Book published by Hutchinson's London.

Simm, J et al, 1998. **“Construction Risk in Coastal Engineering”**, a Book published by Thomas Telford Publishing

Stull RB, 2000. “**Meteorology for Scientists and Engineers**”. A Book published by Brooks / Cole Thompson Learning

SWAN Manual, Version 40.51, August 2006

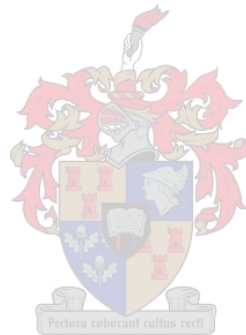
Thurman HV at al, 2002 “**Essential of Oceanography**”, a Book published by Prentice-Hall Inc.

Tyson PD and Preston-Whyte RA, 2000 “**The Weather and Climate of Southern Africa**”, a Book published by Oxford University Press

Watts A, 2004 “**The Weather Handbook**”, a Book published Adlard Coles Nautical

Wells N, 1998. “**The Atmosphere and the Ocean – A Physical Introduction**”, a Book published by John Wiley and Sons

Woodroffe CD, 2002. “**Coasts: Form, Process and Evolution**”, a Book published by Cambridge University Press

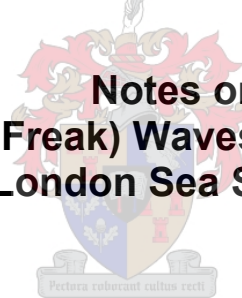


APPENDICES



APPENDIX A

Notes on Very Large (Freak) Waves that occur in the East London Sea Storm Area.



Very Large (Freak) Waves that occur in the East London Sea Storm Area.

1 The Wave Regime

The waves in the East London Sea Storm Area are not only those directly associated with the wind blowing at the time but are a combination of the locally generated waves and those coming up from the Southern and Western Ocean, where they have been generated over vast distances up to 2000km. It has been stated that the centre of the depression, the outskirts of which reach the southern and southeastern shores of South Africa, usually passes over Marion Island during the winter months from May to October. The fetch of the southwesterly wind is 2000 km or more, hence the waves generated by this wind are fully developed and will therefore have reached their maximum height and length by the time they reach the vicinity of Port Elizabeth. These maxima will of course depend upon the velocity of, and the duration for which the wind has been blowing.

Even though the wind along the coast may not be very strong these ocean waves still come rolling in. There may be more than one source generating such fully-fledged waves, having differing wavelengths and frequencies. The locally generated waves are shorter and steeper. All these are greatly affected by the southwesterly flowing Agulhas Current which tends to shorten the wave length and raise the height of the sea, and this effect is of course more pronounced where the opposing current is strongest, i.e. just outside the 100 fathom (200 m) line. Because the wavelengths of the local waves and the long distance waves differ to a considerable degree, they are frequently being momentarily superimposed one upon another, thereby increasing the height.

It may so happen that there are occasions when all the wave trains are in conjunction, and a gigantic wave forms for a few minutes, after which the separate waves become disunited and the wave heights return to normal.

These abnormally high waves are naturally associated with correspondingly deep troughs. If these were of a normal sinusoidal character, a ship would rise up to the approaching wave and no severe damage would occur, other than taking some green water over the bow.

However, this is not the case with these abnormal waves, hence the reason why they have been referred to previously as “freak” waves. It would appear that as the differing orbital motions of the waves become integrated whilst under the influence of the current flowing strongly against the direction of the waves, an abnormally high steep wave is formed. These waves have been reported to be in excess of 18 m in height, and have always been associated with a correspondingly long deep trough – which occurs in advance of a steep wave crest. It is this phenomenon which constitutes the great danger to a vessel steaming into the sea at speed, and which has given rise to the expression “a hole in the sea”. [JK Mallory, 1974]

Lavranov (2003) notes that the phenomenon of abnormal waves cannot be explained from the point of view of a linear wave superposition. In particular, it is impossible to explain the wave shape, its asymmetrical profile with a long deep trough, the “hole in the sea” situated in front of the high steep crest and its sudden appearance .

At present, due to the absence of theory and field measurements, it is practically impossible to forecast abnormal waves. However, on the basis of the above described facts and the analysis of similar events presented by Mallory (1974), it is possible to specify the main hydro-meteorological conditions, under which the occurrence of abnormal waves is most probable in this region. They are as follows: -

- The appearance of waves is most likely in the Agulhas Current in the area with the maximum velocity of 3 to 5 knots, coinciding approximately with a 200 m isobath and deeper. The probability of the appearance of a wave rapidly decreases, approaching the coast from the 200 m isobath.
- Approximately a day before the appearance of abnormal waves, a cyclone with atmospheric pressure of 980-995 hPa is observed on the synoptic map over Marion Island. The isobaths on the map are elongated southwestward to the south of Africa. A cold atmospheric front propagates with a speed of about 15 knots to the northeast along the coast.
- Several hours before the appearance of the abnormal wave a strong persistent northeasterly wind being blowing along the southeastern coast of Africa increasing the maximum current velocity to 4-5 knots.
- There is a rapid change of wind direction while passing the cold atmospheric front. The change of the northeasterly wind with a force of 6 knots to the southeasterly wind with a force of 6-7 knots occurs within 4 hours.
- The local southwesterly wind rapidly increases the wind wave, on which the southwest direction swell is superimposed propagating opposite to the Agulhas Current.

2 The spatial distribution of the speed of the Agulhas Current.

At present there are no theories explaining the abnormal wave phenomenon, appearing under the above described conditions. The propagation of a cold atmospheric front results in so-called “frontal swell waves” which in combination with wind waves can generate waves of a greater amplitude (Ivanenkov et al., 1977). However, the appearance of abnormal waves cannot be explained by these factors alone.

Some other factors will be investigated, in this monograph, in particular, swell transformation in the Agulhas Current, which is a necessary condition for freak wave generation. According to Smith (1976) the appearance of large waves in the Agulhas Current was explained by a local wave pattern generated by wave reflection from the current. However, the problem of large-scale wave transformation in a current was not considered.

Abnormal waves are typically observed on the ocean surface, where the depth approximately coincides with a 200 m isobath. The latter passes parallel to the coastline. It is the boundary of the continental shelf, where the depth increases sharply to 3-4km. That is why it was initially assumed that this abrupt depth change was actually the cause of the abnormal wave formation (Mallory, 1974). But, in reality, the bottom relief in a 200 m depth can influence only waves with lengths more than 500 m. It should be noted that typical horizontal dimensions of abnormal waves are much shorter.

The sharp depth variation at the continental shelf margin results in the maximum values of the Agulhas Current, having a jet profile directed parallel to the shoreline. The transversal profile of the Agulhas Current velocity distribution is not changed much along its entire length from the Mozambique and South Madagascar current confluence at latitude 30-degree south. A typical horizontal profile of the current velocity distribution in the transversal direction (Schumann, 1976) is shown in Figure A1. The Ox axis of the coordinate system is chosen along the current velocity direction, and the Oy axis is in the perpendicular direction.

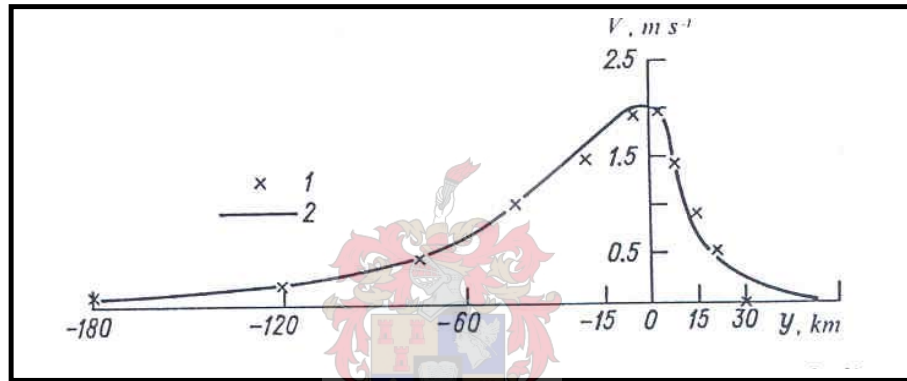


Figure A1: Horizontal current velocity distribution in transversal direction, based on 1-velocity values according to Schuman (1976); and 2-the approximation given on equation 1 [Lavranov, 2003].

The transverse profile of the current velocity $\mathbf{V} = \{V_x(y), 0\}$ in this area can be quite accurately approximated by the relation:

$$V_x = b_1 / (1 + b_2 y^2) \quad (1)$$

where: $b_1 = 2.2 \text{ ms}^{-1}$; $b_2 = 6.25 \times 10^{-10} \text{ m}^{-2}$ at $y < 0$; $b_2 = 10^{-8} \text{ m}^{-2}$ at $y > 0$.

The current velocity distribution (1) is assumed to be valid at $x < 0$ in the chosen coordinate system. The point $\{x = 0, y = 0\}$ is assumed to correspond to the current velocity midstream at the point with coordinates $\{27^\circ\text{E}, 34^\circ\text{S}\}$. The Agulhas Current diverges in a fan-shaped manner at more southern latitudes, becoming weaker.

In accordance with the Atlas (1977), it can be assumed that in the case $x > 0$, the horizontal current velocity components $\mathbf{V} = \{V_x(x, y), V_y(x, y)\}$, satisfying the continuity equation, are approximated by the equations:

$$V_x = b_1 / [(1 + b_2 y^2)(1 + b_3 x^2)] \quad (2)$$

$$V_y = 2b_1 b_3 x (\arctan(b_2^{.5} y)) / [(1 + b_3 x^2) y^{.5}] \quad (3)$$

where $b_3 = 0.6 \times 10^{-11} \text{ m}^{-2}$

The transverse velocity, V_x , has been calculated at 100 km intervals along the centre line of the Agulhas current, proceeding to the north east from the origin defined above, on the basis of the approximation in equation (2), and the different profiles have been shown on Figure A2.

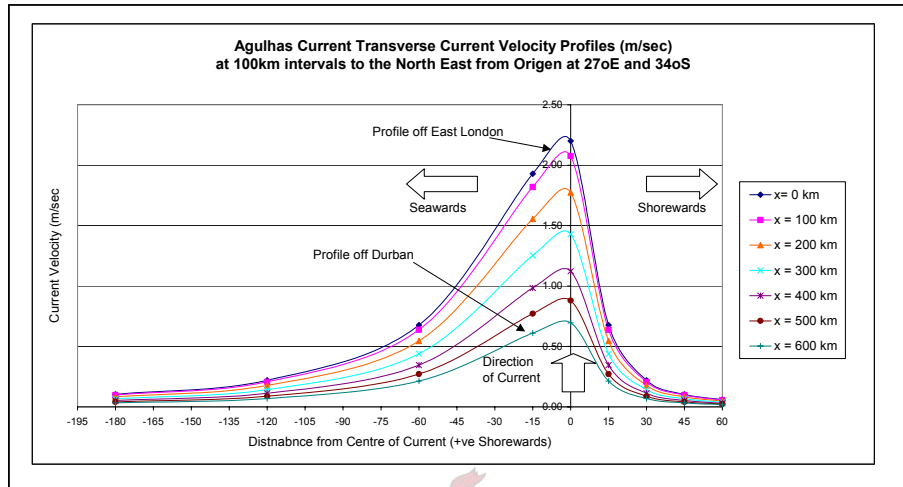
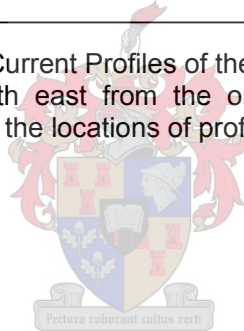


Figure A2: Transverse Current Profiles of the Agulhas Current, at 100 km intervals north east from the origin at {27°E, 34°S}. (Refer to Figure A3 for the locations of profiles).



A surface plot of the Agulhas Current Profile, viewed from the landside, has been shown in relation to the adjacent coastline in Figure A3.

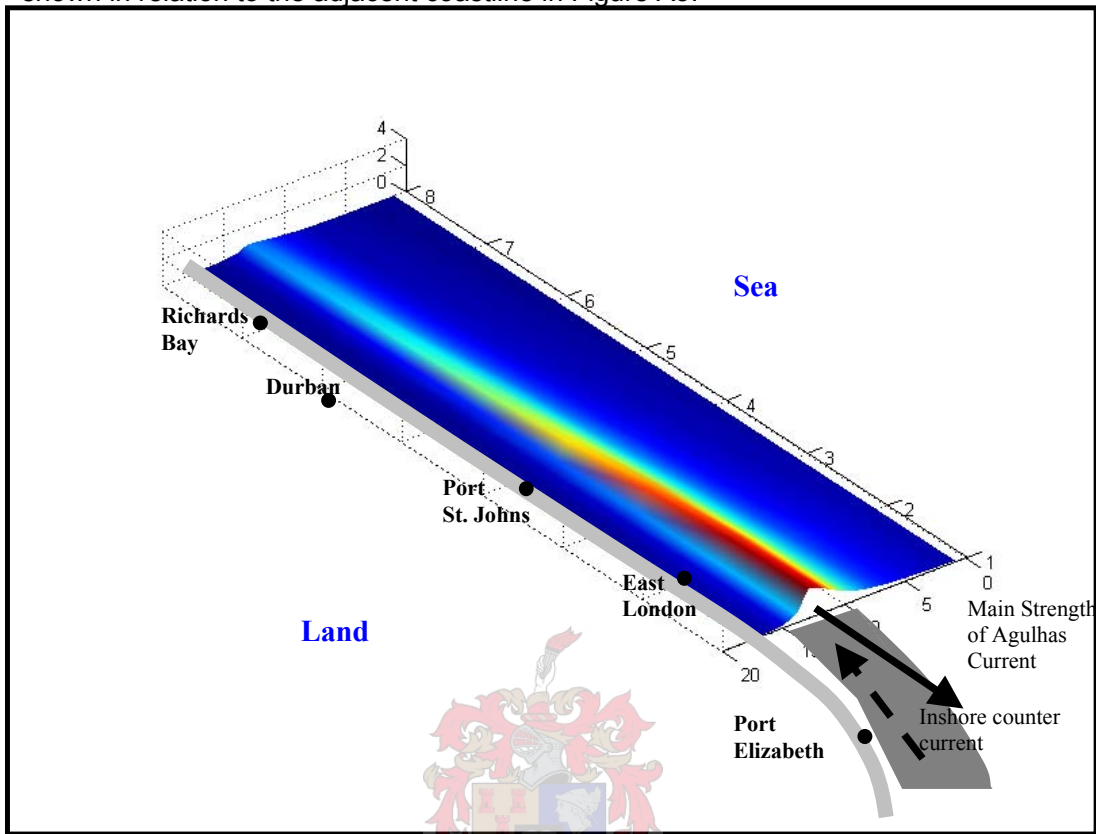


Figure A3: A surface plot of the Agulhas Current Profile, viewed from the landside together with coastal features.

3 The Relative Mean Wave Heights in the Agulhas Current

Lavranov (2003) has found that the relative mean wave height h/h_0 in the current (where h_0 is the initial wave height without any current) varies as shown in Figure A4.

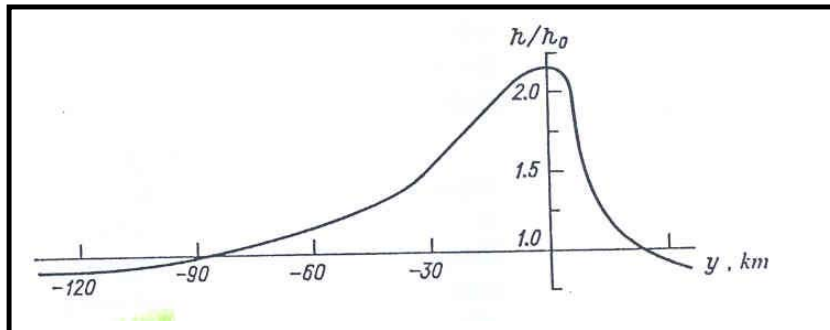
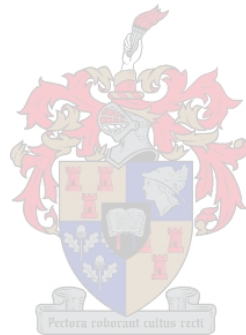


Figure A4: Variation in relative mean wave height h/h_0 in the current

“The maximum value of $h/h_0 = 2.19$ is estimated as being in the midstream. The ratio of h/h_0 is sharply decreased along the distance to the shoreline. The excess of the wave height is not greater than 10% at a distance of $y = 19$ km from the maximum current velocity line. Seaward to the mainstream, the relative height h/h_0 is decreased to a lesser extent with a 10% excess in wave height excess occurring at $y = -70$ km. But the reversed case (i.e., $h < h_0$) is even observed at $y > 90$ km.” [Lavranov, 2003].

The above theoretical estimation of wave height was proved by satellite observation, obtained by Grundlingh and Rossouw (1995).

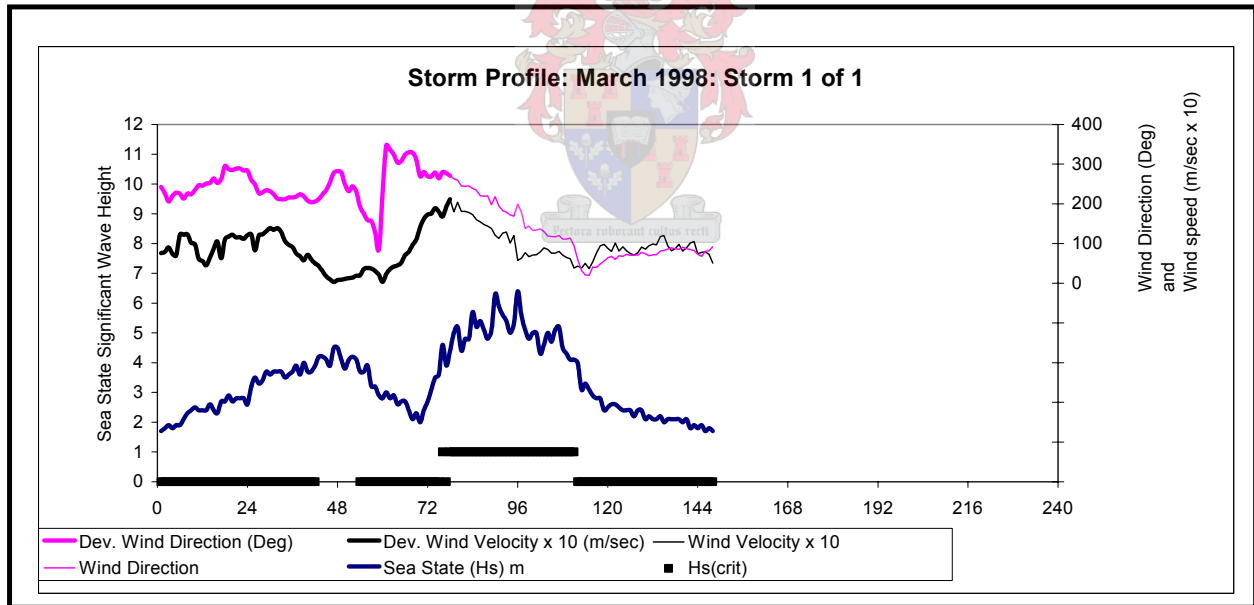
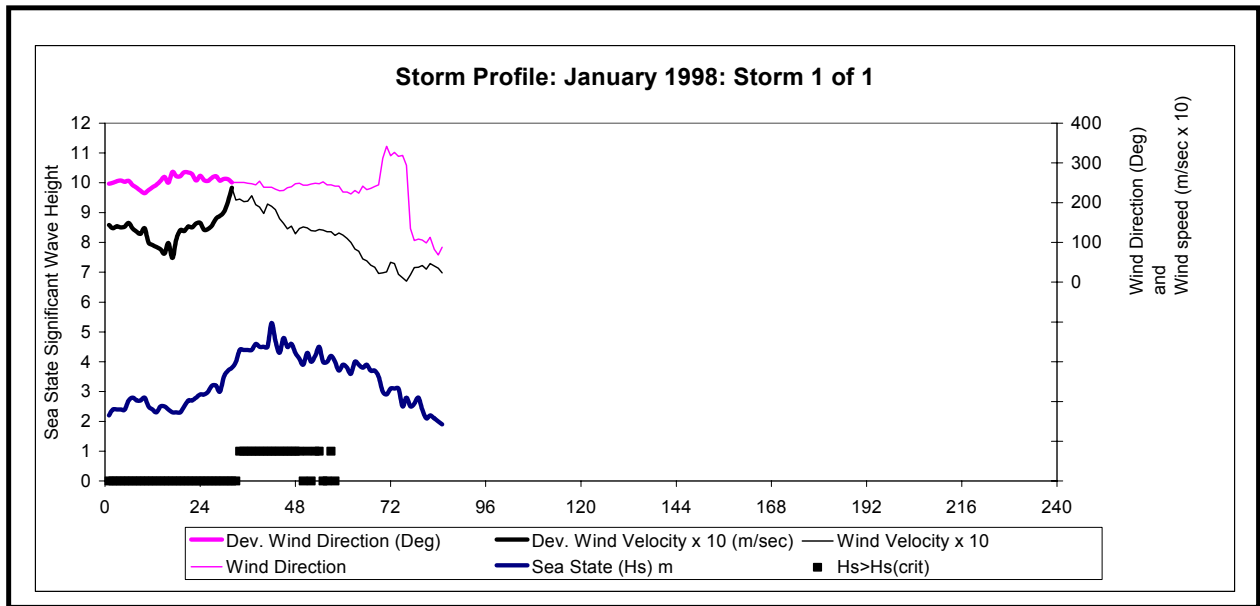
The Raleigh distribution provides for the fact that H_{max} can be as high as 1.5 to 2.0 times H_s (or H_{m0}), depending on the recording interval, which could be 1 hour or 3 hours. In the case of a 1 hour recording interval H_{max} could be $1.5 \times H_s$, and for a 3 hourly recording interval H_{max} could be $2.0 \times H_s$ [Rossouw, 1989]

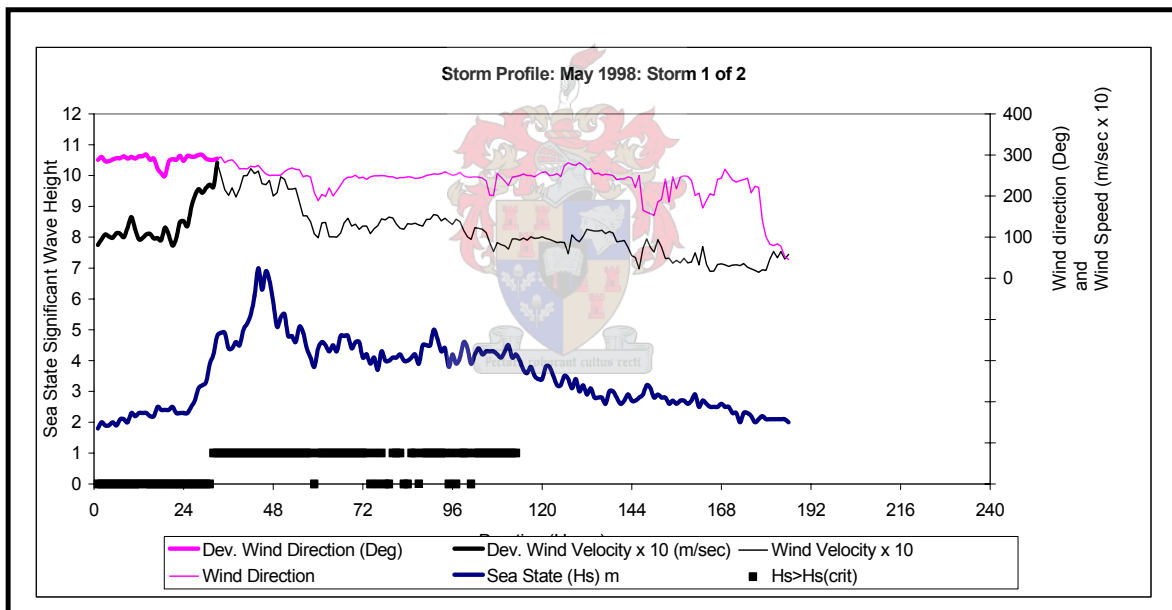
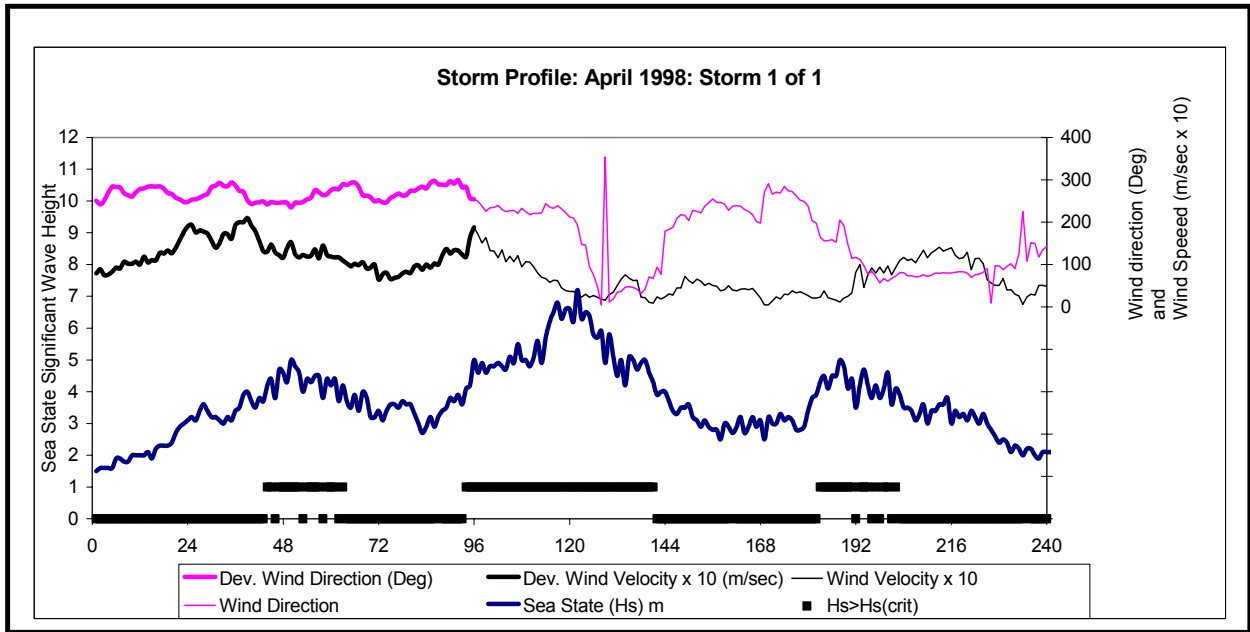


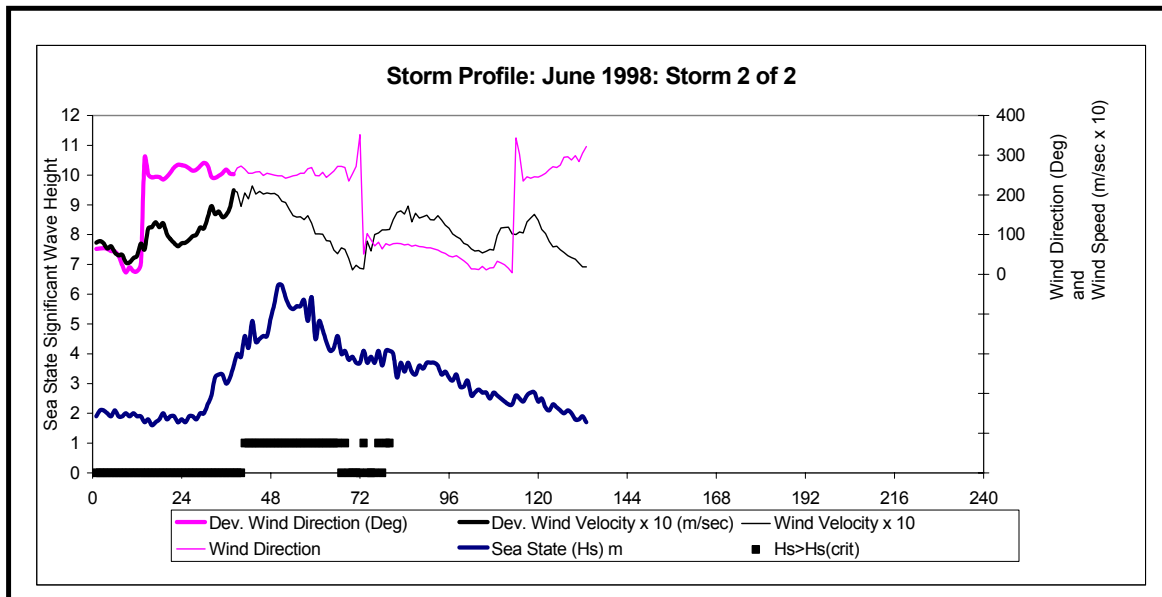
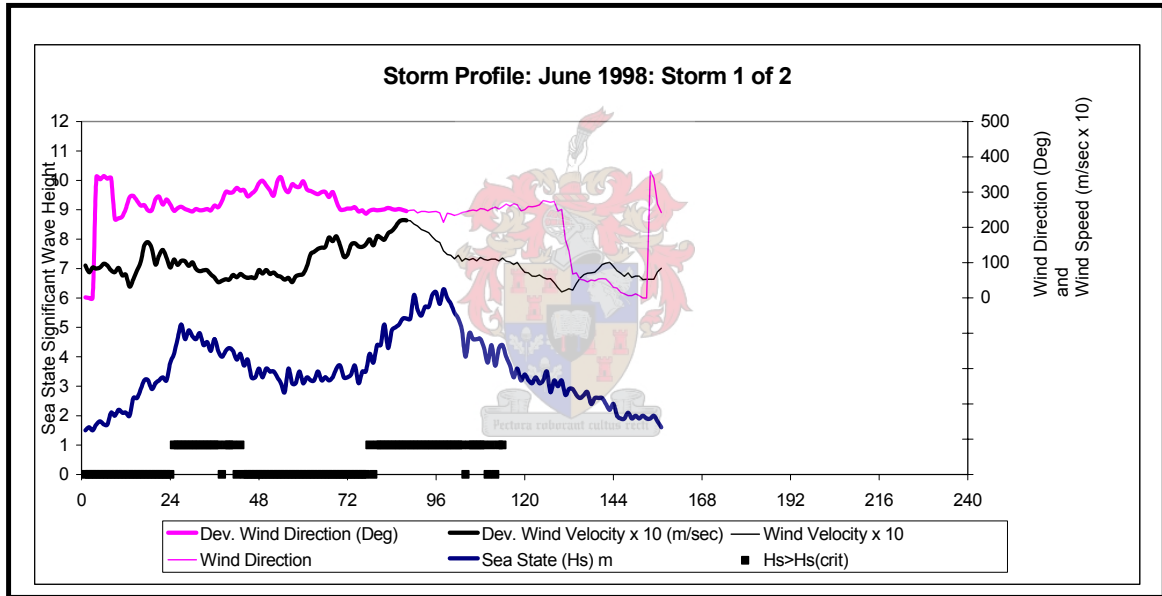
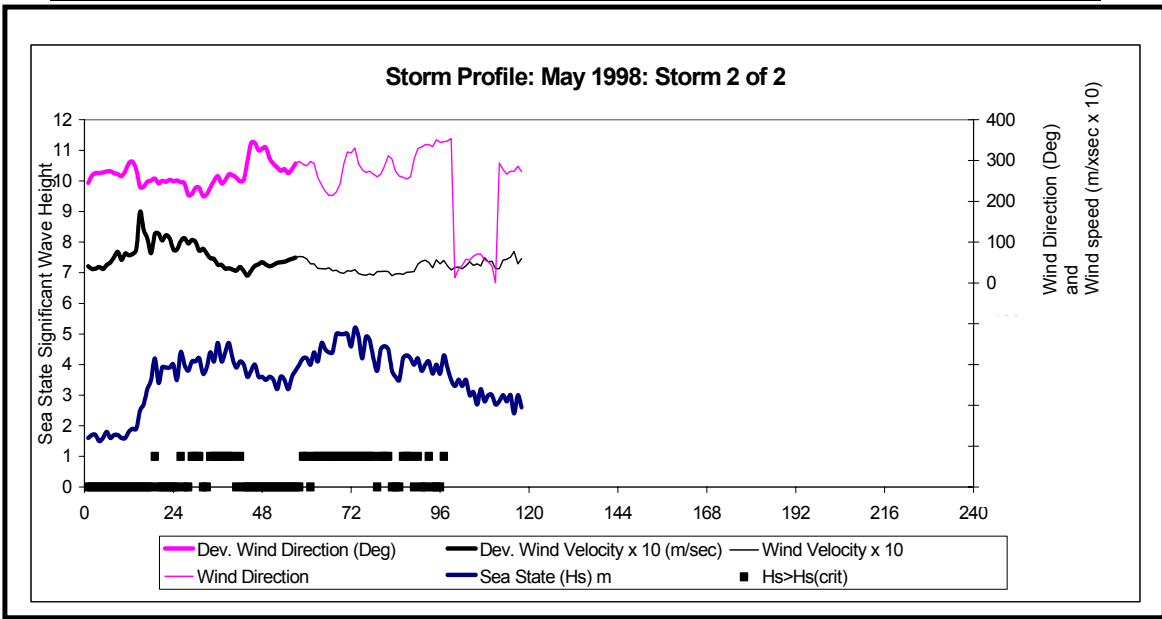


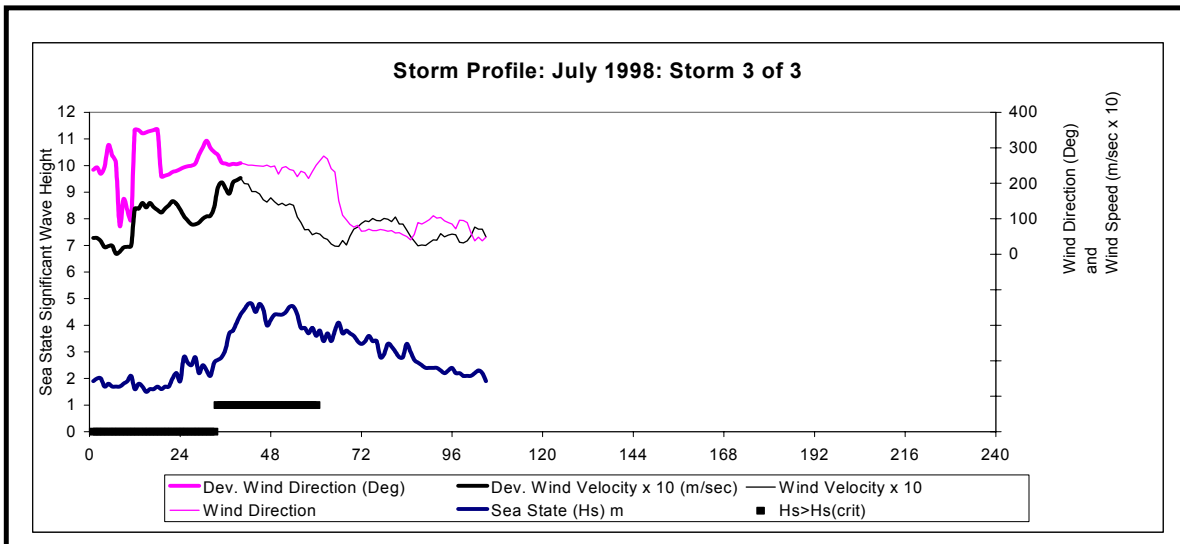
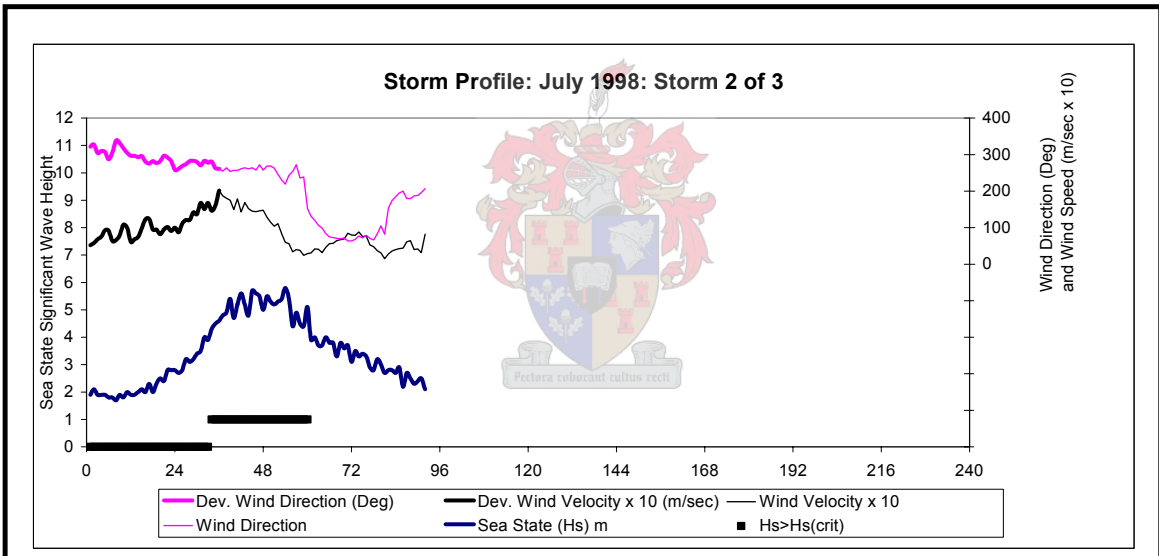
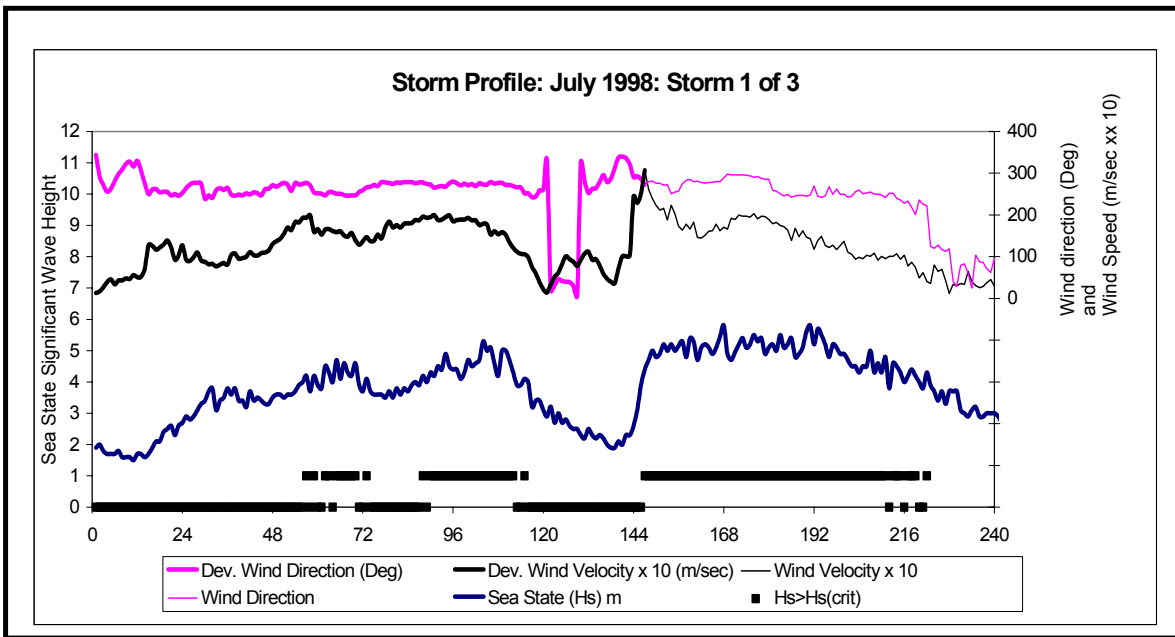
APPENDIX B

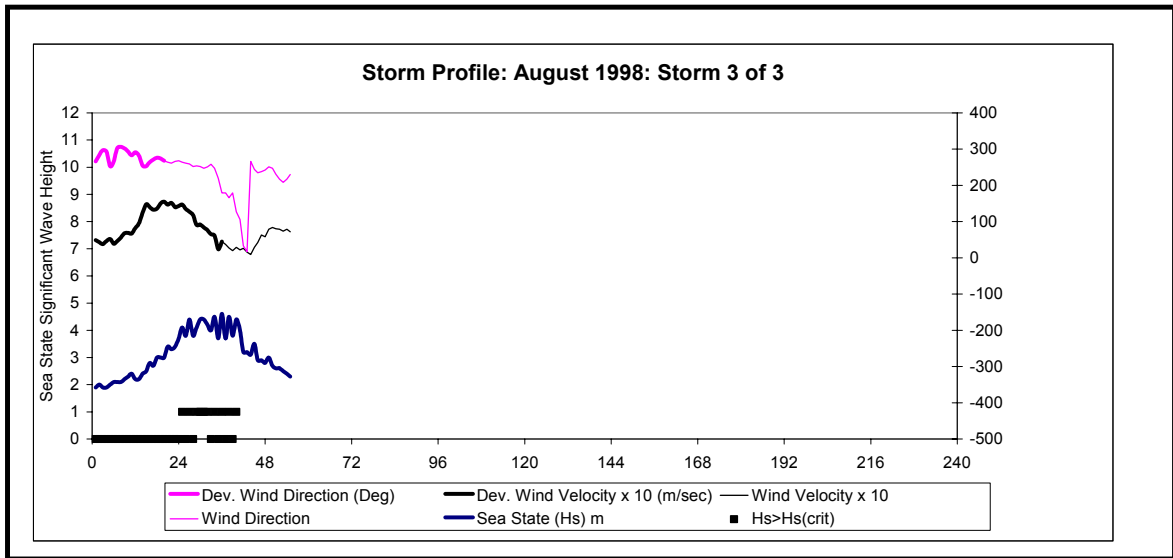
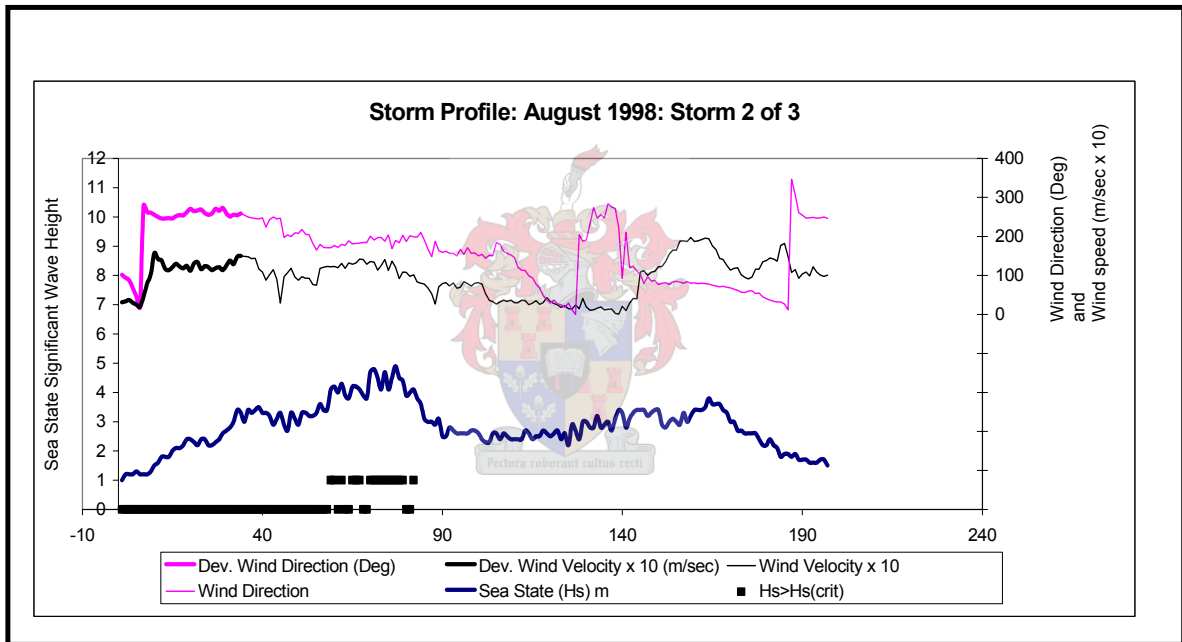
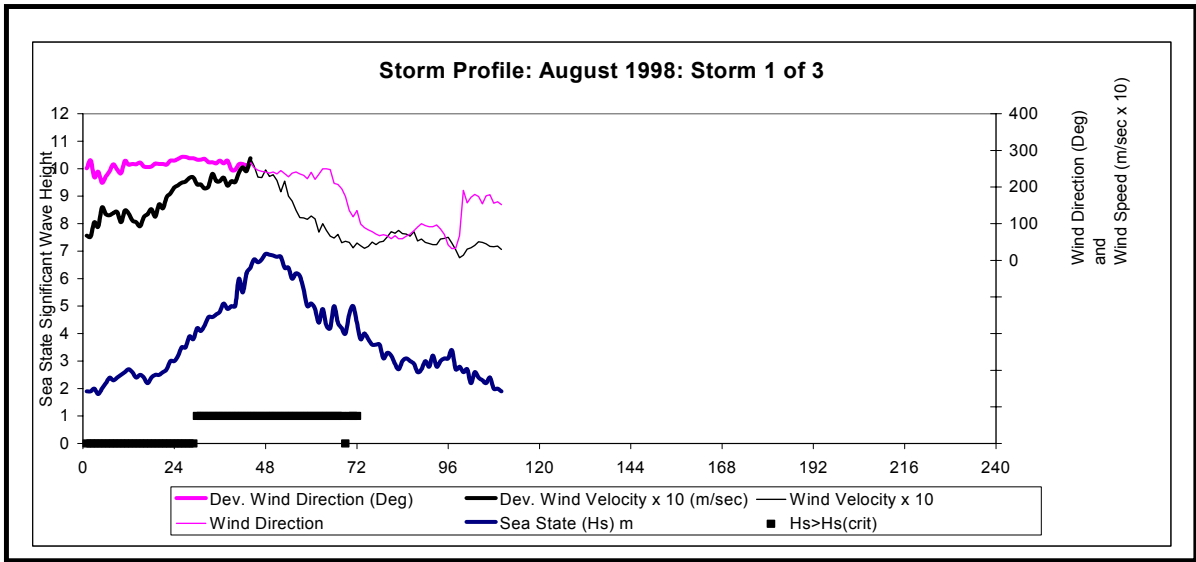
Graphs showing Profiles of Sea Storms in the Agulhas Bank Area for the Year 1998

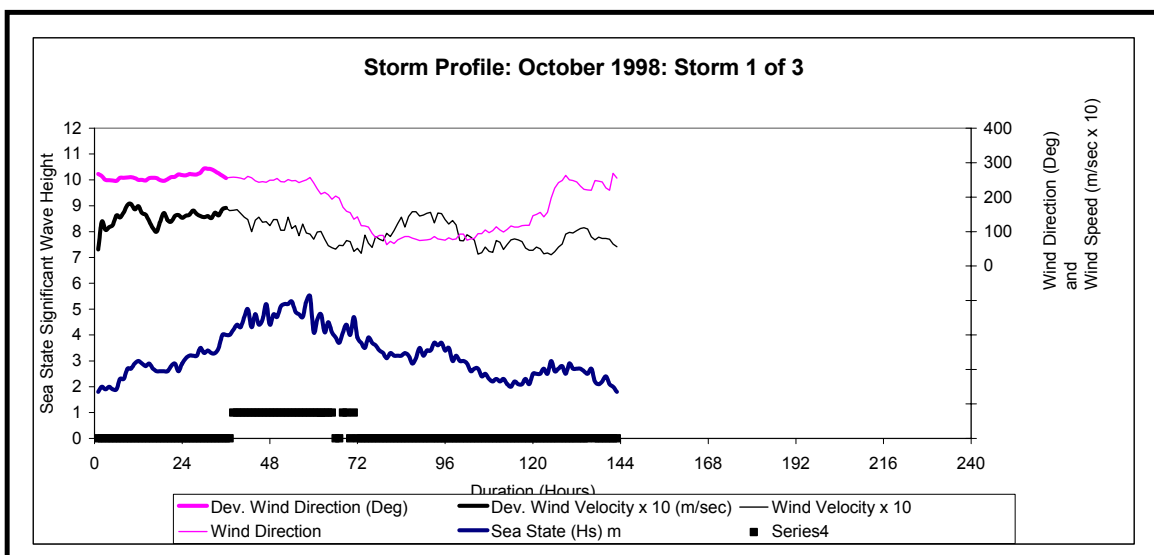
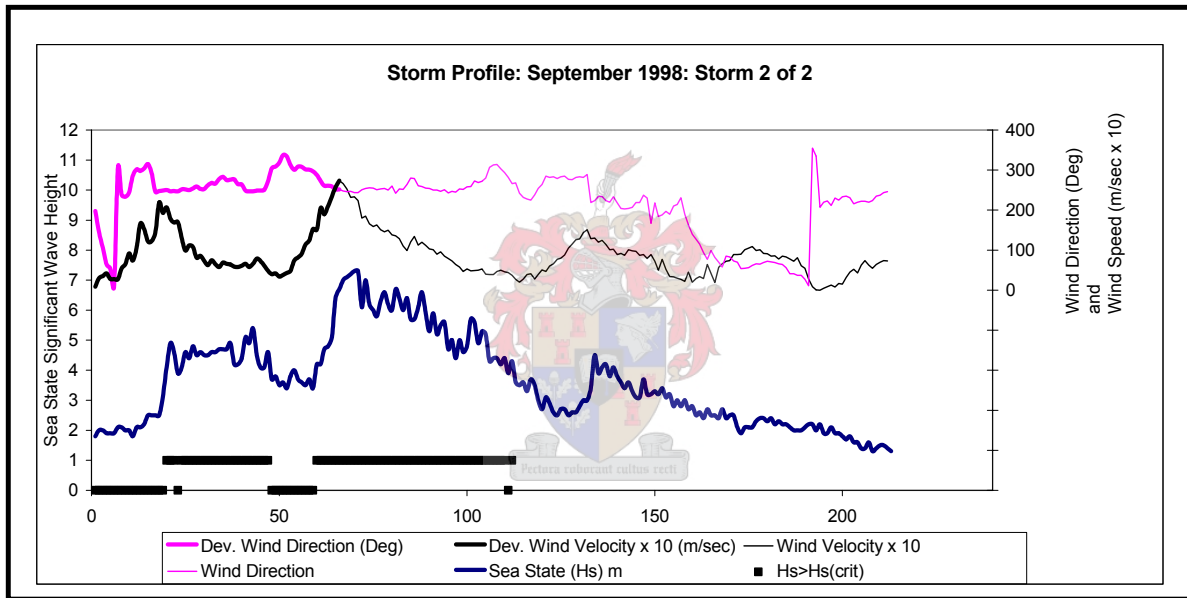
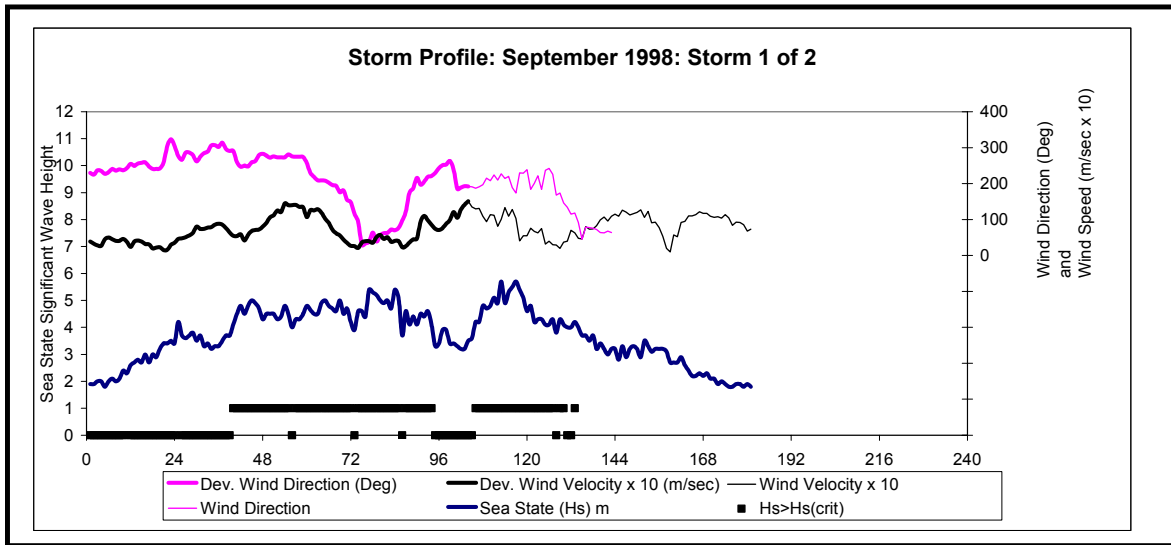


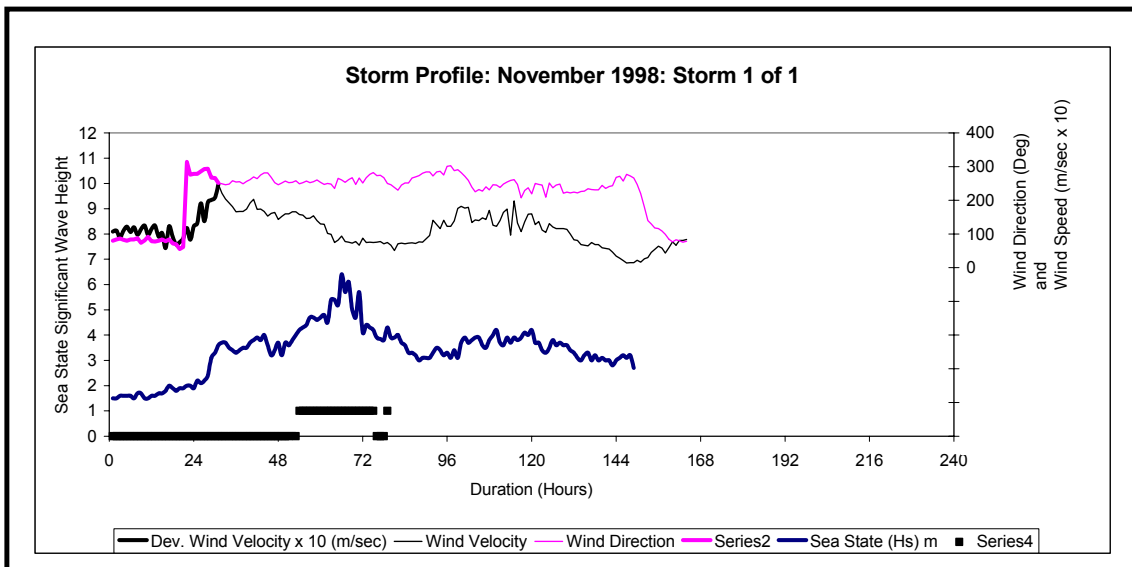
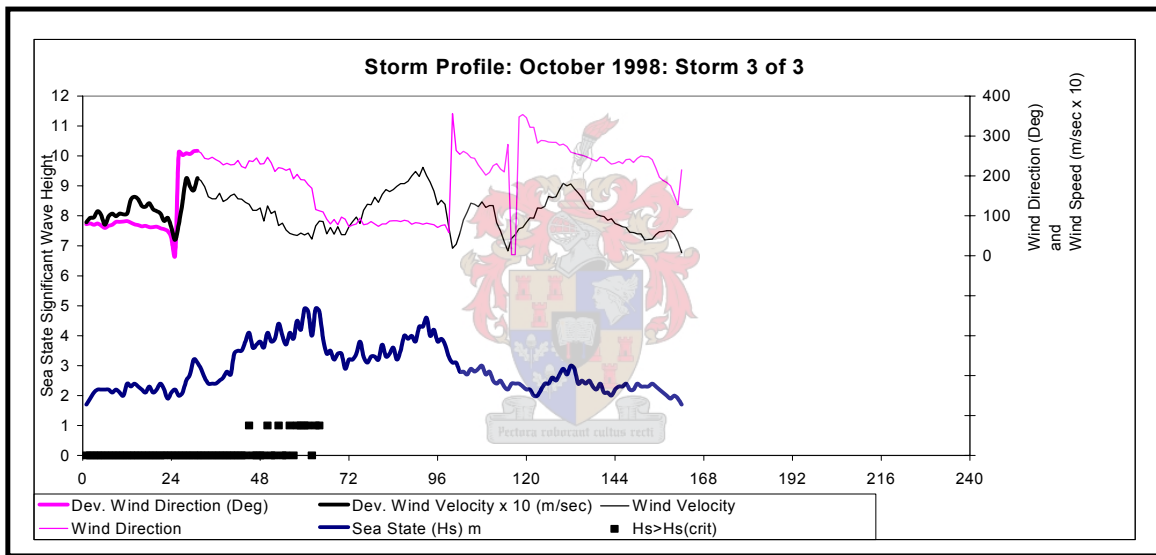
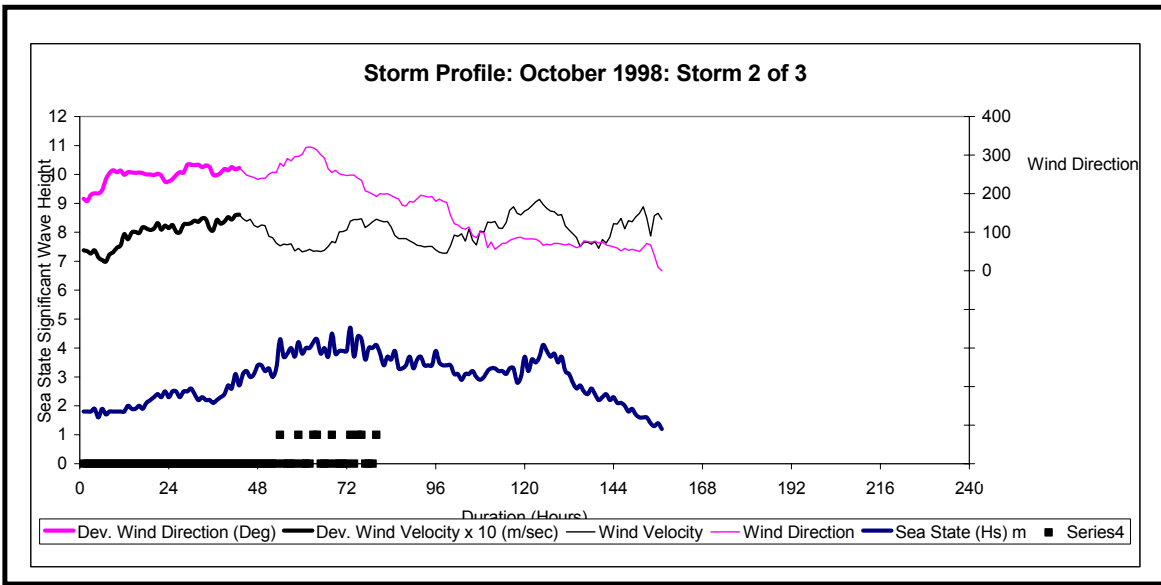


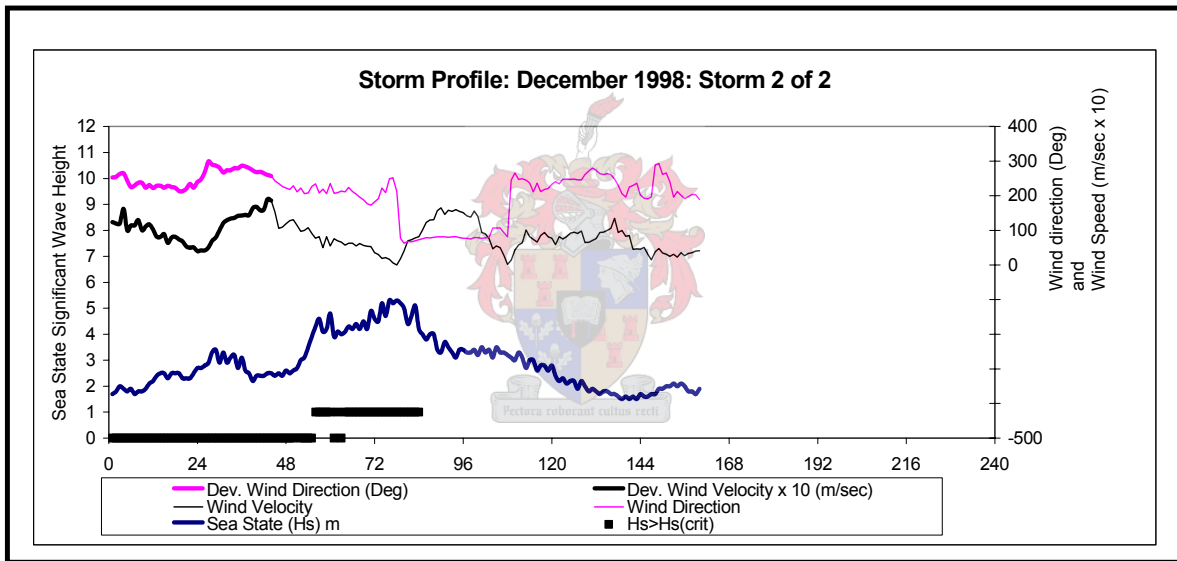
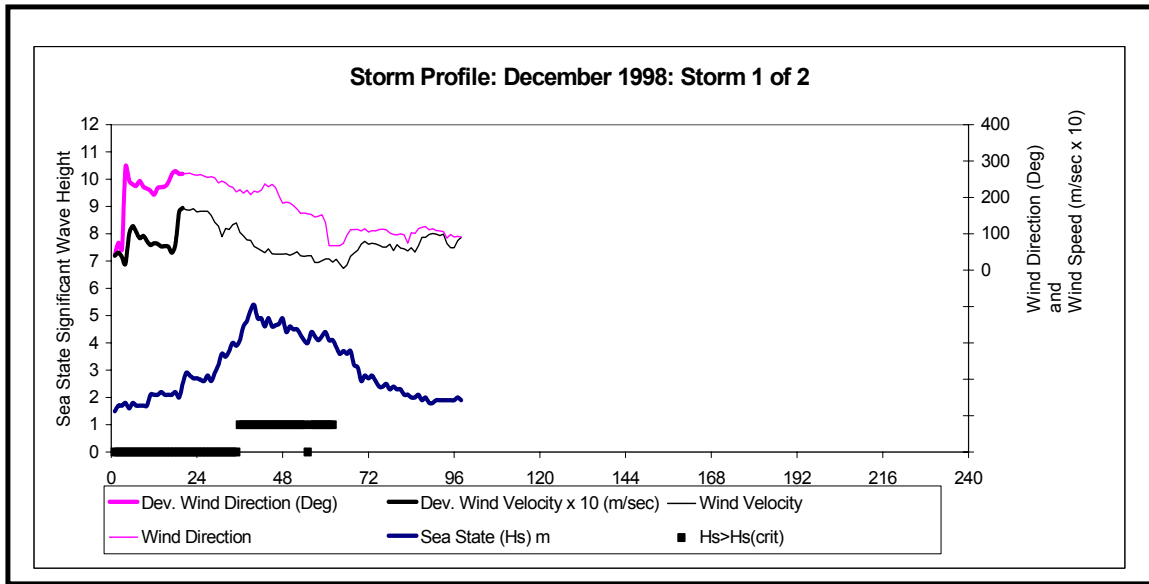












APPENDIX C

Typical Storm Energy Flux Calculations



Hm0	Tp	Wave Energy		
		Peak Hour	Sea State	Storm
m	sec	kWh/m	kWh/m	kWh/m
	14.50	41.23	123.68	7924.09
	13.47	55.09	165.27	
	14.50	53.42	160.27	
	15.52	51.25	153.76	
	14.50	42.62	127.86	
	13.47	35.01	105.03	
	13.47	39.12	117.35	
	13.47	43.45	130.35	
	13.47	44.31	132.93	
	13.47	45.18	135.54	
	13.47	41.76	125.27	
	13.47	38.47	115.41	
	13.47	35.32	105.96	
	13.47	32.30	96.91	
	12.69	27.58	82.75	
	11.91	23.35	70.04	
	11.91	22.88	68.63	
	11.91	22.41	67.24	
	10.37	23.30	69.91	
	8.83	23.36	70.07	
	8.83	26.50	79.50	
	8.83	29.85	89.54	
	9.25	37.41	112.24	
	9.66	46.12	138.35	
	9.66	37.46	112.39	
	9.66	29.71	89.12	
	9.66	29.71	89.12	
	9.66	29.71	89.12	
	11.57	28.37	85.11	
	13.47	25.61	76.83	
	11.57	28.63	85.88	
	9.66	30.19	90.56	
	10.79	46.29	138.88	
	11.91	67.23	201.69	
	12.69	77.28	231.85	
	13.47	88.26	264.77	
	13.47	101.39	304.17	
	13.47	115.44	346.31	
	13.47	123.09	369.26	
	13.47	130.98	392.95	
	14.50	122.43	367.28	
	15.52	112.64	337.93	
	14.50	87.02	261.05	
	13.47	65.56	196.68	
	13.47	63.27	189.81	
	13.47	61.02	183.06	
	12.69	55.97	167.91	
	11.91	51.12	153.37	
	12.69	48.68	146.05	
	13.47	45.88	137.64	
	12.69	33.57	100.70	
	11.91	23.58	70.75	

APPENDIX D

Typical Equivalent Wave Energy Storm Profile Calculations



Equivalent Energy Storm Parameter Calculation				
Storm Energy Flux (kW/m)	Hm0(max.ave./strom) (m)	Storm Threshold (m)	Tp (ave/storm) (Sec)	Duration (hrs)
7,924	4.41	1.95	12.42	126.18
Half Plot Length:				21.00

Profile of EWE Storm		Storm Energy Calculation
Half Profile	Full Profile	
0.00	1.95	70.86
1.00	2.06	79.22
2.00	2.17	70.86
3.00	2.29	79.22
4.00	2.40	107.09
5.00	2.51	117.31
6.00	2.62	127.99
7.00	2.73	139.14
8.00	2.84	150.76
9.00	2.96	162.84
10.00	3.07	175.39
11.00	3.18	188.41
12.00	3.29	201.89
13.00	3.40	215.83
14.00	3.52	230.24
15.00	3.63	245.12
16.00	3.74	260.46
17.00	3.85	276.27
18.00	3.96	292.55
19.00	4.07	309.28
20.00	4.19	326.49
21.00	4.30	344.16
22.00	4.41	362.30
	4.30	344.16
	4.19	326.49
	4.07	309.28
	3.96	292.55
	3.85	276.27
	3.74	260.46
	3.63	245.12
	3.52	230.24
	3.40	215.83
	3.29	201.89
	3.18	188.41
	3.07	175.39
	2.96	162.84
	2.84	150.76
	2.73	139.14
	2.62	127.99
	2.51	117.31
	2.40	107.09
	2.29	97.33
	2.17	88.04
	2.06	79.22
	1.95	70.86
Equiv SEF:		8740.39
Actual SEF:		7924.09
% Difference:		-10.30%